

Department of Chemistry, Faculty of Natural Sciences and Technology

Novel Synthesis of Lipoxine A4 Analogues

Towards Allosteric Modulators for Human Cannabinoid Receptor Type 1

—
AYA ISMAEL

KJE-3900 Masters Thesis in Chemistry – December 2015



ABSTRACT

The synthesis of the benzoid-based lipoxine A4 (LXA4) is the focus of this study specifically, the para substituted benzoid system. LXA4 is an endogenous agonist binding with high affinity to (ALXR) receptor that initiate it to display anti-inflammatory and antioxidant activities. Arachidonic acid is the cascade of LXA4 and its derivatives. These compounds belong to the biological active eicosanoids, which are characterized by its consistent of 20 C-atoms.

Based on structure activity relationship (SAR) of LXA4, several studies postulated wide range of modification and functionalization. Benzoid based LXA4 analogues have studied by several research groups where the focus was on the *O*- and *M*-substituted benzoids. Herein, a total synthesis approach towards some structural mimics of LXA4 was conducted. Where, the target was the benzoid based LXA4. Specifically, the *p*-substituted benzoid suggesting that these analogues could cover the same conformational space as the native LXA4.

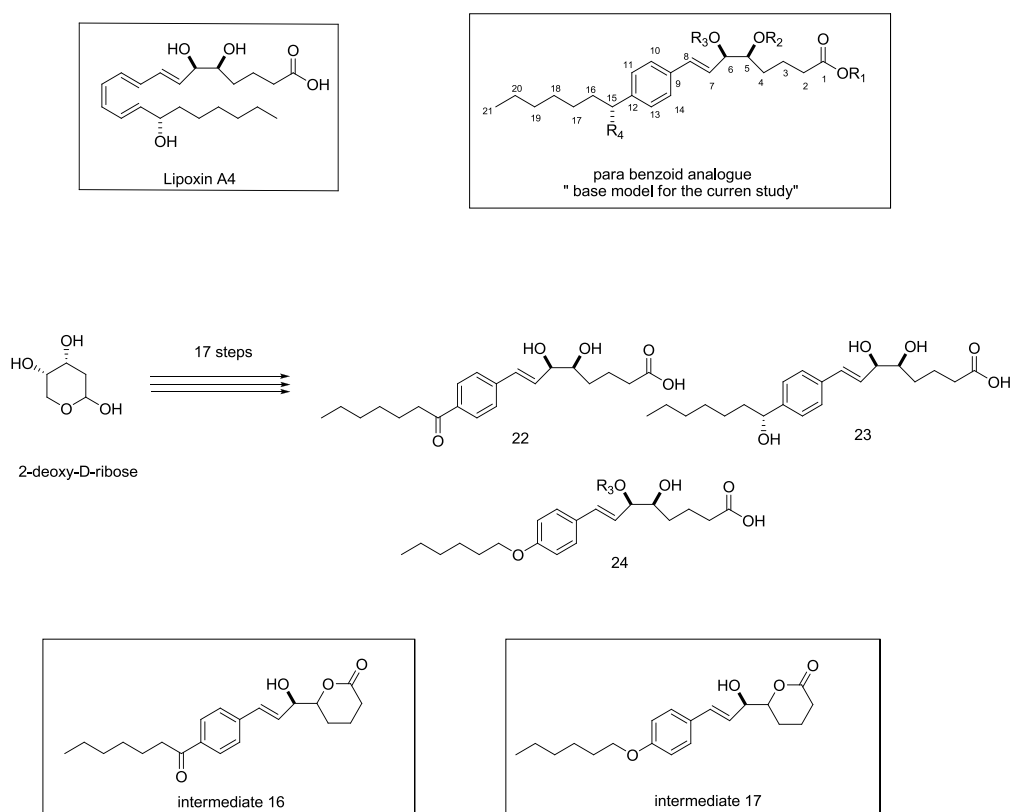


Figure 1. Lipoxin A4 and schematic presentation of the targeted analogues

The project approach is based on using commercially available starting materials such as 2-deoxy-D-ribose, toluene and p-cresol to assemble the desired molecules.

Important reactions in the course of the synthesis includes:

C1-C8 building block: Wittig reaction, Parikh-Doering oxidation, hydrogenation of the alkene, protecting group operations.

C15-C21 building block: Friedel-Craft acylation, O-alkylation, reduction by sodium borohydride.

Key reaction of the synthesis is the Wittig reaction between the two coupling partners. This reaction leads to the selective formation of the trans-olefin. The formation of the lactone ring intermediates **17** and **16** during the de-protection of 1, 2-diol moiety has been studied in details with the help of computational chemistry (Figure 1). The last part of the thesis reveals an initial trial of another suggested approach based on "Ullmann type" reaction. The total synthetic strategy was successfully applied within 14 steps out of 17 were successfully performed obtaining intermediates **16** and **17** in a good yield. The compliment of the steps includes short reactions of lactone ring hydrolysis in basic medium in addition to reduction of the ketone moiety in intermediate **16**.

ACKNOWLEDGEMENTS

“In life you will encounter two kinds of people: those who inspire you and those who bring you down. However, in the end, you will thank both of them”. I fell so blessed because today I don't have to thank anyone that has brought me down, simply because I didn't meet any yet.

My sincere gratitude go to my supervisor Ass. Prof. Jørn Hansen for giving me the opportunity to work as part of his research group. My masters has been a very rich period, full of positive experiences and independency. I am so grateful for your constructive supervision and guidance. It has been a pleasure working under your supervision.

I would like to send my extreme appreciation and thankfulness to my co-supervisor Ass. Prof. Annette Bayer. You were always there when I needed advice whether through my lab work or with correcting my thesis. Thank you for the encouragement and the constructive criticism.

During my study period I always had good study and work environment around me. Therefore, I thank University of Tromsø of such a great experience and opportunity.

I would like to thank Dr Taye Beyene Demissie for being so helping and providing me DFT data.

I am very grateful to Dr. Muhammad Zeeshan and Dr. Krisztian Bogar for being excellent mentors to me in the lab. I owe you with my lab experience. Thank you for the good relation both related to chemistry and to life in general.

To the engineers in tromsø, Truls Ingebrigsten, Arnfinn Kvarnes, Jostein Johansen and Frederick leeson. I thank you from all my heart for your daily help with HRMS, NMR, and IR.

I am also very grateful to my friends and colleagues, Marc Boomgaren, Sundus Akhter, Fatemeh Shouli pour, Emy Darwish, and Phenias Buhire for their overall support and appreciated advices.

A big thank you must be said to Yngve Guttormsen for his support in lab and the big effort he put in correcting my thesis.

A special thanks goes to my mom and my little sisters Ola and Hala. I am blessed to have such a magnificent family I thank you for the love and care you provided me with.

Finally, I would like to dedicate this thesis to my loving dad. You always supported me in everything unconditionally, I wouldn't be the person I am now without your guidance and love.

ABBREVIATIONS

2-AG	2-arachidonoyl glycerol
AA	Arachidonoyl acid
AC	Adenylyl cyclase
AEA	Anandamide
AM251	AM 251 6-iodopravadoline
AM281	1-(2,4-dichlorophenyl)-5-(4-iodophenyl)-4-methyl-N-4-morpholinyl-1 <i>H</i> -pyrazole-3-carboxamide
ATP	Adenosine 5`-triphosphate
cAMP	Cyclic 3`:5`-adenosine monophosphate
CP55,940	[(-)- <i>cis</i> -3-[2-hydroxy-4-(1,1-dimethylheptyl)phenyl]- <i>trans</i> -4-(3-hydroxypropyl)cyclohexanol]
CB1	Cannabinoid receptor subtype 1
CB2	Cannabinoid receptor subtype 2
13C-NMR	Carbon-13 nuclear magnetic resonance
DMP	Di-methoxy propene
DAGL	Diacylglycerol lipase
DMSO	dimethyl sulphoxide
DMF	<i>N,N</i> -dimethylformamide

DCM	dichloromethane
ECS	Endocannabinoid system
ERK1/2	Extracellular signal-regulated kinase-1 and -2
E1, E2	Elimination reaction
FAAH	Fatty acid amide hydrolase
GDP	Guanosinediphosphate
GIRK	Inwardly rectifying potassium channels
GPCR	G-protein-coupled receptor
ΔG	Change in Gibbs free energy
GTP	Guanosine 5'-triphosphate
IP3	Inositoltrisphosphate
JNK	c-Jun N terminal kinase
MAGL	Monoacylglycerol lipase
¹ H-NMR	Proton nuclear magnetic resonance
HRMS	High Resolution Mass Spectroscopy
IR	Infrared (Spectroscopy)
MW	Microwave
m.p	melting point

MAPK	Mitogen-activated protein kinase
NArPE	N-arachidonoylphosphatidyl-ethanolamine
NBS	N-bromosuccinimide
NMR	Nuclear magnetic resonance
ORG 27569	5-chloro-3-ethyl-N-(4-(piperidin-1-yl)phenethyl)-1 <i>H</i> -indole-2-carboxamide
PI3K	Phosphoinositide 3-kinase
PIP2	Phosphatidylinositolbisphosphate
PSNCBAM-1	1-(4-Chlorophenyl)-3-[3-(6-pyrrolidin-1-ylpyridin-2-yl)phenyl] urea
Ppm	Parts per million
PPTS	Pyridinium <i>p</i> -toluenesulphonate
PES	Potential energy surface
R _f	Retention factor
SR141716A, Rimonabant	5-(4-chlorophenyl)-1-(2,4-dichlorophenyl)-4-methyl-Npiperidino pyrazol-3-carbamide
SAR	Structure Activity Relationship

SN	Nucleophilic substitution
TFT	Trifluoro toluene
ΔS	change in the entropy
Δ^9 -THC	Δ^9 -tetrahydrocannabinol
TFA	Trifluoroacetic acid
THF	Tetrahydrofuran
TLC	Thin layer chromatography
TBAF	Tetrabutylammonium fluoride
TMS	tetramethylsilane
UV	Ultra Violet
WIN 55,212-2	(<i>R</i>)-(+)-[2,3-dihydro-5-methyl-3-(4-morpholinylmethyl) pyrrolo [1,2,3-de]-1,4-benzoxazin-6-yl]-1-naphthalenylmethanone mesylate

LIST OF FIGURES, TABLES AND SCHEMES

Figure 1. Lipoxin A4 and schematic presentation of the targeted analogues.....	iv
Figure 2. LXA4 and some benzoid based analogues.....	2
Figure 3. Proposed p- benzoid analogues	4
Figure 4. Schematic representation of rat CB1.....	10
Figure 5. Model of the GPCRs life cycle.....	11
Figure 6. GPCR activation states.....	12
Figure 7. Tissue distribution of the human CB1 and CB2 receptors in the body	14
Figure 8. Model of CB1 signal transduction.....	15
Figure 9. The structures of several CB1- cannabinoid ligands	18
Figure 10. Chemical structure of representatives for CB1 allosteric modulators.....	21
Figure 11. Catalytic hydrogenation mechanism	28
Figure 12. B3LYP/6-311G (d, p) calculated change in standard Gibbs free energy and change in entropy.....	56
Figure 13. Potential energy surface (PES) for the internal cyclization of compound 6	58
Figure 14. Optimized structure of compound 16.	64
Figure 15. Optimized structure of compound 17	65
Table 1. Reaction optimization towards the bromination of the benzylic ether	50
Table 2. Initial optimizations of Ullmann reaction conditions.	54
Table 3. The trials towards the O-alkylated product.	74
Scheme 1. Retrosynthetic analysis of LXA4.....	6

Scheme 2. Forward synthesis of the designed reaction sequence.....	23
Scheme 3. Earlier synthetic research on the key intermediate	24
Scheme 4. Protection of 2-deoxy-D-ribose	24
Scheme 5. General mechanism of acetal formation	25
Scheme 6. Mechanism of acetonide formation.....	26
Scheme 7. Synthesis of the unsaturated alcohol.....	26
Scheme 8. Mechanism of the Wittig reaction	27
Scheme 9. Reduction of the alcohol's bi bond	28
Scheme 10. Parikh-Doering oxidation of the 1° alcohol.....	29
Scheme 11. Mechanism of Parikh- Doering oxidation.	29
Scheme 12 . Synthesis of the acylated toluene	30
Scheme 13. Friedel-craft acylation mechanism.....	30
Scheme 14. Benzylic bromination of the acylated toluene.....	31
Scheme 15. Mechanism of the benzylic bromination using NBS in visible light.	32
Scheme 16. Synthesis of the Wittig salts.	32
Scheme 17. Nucleophilic attack by the triphenyl phosphine on the electrophilic carbon.....	33
Scheme 18. SN2 reaction mechanism.....	33
Scheme 19. O-alkylation of para cresol.....	33
Scheme 20. Benzylic o-alkylation mechanism "SN2"	34
Scheme 21. Benzylic bromination.	34
Scheme 22. Mechanism of the benzylic bromination by NBS.	35
<i>Scheme 23. Wittig reaction of the ylid and the aldehyde.</i>	<i>36</i>
Scheme 24. Mechanism of the Wittig reaction.	37
Scheme 25. Deprotection of the diol in acidic medium.....	38

Scheme 26. NaBH ₄ reduction “general mechanism “	38
Scheme 27. Carbonyl group reduction mechanism.	39
Scheme 28. Lactone formation mechanism.	40
Scheme 29. Classic Ullman reaction	40
Scheme 30. “Ullmann Type” reaction	41
Scheme 31. Catalytic mechanism of Ullmann reaction.	41
Scheme 32. Proposed analogues.	43
Scheme 33. Synthesis of the protected sugar	44
Scheme 34. Synthesis of the alkene via Wittig reaction.	45
Scheme 35 synthesis of the reduced alcohol.	46
Scheme 36. Synthesis of the aldehyde.	46
Scheme 37. Synthesis of the acylated toluene	47
Scheme 38. Synthesis of the brominated acyl.	47
Scheme 39. Synthesis of the Wittig salt.	48
Scheme 40. Synthesis of the benzylic ether.	48
Scheme 41. Synthesis of the brominated benzylic ether.	49
Scheme 42. Synthesis of the Wittig salt of the benzylic ether	50
Scheme 43. Synthesis of the coupled alkene.	51
Scheme 44. Hydrolysis of the acetal in the ketone containing compound	51
Scheme 45. Synthesis of the coupled alkene of the benzylic ether	52
Scheme 46. Hydrolysis of the acetal in the ether containing compound	52
Scheme 47. Synthesis of the O-alkylated phenol	53
Scheme 48. Synthesis of the Ullmann ether	53
Scheme 49. Strategies for structural diversity of LXA4 analogues library	60

Scheme 50. Late stage functionalization strategy	61
Scheme 51. New proposed analogues with suggested approaches	61
Scheme 52. Summary of Reagents and conditions	63

TABLE OF CONTENTS

TABLE OF CONTENTS

Abstract.....	iv
Acknowledgements.....	viii
Abbreviations.....	x
List of figures, tables and schemes.....	xiv
1 Introduction	xxi
1.1 The Goals and Design of the Project.....	3
1.2 Retrosynthesis.....	5
1.3 Biological Background.....	7
1.3.1 Cannabis and cannabinoids.....	7
1.3.2 The endocannabinoid system.....	8
1.3.3 Cannabinoid receptors type 1.....	9
1.3.4 GPCR receptors life cycle.....	10
1.3.5 Receptor activation states.....	11
1.3.6 CB1 receptors tissues distribution.....	13
1.3.7 CB1 Signal transduction.....	14
1.3.8 CB1 receptor agonists.....	15
1.3.9 Cannabinoid antagonists – inverseagonists.....	17
1.3.10 Allosteric modulation.....	19
1.3.11 Allosteric Modulators of the CB1 Receptors.....	20
1.3.12 Lipoxin A4 is an endogenous allosteric ligand for CB1.....	21
1.4 Chemical background toward the synthesis of LXA4 analogues.....	23

1.4.1	Preparing the aldehyde from the sugar	24
1.4.2	Preparing of the Wittig salts	30
1.4.3	Wittig reaction	36
1.4.4	De-protection of the acetonide	37
1.4.5	Reduction of benzylic ketone.....	38
1.4.6	Lactone formation	39
1.4.7	Ullmann approach	40
2	Result and Discussion.....	43
2.1	The scope of the chapter.....	43
2.2	Protection of 2-deoxy-D ribose	44
2.3	Synthesis of the alkene from the sugar	45
2.4	Reduction of the alkene.....	46
2.5	Oxidation of the 1° alcohol to aldehyde.....	46
2.6	Friedel-Craft acylation of the toluene	47
2.7	Benzylic bromination of the acylated toluene.....	47
2.8	Wittig salt from the benzyl brominated toluene derivative	48
2.9	Preparation of the O-alkylated <i>p</i> -cresol.....	48
2.10	Benzylic bromination of the ether.....	49
2.11	Wittig salt from the bromo-benzylic ether	50
2.12	Wittig reaction of the aldehyde and the ketonic Wittig salt.....	51
2.13	Hydrolysis of the acetal in the ketonic moiety containing product.....	51
2.14	Wittig reaction of the aldehyde and the aldehydic Wittig salt	52
2.15	Hydrolysis of the acetal in the aldehydic moiety containing product	52
2.16	Ullmann approach	53

2.16.1	Preparing the O-alkylated phenol derivative.	53
2.16.2	Preparing the Ullmann ether	53
2.17	A total computational study on the lactone case.....	55
2.17.1	Density functional theory (DFT) calculations	55
2.17.2	Discussion of the calculated results	55
3	Future Directions.....	59
4	Summary and Conclusions.....	63
5	Experimental Section	67
5.1	General experimental Considerations.....	67
5.2	Detailed experimental procedures and characterizations.....	68
5.2.1	Synthesis of the aldehyde	68
5.2.2	Synthesis of the Wittig salts.....	71
5.2.2.1.1	<i>Synthesis of the acylated toluene</i>	71
5.2.3	Synthesis of the alkene via Wittig coupling of the ketone partner.	76
5.2.4	Synthesis of the alkene via Wittig coupling of the ether partner	77
5.2.5	Hydrolysis of the acetonid in the ketone containing analogue.....	78
5.2.6	Hydrolysis of acetonid of the ether containing analogue	79
5.2.7	Ullmann approach	79
6	References	83
7	Appendices	95

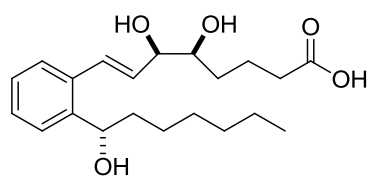
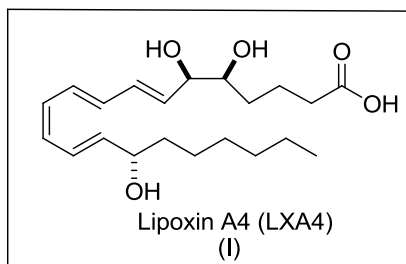
1 INTRODUCTION

LXA4 is an endogenous agonist binding with high affinity to (ALXR) receptor. It is known as formyl peptide receptor 2 (FPR2), which displays anti-inflammatory and antioxidant activities [1-3]. LXA4 also shows partial agonist activity on binding with cysteinyl leukotriene receptors 1 and 2 [3, 4]. LXA4 can suppress cytokine signaling² when binding to nuclear receptor aryl hydrocarbon [5]. Furthermore, LipoxinA4 interacts with CB1 receptor and exhibits positive allosteric modulation [6, 7]. LXA4 involved in modulation of several inflammatory disorders such arthritis, asthma and ischemia [8-10, 132]. According to Pamplona et al. LXA4 is positive allosteric modulator (PAM) of CB1 cannabinoid receptor whether it is administered exogenously or it is produced endogenously [6, 7].

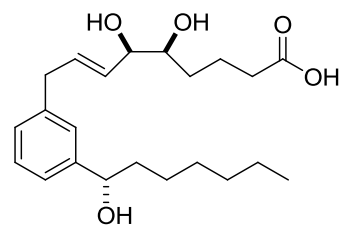
As a natural product LXA4 can only be isolated in minimal quantities as many other natural products. It is produced in the body on demand and rapidly metabolized, which means that its accumulation at the site of the inflammation is short lived. These obstacles were realized upon the investigation and the study of these compounds. Thus, it reduces the possibility of applying further studies and investigations on these important pharmacological agents. Subsequently, a novel range of LXA4 analogues were designed and synthesized to get the structure activity relationship (SAR). In addition to, the evaluation of these novel analogues for pharmacological activity and resistance to the degradation for enhanced biological properties. Several research groups have conducted extensive studies indicating some functionalities and stereocenters that are essential to retain the biological activity according to SAR [9, 11-14].

This thesis describes our contribution in the continuous efforts towards mimicking the structure of the native LXA4. Our approach targeted a class of LXA4 analogues that are based on replacing the triene unit with a stable aromatic moiety in a substituted benzoid system. Benzoid based LXA4 analogues have been under the spot of study for many research groups where the focus was on the *O*-and *M*-substituted benzoids (Fig 2).

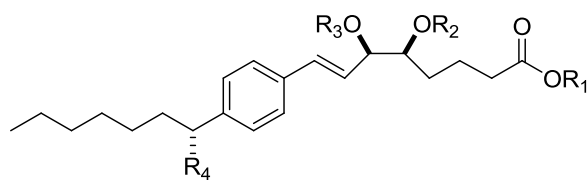
Herein, we present in our research a total synthesis approach where the focus is on the *p*-substituted benzoid suggesting that these analogues could cover the same conformational space as the native LXA4.



O-benzoid analogue
(II)



M-benzoid analogue
(III)



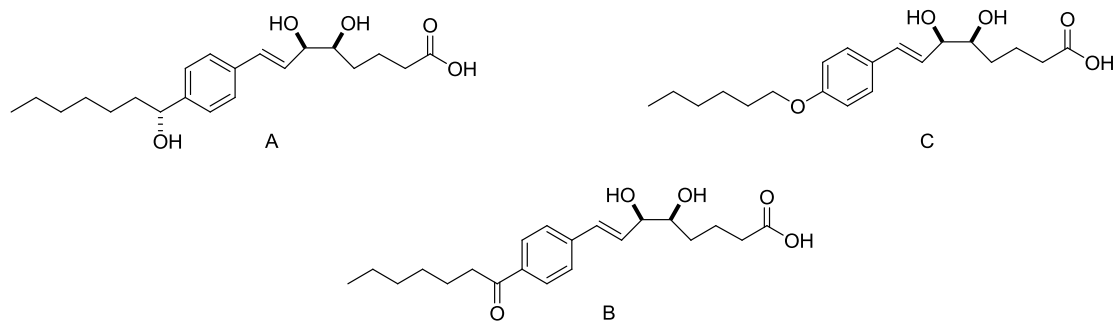
Proposed modification for SAR-studies
(IV)

Figure 2. LXA4 and some benzoid based analogues.

1.1 THE GOALS AND DESIGN OF THE PROJECT

Herein is proposed the construction of LXA4 analogues based on benzoid system (Fig 2, 3). The benzoid scaffold allows for a more effective and modular construction of the basic framework and the formation of a variety of analogues in a relatively straightforward manner. It is assumed that the various analogues cover the same conformational space as LXA4. However, each analogue is restricted to a particular configuration of the triene-portion of LXA4. This could impose entropically very favorable binding characteristics, which means that the analogue would not need to lose too many degrees of freedom in the binding process compared to the LXA4 itself. The construction of the proposed analogues will be first attempted. Our project goal is to introduce an appropriate organic synthesis strategy to produce the proposed analogues see (Fig 3) from easy and commercially available starting materials. The aims of the thesis are:

1. Plan and design a synthetic route to benzene analogues of lipoxin A4
2. Develop the synthetic route towards lipoxin A4 analogues
3. Prepare some structurally similar analogues.
4. Investigate alternative synthetic routes to generate simpler analogues
5. Submit pure samples for pharmacological profiling.



Proposed analogues A,B,C

Figure 3. Proposed p- benzoid analogues

1.2 RETROSYNTHESIS

The targeted molecules **17** and **18** consist of two main partners that show from the central disconnection A. The first disconnection A removes the aldehyde moiety **5** revealing the Wittig salts **9** and **13**. In the forward direction, this is envisioned using Wittig coupling reaction.

Further disconnection of both Wittig salts **9** and **13** removes the phosphate group retaining the benzylic brominated compounds **8** and **12**. While in forward synthesis, they could be performed by SN2 reaction with the triphenylphosphine

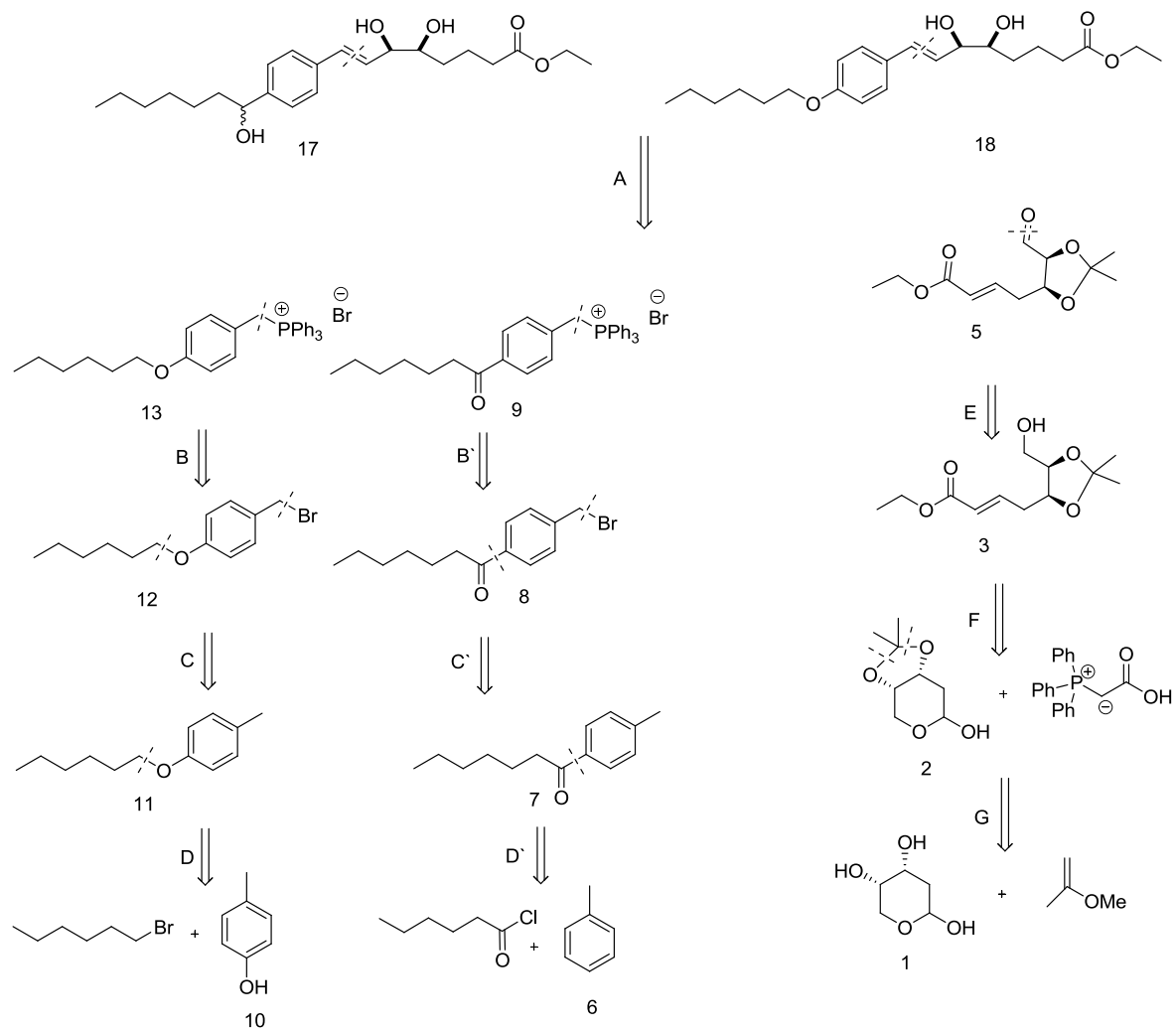
Disconnection of the benzylic brominated para benzoids **8** and **12** reveals the para alkyl benzoids **7** and **11**. While the forward synthesis in case of compound **7** is based on the use of NBS within a thermal reaction where the heat is the radical initiator. On the other hand, the forward synthesis of compound **11** is based on the use of NBS with benzoyl peroxide as the radical initiation in a benzylic bromination induced by visible light reaction

Latest disconnection D of the benzylic ether **11** gives the alkyl bromide and the para cresol, which is forward synthesized by O-alkylation in an SN2 reaction mechanism. While in case of the acylated toluene **7** the disconnection gives the toluene and its acyl chloride partner. The forward synthesis can be performed using Friedel-Craft acylation on the toluene to give the para acylated toluene.

On the other pathway, further disconnection of the aldehyde **5** gives the alcohol **3**. While, the forward synthesis of this aldehyde can be performed by the oxidation of the corresponding saturated alcohol of the alcohol **3** using Parikh-Doering oxidation.

Disconnection F removes the ethyl acetate moiety revealing the original protected sugar **2** and the phosphate salt. Compound **3** can be forward synthesized by Wittig reaction between the Wittig salt and the protected sugar **2**.

As 1, 2-diol containing sugar **1** it could be protected in a form of acetonide **2** when it couples with 2-methoxypropene as it shows in disconnection G.



Scheme 1. Retrosynthetic analysis of LXA4

1.3 BIOLOGICAL BACKGROUND

1.3.1 Cannabis and cannabinoids

The plant *Cannabis sativa L.*, family (Cannabaceae), is an Indian hemp represents one of the oldest cultivated plants. Its origin is the plains of Central Asia and from there has been distributed widely around the world [15, 16]. Cannabis was cultivated for its herbal contents, natural fiber and oil. Cannabis derivatives have been used as therapeutic agents across the ancient world for more than 4000 years. Several therapeutic uses have been reported such as digestive, appetite stimulant, analgesic, anticonvulsant, tranquilizer, anesthetic, anti-inflammatory, antibiotic, antiparasite, antispasmodic, and others [17]. The two most referenced cannabinoids preparations, are marijuana (dried leaves and female flower heads) and hashish (cannabis resin) [18]. In 19th century Europeans used cannabis extracts in the treatment of epilepsy, rheumatism, menstrual cramps, convulsions, chorea, hysteria, depression, tetanus, gout, and neuralgia [19].

Cannabis extracts contains more than 460 compounds around 70 out of them are considered as phytocannabinoids [20]. The prototype psychoactive phyto cannabinoid of cannabis is Δ^9 tetrahydrocannabinol, commonly known as Δ^9 -THC, The identification of the Δ^9 -THC was the first step to develop novel synthetic cannabinoids, The chemical synthesis of the cannabinoids was followed by accumulating research into basic structure activity relationships {SAR} and their metabolic routs [21, 22]. The need for more potent and less lipophilic analogues that avoid the unwanted psychoactive effects led to the first synthetic drug mimics the action of Δ^9 THC “nantradol” synthesized by Pfizer Inc. in 1980. Soon after, replaced by levonantradol (Nantrodolum[®]) [23]. The term “Cannabinoid” refers to a set of oxygen-containing C21 aromatic hydrocarbon compounds that occur naturally in the plant *Cannabis sativa*. Now, the term is expanded to involve all naturally occurring or synthetic compounds that can mimic the actions of plant-derived cannabinoids or that have structures similar to those of plant *Cannabis sativa* [24-26].

A separate term” phytocannabinoid” (pCB) refers to lipophilic molecules naturally occurring in the *cannabis sativa L.* with similar chemical structures as Δ^9 -THC [27].

1.3.2 The endocannabinoid system

The endogenous cannabinoid system is comprised of cannabinoid receptors (CBs), their endogenous ligands, i.e. endocannabinoids, and enzymes for their biosynthesis and degradation [28]. Endocannabinoids comprise a family of eicosanoid CBs [29, 30] present in the brain and in peripheral tissues. Wilson and Nicoll [31] described that endogenous cannabinoids mediate retrograde signaling that may be involved in the inhibition of neurotransmitter release. Endocannabinoids differ from neurotransmitters as they are synthesized rapidly on demand, not in advance, from membrane phospholipids precursors upon stimulation and they are not stored in vesicles rather their precursors [32].

N-arachidonoyl ethanolamine (anandamide, AEA) and 2-arachidonoyl glycerol (2-AG) are the major endocannabinoid ligands act basically at cannabinoid receptors CB1 and CB2. Other endocannabinoids have also identified such as noladin ether, virodhamine, and N-arachidonoyl dopamine (NADA) but their biological activity and metabolism has not yet been fully identified [20]. Most of endocannabinoids have greater affinity for CB1 Than CB2 except 2-AG that has relatively equal affinity for both CB1 and CB2,while virodhamine, unlike the others, acts as CB1 antagonist /invers agonist and has greater affinity for CB2 receptors [33, 34]. Endocannabinoids mediate several signals that regulate numerous aspects of mammalian neurophysiology, including suppress pain sensitivity, feeding, emotional state, learning and memory, and reward behaviors [35-37].Anandamide and 2-AG are widely distributed throughout the body. They are the main ligands among other endocannabinoids, though 2-AG expressed at much higher concentrations than anandamide. These endocannabinoids have been found in the brain, retina, and several peripheral tissues that involve the heart, spleen, liver, kidney, thymus, reproductive system and skin [38].The biosynthesis of endocannabinoids has not yet fully understood. It is known that anandamide is synthesized by calcium dependent transacylase enzyme (CDTA) that led to migration of arachidonic acid (AA) from the sn-1 position of membrane phospholipids to the primary amine of phosphatidylethanolamine (PE) to form N-arachidonoylphosphatidyl-ethanolamine (NArPE).Hydrolysis of (NArPE) to produce anandamide seems to go through Multiple enzymatic routes [39, 40].

2-AG is synthesized from arachidonoyl acid and preceded by formation of diacylglycerol (DAG) species by sn-1-specific diacylglycerol lipase- α and $-\beta$ (DAGL α and DAGL β [41]).

DAGL α is required for 2-AG formation in the brain while DAGL β in peripheral tissues such as the liver and spleen [42, 43]. DAG precursors are synthesized from membrane phospholipids to form sn-2 arachidonoyl phosphatidylinositol 4, 5-bisphosphate (PIP2) then hydrolyzed by phospholipase C (PLC β) to form 2-AG [44].

Anandamide transfers to its target cells by passive diffusion where exert its biological effects and rapidly degraded. Anandamide degradation seems to be happened by the serine hydrolase enzyme fatty acid amide hydrolase (FAAH) to form arachidonic acid and ethanolamine [33]. Soon after 2-AG migrates into cells by simple and passive diffusion, it is degraded by enzymatic hydrolysis of the ester bond. Presynaptic monoacylglycerol lipase (MAGL) is the major enzyme that hydrolyze 2-AG, serine hydrolases (SH) and FAAH enzymes may regulate 2-AG hydrolysis [45, 46].

1.3.3 Cannabinoid receptors type 1

The existence of unknown (GPCRs) receptors bind to cannabinoids and couple to inhibition of adenylyl cyclase to decrease the (cAMP) accumulation was first demonstrated by Howlett [47, 48]. In 1988 the same group characterized CB1, receptor needed for cannabinoids to mediate their action [49]. The cannabinoid receptor, CB1, was first cloned from rat in 1990 [50] followed by the second cannabinoid receptor CB2, which was cloned in 1993 [51]

The two different cannabinoid receptors CB1 and CB2 belong to G Protein Coupled Receptors (GPCRs), The largest family of cell surface receptors responsible for transducing signals from the outside to the inside of the cell. GPCRs are divided into 6 classes (A-F) based mainly on sequence homology and functional similarity. The largest and most studied class is the rhodopsin-like class A. This class, which includes rhodopsins, adrenergic, and cannabinoid receptors [52], is characterized by a heptahelical arrangement of membrane spanning α – helical transmembrane domains (TMDs). They are connected by intervening three extracellular loops (EC1-EC3) preceded by Extracellular amino terminal (N terminus) and three intracellular loops (IC1-IC3). TM7 followed directly by intracellular cytoplasmic H8 and a carboxyl terminus (C- terminus).

The 7TM bundle also known by highly conserved motifs that are characteristic of GPCRs. These include the S(N)LAXAD in TM2, the E/DRY motif in TM3, the WX(9)P in TM4, the CWXP in TM6 and the NPXXY motif in TM7 [53,54]. It was found that human CB1 receptors are composed of 472 amino acids and those in rats are 473 amino acids long [50] (Fig. 4). The CB2 receptor was determined to be 360 amino acids long and shares 44% of its overall sequence with the CB1 receptor, with 68% similarity through the transmembrane domains [51].

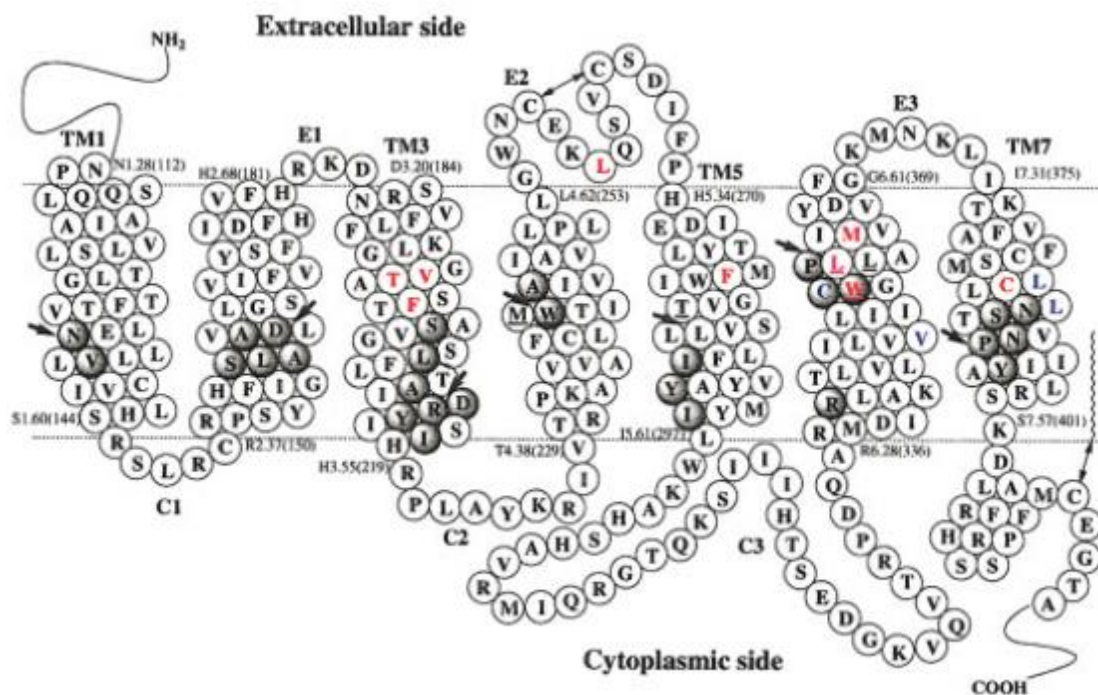


Figure 4. Schematic representation of rat CB1 with three extracellular loops E1 – E3 and three intracellular loops C1 - C3, extracellular N-terminus, transmembrane α helix TM1 – TM7 and intracellular C-terminus ended with helical segment H8 and palmitoylation site on Cys residue denoted to by two sided arrows. Shaded circles marked the highly conserved residues while the arrows denote the most highly conserved residues of each helix. A conserved disulfide bridge Cys – Cys residues on E2 loop marked also by two sided arrows. (From Shim et al., [54]).

1.3.4 GPCR receptors life cycle

It seems that GPCRs are synthesized, folded, and assembled through the endoplasmic reticulum (ER). Then migrate to Golgi complex where they subject to final modifications. After this modifications (e.g. palmitoylation methylation and glycosylation) GPCR receptors transfer to embedding themselves through the plasma membrane in inactive state. GPCR undergoing conformational changes when binding to a distinct agonist and associate G-protein to

commence downstream signaling pathways [55]. The level and duration of CB1 signaling activity is controlled by desensitization process. It first begins with phosphorylation of activated receptors by GPCR protein kinases (GRKs) blocking the receptor from binding to G proteins. Phosphorylation of CB1 sets the stage for the second step, which is binding to protein β -arrestin1 and β -arrestin2 immediately [56].

The agonized CB1-arrestin complex associates with clathrin-coated pits to initiate GPCR internalization. β -arrestins also acts as scaffolds in CB1- endosome - based signaling pathways. The arrestin bound CB1 may be dephosphorylated leaving CB1 free to migrate to plasma membrane. Internalized CB1 may also traffic from endosomes to lysosomes where they are degraded [56, 57].

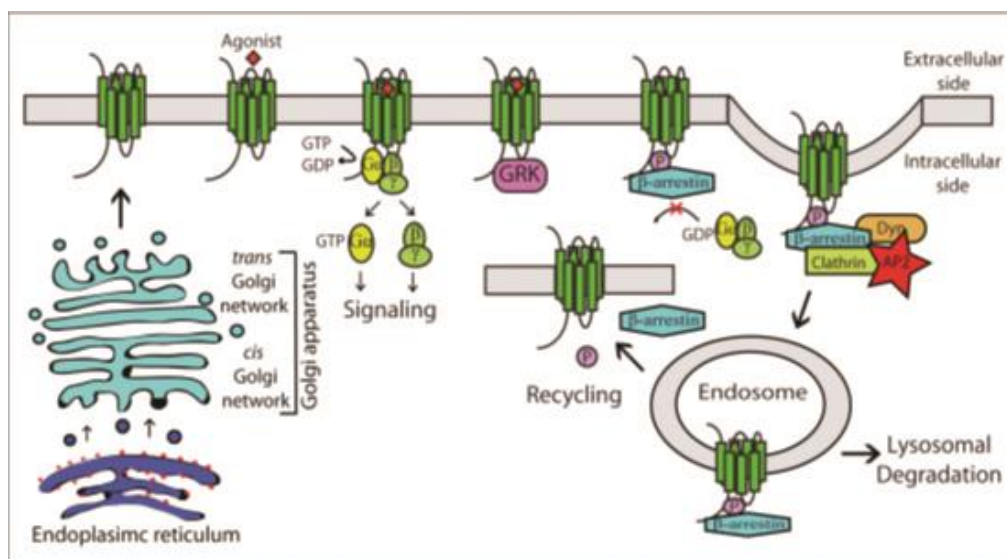


Figure 5. Model of the GPCRs life cycle. GPCRs are synthesized at the endoplasmic reticulum (ER) and sent to the Golgi complex where they are modified then transfer to the plasma membrane. Upon agonist stimulation, GPCRs bind and activate a G protein commencing downstream signaling pathways. Duration of CB1 signaling activity controlled by desensitization a process begins with phosphorylation and removal of the receptors from the cell surface (internalization) by GRK and β -arrestins proteins. Internalized receptors may targeted to lysosomes for degradation, or resensitized by recycling back to the cell surface. (Stadel et al., [55]).

1.3.5 Receptor activation states

A two-state model of GPCR activation suggested by Leff [58], a receptor can exist in two states, the fully active state R^* and the inactive state R . Both states, R^* and R , are in dynamic equilibrium. The different states of the receptor can be stabilized according to the

pharmacophoric features of the ligand binding to the receptor. Agonists can alter the equilibrium to the active state R^* , while the antagonists alter the equilibrium to the inactive state R [59]. Most GPCRs possess some degrees of constitutive activity R' (a basal level of activation in the absence of any endogenous or exogenous agonist) so, we can look at the Inverse agonists as ligands that decrease the level of receptor activation below basal levels and suppress signal transduction [60]. Neutral antagonists bind to the receptor keeping the basal levels without stimulating or inhibiting the receptor, they occupy the binding sites and can prevent other ligands from binding to the receptor. Full agonists induce the maximal possible level of activation, while partial and weak partial agonists activate the receptor above basal levels but not maximally, they cannot elicit full activity even at saturating concentrations [61]. This observation led to adaptation of the model of GPCR two state activation to suite multiple activation states [62] with distinguishing biochemical characteristics, including extent and selectivity of promiscuous G protein coupling and arrestins for signaling.

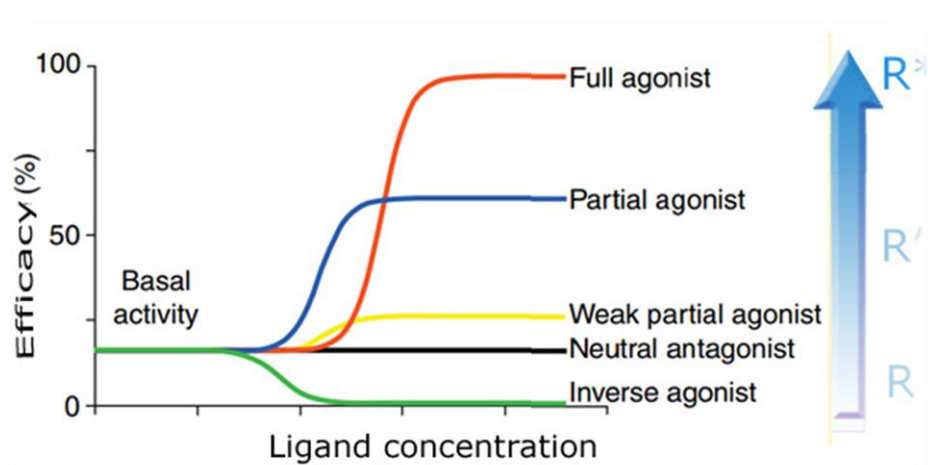


Figure 6. GPCR activation states. Full agonists promote the maximum active R^* state of the receptor and enhance the biological activity and signal transduction of the receptor while inverse agonists decrease the level of receptor activation below R' levels and suppress signal transduction. Antagonists bind the orthosteric site competitively but do not alter the equilibrium of R and R^* and do not directly affect signal transduction levels. (Tat, [60]).

1.3.6 CB1 receptors tissues distribution

CB1 receptors are found in rat and human brain tissues predominantly in the central and peripheral nervous system [50], where they mediate presynaptic inhibition of transmitter release that include acetylcholine, noradrenaline, dopamine, 5-hydroxytryptamine, g-aminobutyric acid, glutamate, D-aspartate and cholecystokinin [52,63].

CB1 has been expressed with a high level in cerebral cortex, hippocampus, basal ganglia, and cerebellum, less abundant in hypothalamus and spinal cord, and very low level in the brainstem [52, 64]. However, it has also been identified in a number of peripheral organs and tissues with a lower level than in the central and peripheral nervous system .It is found in heart, kidney, colon, pancreas, spleen, placenta and liver [65]. It can also expressed in gastrointestinal tract, adipose tissue, thyroid, adrenals, skeletal muscle, hepatocytes, and reproductive organs and endocrine cells of the pancreas [66, 67].

The CB1 receptor along with its agonist and antagonist cannabinoids are a valuable therapeutic target for a number of disorders. including neurodegenerative diseases , cancer, neuropathic and inflammatory pain, obesity [68] treatment of anorexia in patients who suffer from AIDS wasting syndrome, reducing nausea and vomiting associated with chemotherapy treatment [69], and relief of neuropathic pain in multiple sclerosis [70]. Their activation can affect processes such as cognition and memory, alter the control of motor coordination, and induce signs of analgesia, autonomic function and sensation [71].

Cannabinoid drugs produce a “tetrad” of characteristic pharmacological effects: antinociception, hypothermia, a decrease in general mobility (sedation), and catalepsy, these combinations of pharmacological side effects have been accepted as a screening procedure [72]. The CB1-selective antagonist SR141716 was able to block the unwanted effects of most cannabinoid drugs in the mouse tetrad model [73, 74].

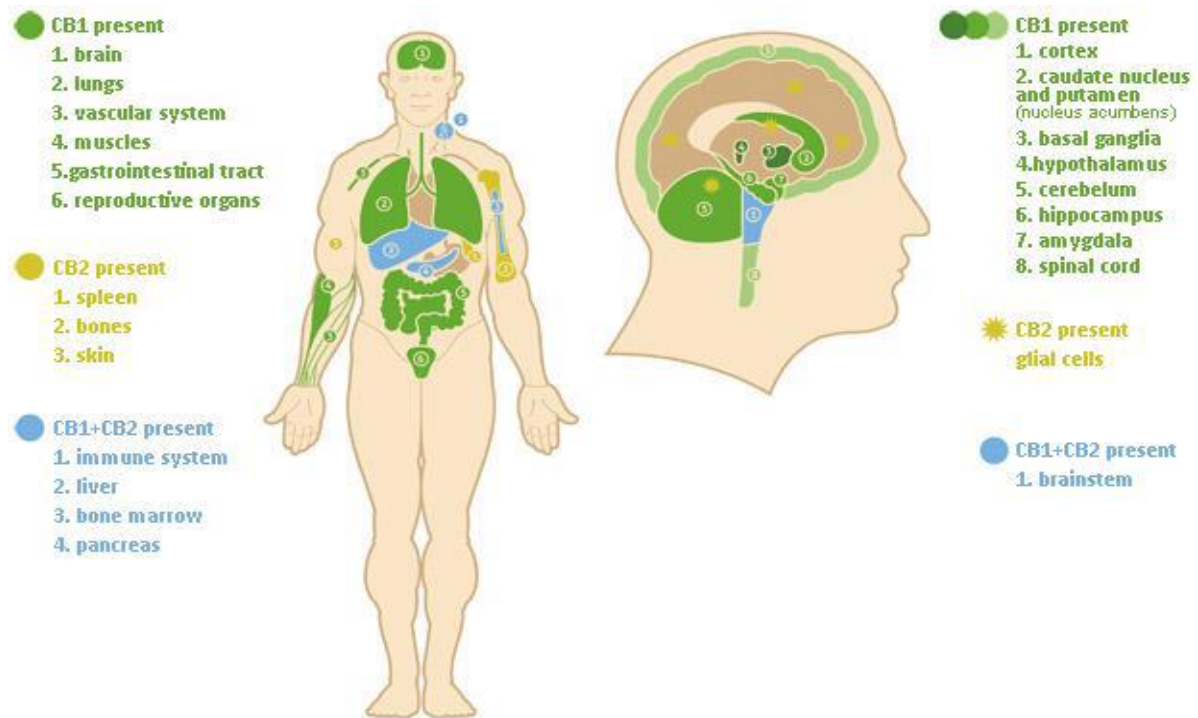


Figure 7. Tissue distribution of the human CB1 and CB2 receptors in the body [75].

1.3.7 CB1 Signal transduction

CB1 receptor when activated, couples to the inhibitory Gi/o proteins. The activation of these inhibitory G-proteins by CB1 linked to the inhibition of adenylatecyclase .The enzyme responsible for synthesizing cAMP production from ATP. That leads to decrease of cAMP accumulation. The cAMP acts as a cellular secondary messenger andmediates processes including the metabolism of glycogen, sugar and lipids [47, 48]. However, in certain circumstances, CB1R can couple to Gs proteins. , It has been reported that in pertussis-pretreated cells, CB1R stimulation leads to adenylyl cyclase activation [76, 77]. The ability of cannabinoids to modulate cellular levels of cAMP has been demonstrated to regulate many aspects of cellular function, such as the contractile activity of smooth muscle, the gating properties of ion channels on neuronal cell [78]. CB1receptor couples predominantly through Gi/o proteins to certain subtypes of voltage-gatedcalcium (Ca²⁺) channels associated with the inhibition of N, P/Q and L-types voltage-dependent (Ca²⁺) channels [79] and activation of A-subtype and inward-rectifying K⁺ channels [80,81]. Cannabinoids suppress neuronal excitability and play a role in regulating neurotransmitter release [82].

CB1 activation may also stimulate mitogen-activated protein kinase (MAPK). The (MAPK) pathways can regulate cell proliferation, cell differentiation, cell movement and cell death [83]. MAPK cascades include pathways leading to activate ERK1/2 [84], c-Jun N-terminal kinase (JNK), p38 MAPK [85, 86], and (PI3K) phosphatidylinositol 3-kinase [87].

CB1 receptor-mediate production and release of NO from endothelial and neuronal cells. CB1 stimulation of NO-sensitive guanylylcyclase leads to increasing of cyclic GMP production [88, 89]. NO is synthesized in most biological tissues and it involves in several biological functions including neurotransmission, vasodilatation and macrophage function [90].

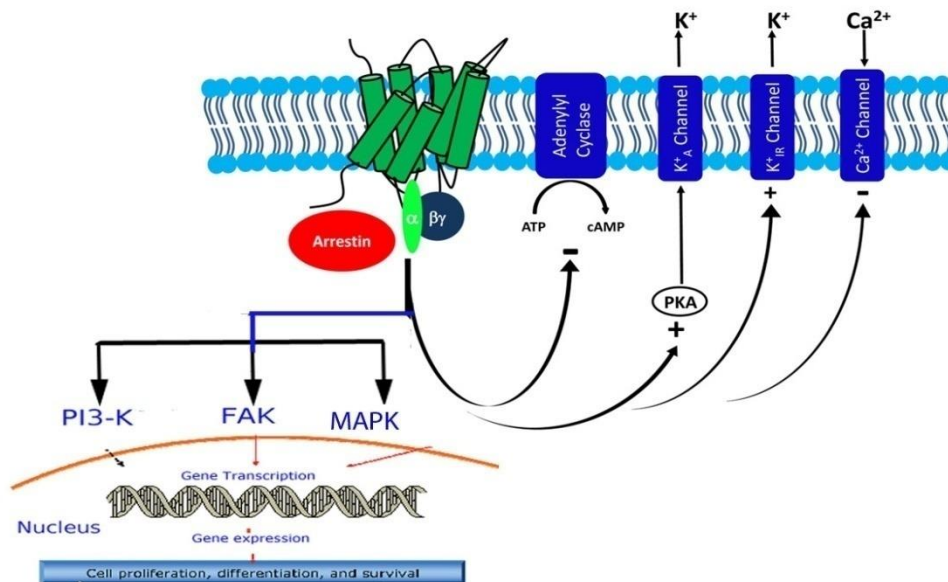


Figure 8. Model of CB1 signal transduction. On stimuli CB1 associates to heterotrimeric G-protein results in a release of (α - $\beta\gamma$) subunits of G- protein, which have a negative impact on cellular production of cAMP, activates K^+_A and K^+_{IR} channels, and inhibits Ca^{2+} channels. It can also recruit β -arrestin to the plasma membrane. When stimulated, CB1 can activate MAPK, phosphatidylinositol 3-kinase, and FAK, among other pathways. (Modified from [65]).

1.3.8 CB1 receptor agonists

CB1 receptor agonists can be divided into five different groups: Classical cannabinoids, Non-classical cannabinoids, aminoalkylindole cannabinoid, and eicosanoid cannabinoids that related to endocannabinoids and miscellaneous compounds “Hybrid ligands” [52, 91].

Classical cannabinoids are ABC - tricyclic terpenoid derivatives bearing a benzopyran moiety. They are insoluble in water but soluble in lipids, alcohols, and other nonpolar organic solvents. (Δ^9 -THC) Δ^9 -tetrahydrocannabinol the prototype of the classical cannabinoid agonists is the main constituents of the plant *cannabis sativa*, this phytocannabinoid agonist which was known by its psychoactive effects long before discovery of CB1/CB2 receptors. Δ^9 -THC exhibit low affinity for both receptors and acts as partial agonist. Other pharmacologically active constituents of the plant *cannabis sativa* is (-)- Δ^8 -THC (*cannabinol*. [92]).

HU-210 is a synthetic analogue produced by replacing the pentyl side chain of Δ^8 -THC with a dimethylheptyl side chain. It is developed by Mechoulam to work as a radioligand labeled probe binding to cannabinoid receptors [93]. It has a high affinity for both CB1 and CB2 receptors. It also displays high potency and acts as a cannabinoid receptor agonist and exhibits a long term of action in vivo [24].

Non classical agonists consist of bicyclic and tricyclic analogues that are biological mimetic of Δ^9 -THC, identified by lack of the pyran ring of Δ^9 -THC. They are represented by CP55, 940 developed by Pfizer [94]. The [3H]CP55, 940 exhibits high affinity and efficacy for both CB1 and CB2 receptors and acts as a standard research tool for probing the cannabinoid receptors, used as a key radioligand to identify CB1 receptor [49]. CP55244 and HU-308 are examples for this class. They are closely related to the classical cannabinoids.

Aminoalkylindoles structure, from the pharmacophoric point of view may have a three-point attachments i) the morpholinoethyl group ii) the carbonyl group iii) the naphthalene ring at the C7 position[95]. The morpholinoethyl group or another cyclic structure was required for binding and exert activity of aminoalkylindoles [96]. Aminoalkylindoles represented by WIN55, 212-2, it is important research tool for investigation of the endocannabinoid system. Its potential as non-steroidal anti-inflammatory agent showing a 7-fold difference in potency for hypomotility *versus* potency for antinociception and hypothermia [97] with a higher affinity for (CB2) receptors than for CB1 receptors in the brain ($K_i = 1.89$ nM (CB1) and 0.28 nM (CB2), [98]).

Eicosanoids, since the discovery of endogenous cannabinoids especially anandamide and 2AG, discussed earlier. Several eicosanoid analogs have been developed. Anandamide has

considered a template for the modification of CB1 agonists for eicosanoid compounds [99,100]. The modification of a polar ethanolamido head group of anandamide produce several CB1 agonists. The (*R*)-Methanandamide is similar to anandamide except for a methyl group added to the 1' carbon [101].

The importance of this compound came from its ability to resist the anandamide hydrolysis by amidohydrolase. Its enzymatic resistance and relatively high potency, 4 folds higher than anandamide, make it effective biological tool with selectivity for the CB1 receptor [102]. The modification of anandamide head group by substitution of chloro or fluoro group instead of 2-hydroxyl group resulted ACEA (AM881) and (O-585) ligands respectively. Both ligands are CB1 selective and exhibit high affinity and efficacy [88, 99].

Hybrid cannabinoids resulted from the combination of classical and non-classical cannabinoids structural features. The modification of The Southern aliphatic hydroxyl (SAH) pharmacophore have been developed to produce novel analogs [103-105]. The β -hydroxypropyl analogue is a good representative for this class. It has a higher affinity than the α -axial epimer.

1.3.9 Cannabinoid antagonists – inverseagonists

Most Endocannabinoid antagonists or inverseagonists are diarylpyrazole compounds. The selective CB1 receptor antagonist SR141716A (Rimonabant) was developed by Sanofi [74,107]. It is used in medicinal treatment for a number of disorders such as Alzheimer's disease, schizophrenia and obesity [106]. It binds selectively to CB1 receptor with a very high potency. SR141716A has the ability to block or reverse the effects induced by cannabinoid agonists at CB1 receptors, both in vitro and in vivo [52,108]. Structural analogues of SR141716A have been developed, AM251 and AM281 are both selective to CB1 receptor with lower affinity than SR141716A [109]. They are able to displacing [3H] SR141716A and [3H] CP-55,940 in CB1 receptor membrane preparations and they can block or reverse the effects induced by cannabinoid agonists at CB1 receptors [110,111].

Another CB1 receptor selective antagonist LY320135 developed by Eli Lilly, it is less potent than SR141716A and exhibit inverse agonist for CB1 receptor [112].

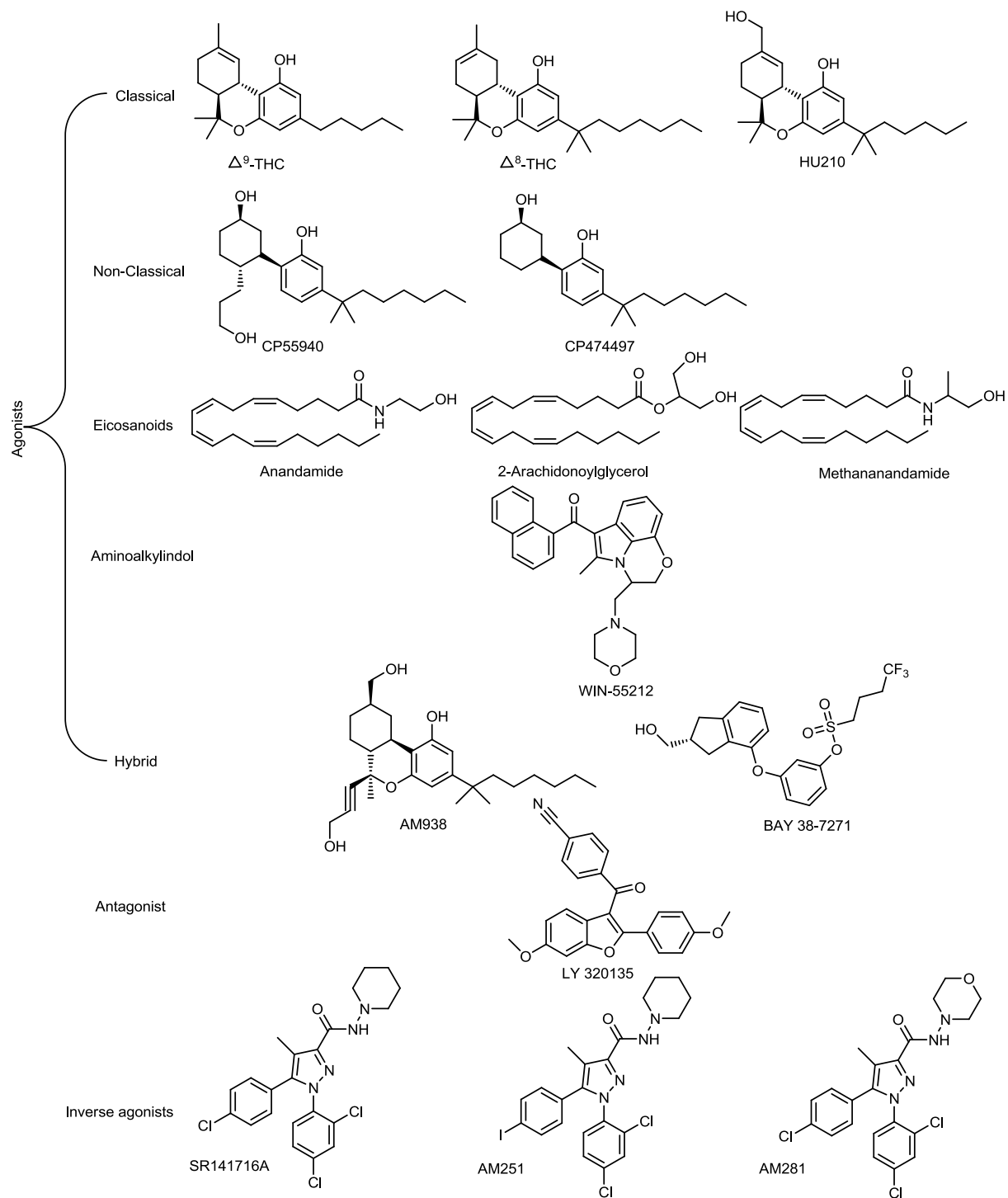


Figure 9. The structures of several CB1- cannabinoid ligands [22].

1.3.10 Allosteric modulation

In 1963, “Monod, Changeux and François Jacob on *‘allosteric proteins and cellular control systems’*” noticed, In the field of enzymology, that the chemical structure of inhibitors was often very different from the substrate of the enzyme suggesting another binding site referred to as “allosteric site” accommodated these inhibitors through which they transmitted their effect to the substrate site [113]. According to this concept, the activity of a receptor can be modulated by ligands that bind to allosteric sites – sites which are located away from the orthosteric sites and does not exhibit any overlap with the orthosteric site. The binding of a ligand to allosteric site can alter the receptor conformation, thereby either enhancing (positive allosteric modulator, PAM) or slowing (negative allosteric modulator, NAM) the interactions carried out at the orthosteric site [114,115]. Allosteric ligands have several advantages over orthosteric ligands. Probe dependant which mean that allosteric modulators exert their effects only in the presence of orthosteric ligands and thereby we can look at them as fine tuners. Additional advantage of allosteric modulator is their saturable effects which known as “ceiling-effect” and no more amount of allosteric ligand can affect orthosteric / allosteric ligands cooperativity [116].

This advantage enabled the allosteric modulators to avoid the harmful and unwanted physiological side effects of the orthosteric agonists [117]. Toxicity, desensitization, long-term changes in receptor up/down regulation and psychoactivity can be adjusted by allosteric modulators that have the potential to overcome these negative effects [114].

Functional assays along with kinetic association and dissociation assays of the (radio) ligand-receptor interaction are often used to determine an allosteric ligand potentiality [115]. The binding of an allosteric ligand induces a conformational changes in the receptor, thereby altering the rates at which the orthosteric ligand associates or dissociates from its binding site [118]. The need to describe different interactions of receptor – ligand have been met by Several mathematical models. One of the first and most simple models is the allosteric two-state model ATSM also known as cubic ternary complex.

1.3.11 Allosteric Modulators of the CB1 Receptors

Allosteric ligands that modulate CB1 Receptor have been developed soon after identifying CB1 allosteric sites. Org 27569 the prototype of allosteric ligands exhibits interesting effects on CB1, it increases the affinity and decreases the efficacy of CB1 agonists, [117,119], by blocking the agonist-induced conformational change at TM6. Org 27569 traps the receptor in a distinct agonist-bound, but inhibiting conformational changes required for receptor signaling [120]. 1-(4-Chlorophenyl)-3-[3-(6-pyrrolidin-1-ylpyridin-2-yl) phenyl] urea (PSNCBAM-1) [121] is another allosteric modulator type for CB1. These compounds modulate electrically evoked contractions in the mouse *vas deferens* [117], affects CB1 ligand modulation of synaptic transmission [122] and have hypophagic effects *in vivo* [121]. They display a contradictory pharmacological profile increasing the specific binding of the CB1 receptor agonist [³H] CP55940 but producing a concentration-related decrease in CB1 receptor agonist efficacy. The 3b-(4-methylphenyl)-2b-[3-(4-chlorophenyl)isoxazol-5-yl]tropane (RTI-371) is the positive CB1 allosteric modulator has been discovered by the way, when Navarro and his colleagues were searching for treatment of cocaine addiction investigating indirect dopamine agonists, they noticed that RTI-371 blocks cocaine-induced locomotor stimulation. They subject this compound for screening through functional assays for activity at other CNS receptors. They demonstrated that RTI-371 is a positive allosteric modulator of the human CB1 receptor. Other DAT-selective inhibitors on CP55940-stimulated calcium mobilization was characterized in a calcium mobilization-based functional assay for the *hCB1* receptor [123]. Recently, a new allosteric modulator (Lipoxin A4) has been identified [6, 7] which will be discussed in more details.

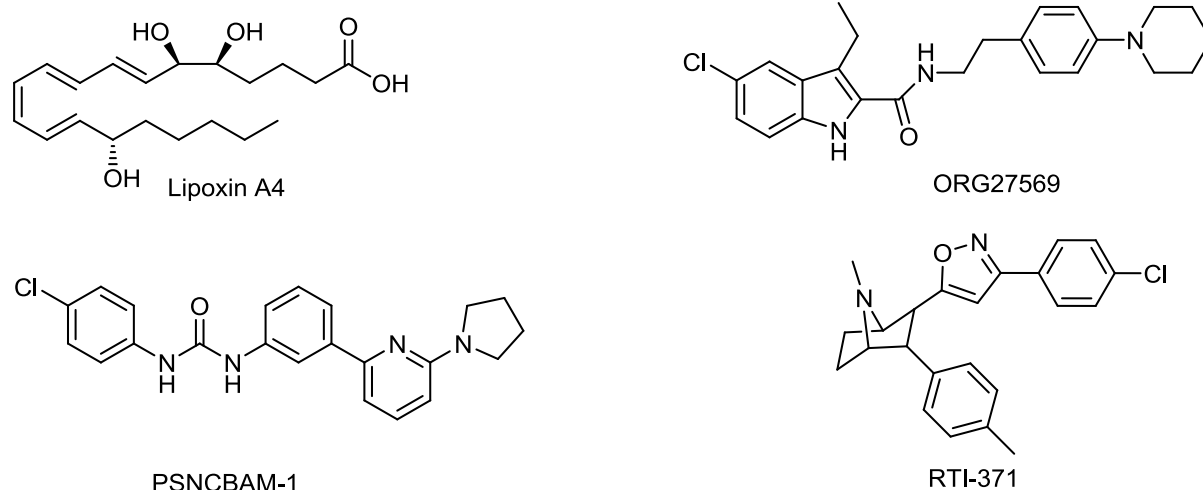


Figure 10. Chemical structure of representatives for CB1 allosteric modulators.

1.3.12 Lipoxin A4 is an endogenous allosteric ligand for CB1

Lipoxins are trihydroxy-eicosatetraenoic acids, derived from arachidonic acid with the four double bonds in conjugation, which were the first lipid mediators to be discovered that were involved in the resolution phase of inflammation. There are at least three routes to the biosynthesis of lipoxins through cell-cell interactions when distinct types of cells are in close proximity during inflammatory responses. The two enzymes lipoxygenase (LO) and cyclooxygenase (COX)-2 have a crucial role in lipoxins biosynthesis [124,125]. One of the recognized mechanisms of lipoxins biosynthesis is catalyzing arachidonic acid into 15S-hydroxyeicosatetraenoic acid (15S-HETE) by lipoxygenase (15-LO) via Monocytes, eosinophils, and airway-epithelial cells. 15S-HETE is rapidly taken up by neutrophils and converted to lipoxin A4 by a 5-LO-catalyzed reaction [124].

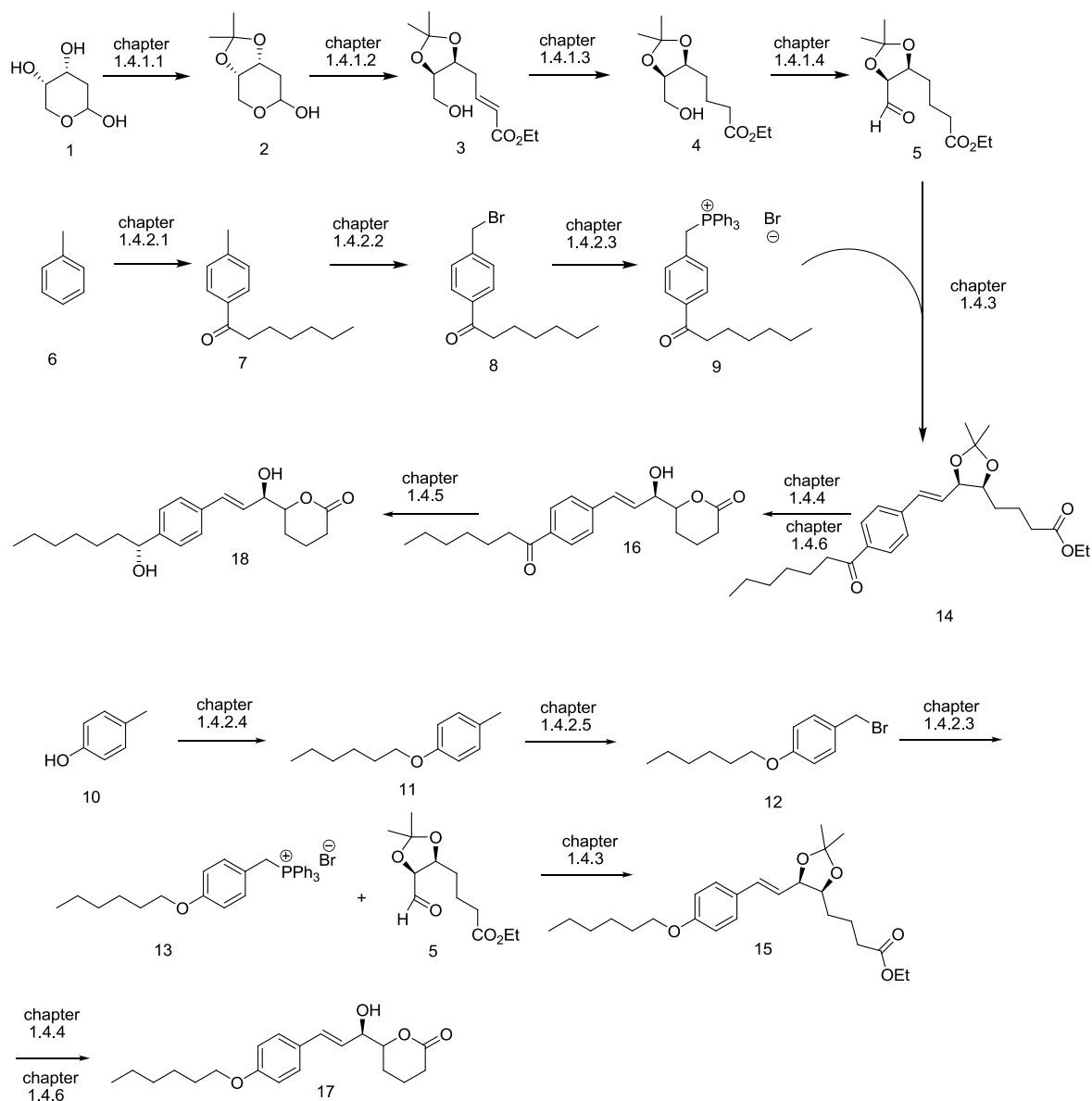
The second pathway goes through the vasculature that activates 5-LO, present in myeloid cells, [126] to produce leukotriene A4 (LTA4) and then converted to lipoxins by 12-LO, which is present in platelets. This process is determined by cell-cell interaction [127]. The third important route is known by the aspirin-triggered 15-epi-LX (ATLs) pathway. The reaction is initiated by aspirin to acetylate the cyclooxygenase COX-2, in the stimulated endothelial and epithelial cells, altering the catalytic activity of the enzyme to produce 15R-HETE in lieu of prostanoid biosynthesis. The 15R-HETE is released from endothelial and epithelial cells and converted to 15-epimer lipoxins (aspirin-triggered lipoxins or ATL) via leukocyte 5-LO enzyme

[128]. The 15-epimer lipoxins possess most of the parent lipoxins biological features added to its higher potency and efficacy [129]. Lipoxins can serve for pro – resolution of inflammation and acts as endogenous mediator that is anti-inflammatory agent. Lipoxins exhibit vasodilatory and counter regulatory roles in vivo and in vitro models. Lipoxins promote vasorelaxation and relax the aorta and pulmonary arteries [130,131].

Lipoxin A4 is an endogenous agonist binding with high affinity to (ALXR) receptors, also known as formyl peptide receptor2 (FPR2), where display anti-inflammatory and antioxidant activities [1-3]. LXA4 also shows partial agonist activity on binding with cysteinyl leukotriene receptors 1 and 2 [3, 4]. LXA4 can suppress cytokine signaling² when binding to nuclear receptor aryl hydrocarbon [5]. Furthermore, LipoxinA4 interacts with CB1 receptor and exhibits positive allosteric modulation [6, 7]. LXA4 involved in modulation of several inflammatory disorders such as pain, arthritis, asthma and ischemia [8-10,132].

1.4 CHEMICAL BACKGROUND TOWARD THE SYNTHESIS OF LXA4 ANALOGUES

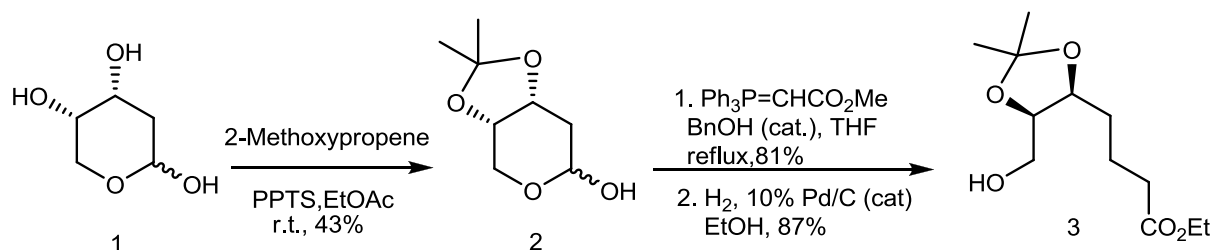
Based on the retro synthesis study (Scheme 1) we were able to design the forward synthesis. This part of the introduction includes an overview on the methodology applied in order to obtain the desired analogues. Furthermore, it discusses the theory behind the reactions by discussing the proposed mechanism of each reaction.



Scheme 2. Forward synthesis of the designed reaction sequence

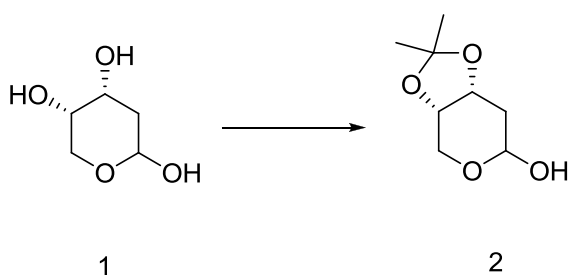
1.4.1 Preparing the aldehyde from the sugar

This part of the synthesis was based on the strategy postulated earlier by Philips ED et al. as shown (scheme 3). Minor modifications were applied on the same strategy in order to obtain the intermediate **3**. Different strategy was applied in this thesis starting from intermediate **3** until the key intermediate **5** (section 1.4.1.4).



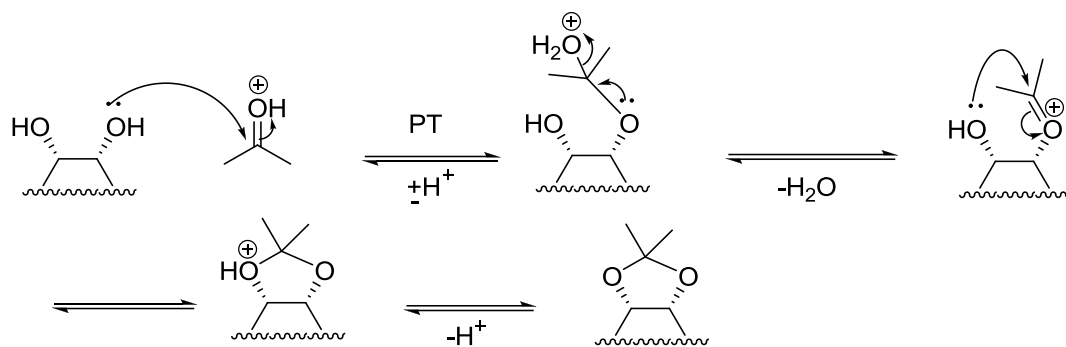
Scheme 3. Earlier synthetic research on the key intermediate

1.4.1.1 1, 2-diol protection of the 2-deoxy-D-ribose.



Scheme 4. Protection of 2-deoxy-D-ribose

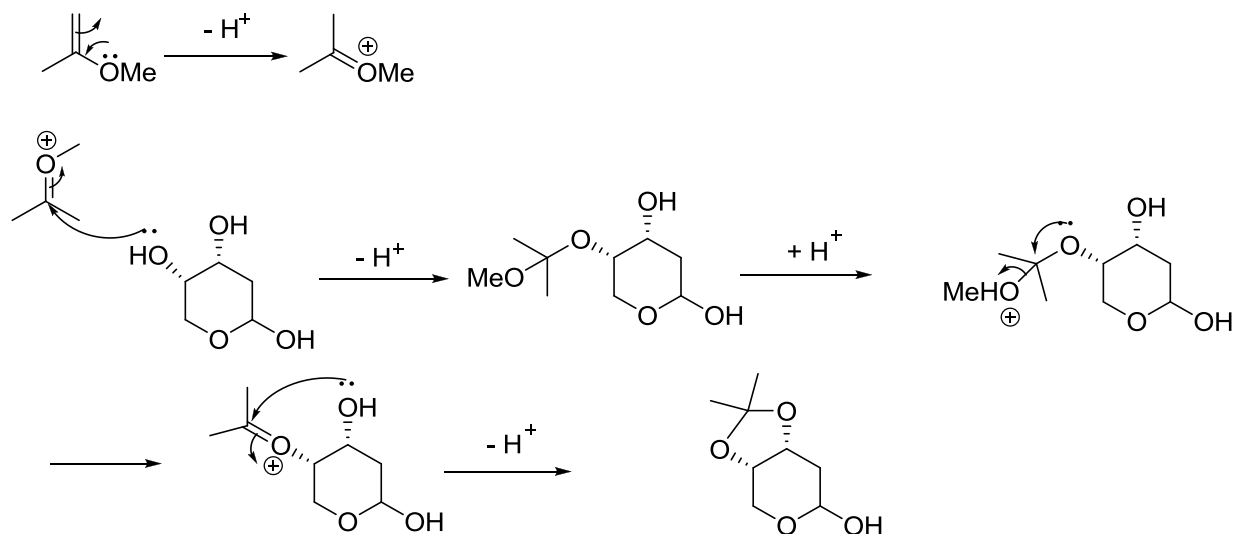
There are many protecting groups that show great efficiency in protecting alcohols as trialkylsilyl (R_3Si), tetrahydropyranyl (THP), benzyl ether (OBn) and they are used in different conditions. In this case we are dealing with the protection of a 1, 2-diol system (two adjacent hydroxyl groups). This kind of protection could be performed by making an acetals from these two adjacent hydroxyl groups. The acetal formation reactions are a reversible process and includes several proton transfer (Scheme 5).



Scheme 5. General mechanism of acetal formation

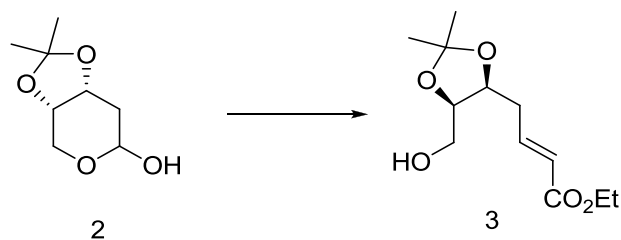
In this reaction 2-methoxypropene was the protecting agent for the 1, 2-diol system in a reaction of acetonide formation. 2-methoxypropene is an electron rich used in the monoprotection of several groups, such as alcohols of different types like aliphatic and allylic alcohols, peroxides, cyanohydrins, alpha hydroxyl ketones , 1,2 diols and 1,3 diols. In addition, it is used in other applications such as formation of 2-methoxyallyl halides and substituted furans its participation in pericyclic reactions [133]. Acetonide formation proceed when the lone pair of the hydroxyl group act as a nucleophile and attack the electrophile, which expressed in the protecting group. This leads to the formation of a new O-C bond between both of them, in a process of proton transfer leads to some resonance movement. As a result a new electron rich position which is the formed carbonyl group with a positive charge on the oxygen after the removal of methanol fraction from the compound. The lone pair on the other alcohol partner will have the tendency to attack on this carbonyl group completing the protection reaction after another deprotonation step [134].

Mechanism



Scheme 6. Mechanism of acetonide formation

1.4.1.2 Wittig reaction of the protected sugar.



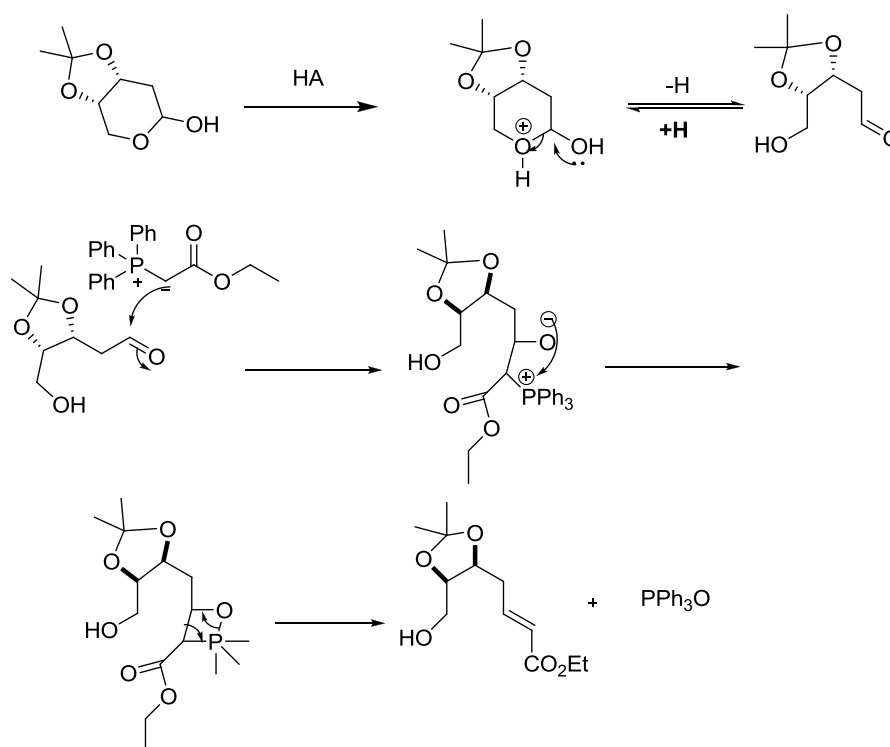
Scheme 7. Synthesis of the unsaturated alcohol

Wittig reaction is one of the common reactions known for replacing the carbonyl group ($\text{C}=\text{O}$) with an alkene group ($\text{C}=\text{C}$). In general, the reaction is based on the nucleophilic attack on the carbonyl group (electrophile) by the carbanion part of the phosphonium ylid.

Consequently, negative charge on the aldehydic oxygen is formed. The negative charge will attack the phosphorus positive charge, giving rise to four membered ring transition state called oxaphosphetane, which cleaves forming the desired alkene with triphenylphosphine oxide as by product (scheme 8). The phosphonium ylid is originally formed from the deprotonation of the phosphonium salt, which can be readily synthesized in a reaction between triphenyl phosphine and an alkyl halide. Opening the acetal is required to reveal the carbonyl group. This is done by a simple process of proton transfer. Where the lone pair of the ether receives a

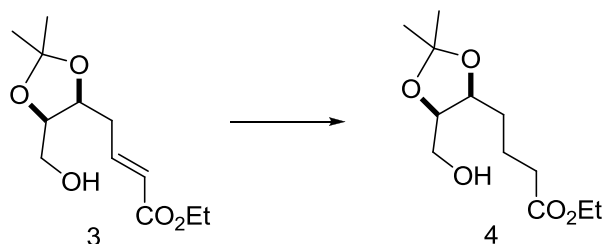
proton from the benzoic acid, forming a positive charge on the oxygen. This will push the lone pair of the alcoholic oxygen to make a resonance movement in order to open the pyran ring. The alcohol will be in one side and the aldehyde group on the other after removal of the proton. At this stage the Wittig reaction could proceed. The stereo chemistry of the resulted alkene depends on whether the ylid is stabilized or not. In case of a stabilized ylid by the presence of adjacent carbonyl group, gives the E alkene selectively. On the other hand, the unstabilized ylid forms the Z alkene selectively [135,136]. Wittig reaction is widely applied for many synthetical uses [137,138].

Mechanism



Scheme 8. Mechanism of the Wittig reaction

1.4.1.3 Reduction of the alkene.



Scheme 9. Reduction of the alcohol's bi bond

A Pd/C-catalyzed hydrogenation is one of the most common C-C double and triple bond reduction reactions. This method of hydrogenation based on the absorption of the H₂ on the surface of the metal catalyst. The H-H bond cleaves, each hydrogen attaches to the metal catalyst surface, forming metal-hydrogen bonds. In addition, the alkene itself will be absorbed on the surface of the metal catalyst. At this stage, one of the hydrogen atoms will transfer to the alkene forming a new C-H bond. The other hydrogen atom will transfer to the alkene forming another C-H as well, with the other carbon of the c-c double bond. According to the physical arrangement of the alkene and the hydrogen on the flat surface of the metal catalyst, the two hydrogen atoms pictured to be added as syn addition. It means that they both come on the same phase or the same side of the alkene [139, 140]. This metal catalyzed hydrogenation have been widely applied in many industrial and research work [141]. It is also used in the food industry to make a large variety of manufactured goods [142].

Mechanism

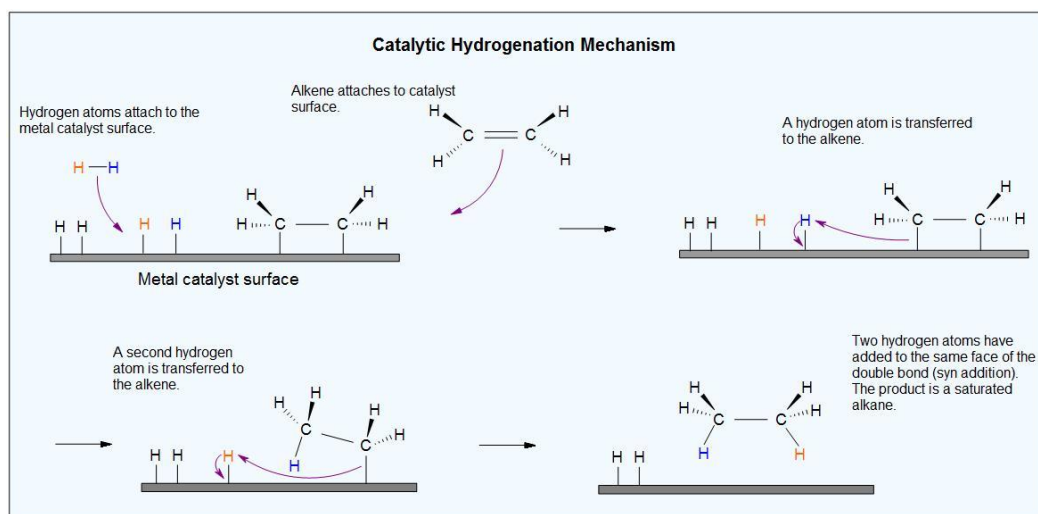
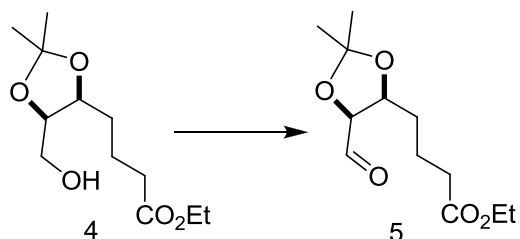


Figure 11. Catalytic hydrogenation mechanism [143].

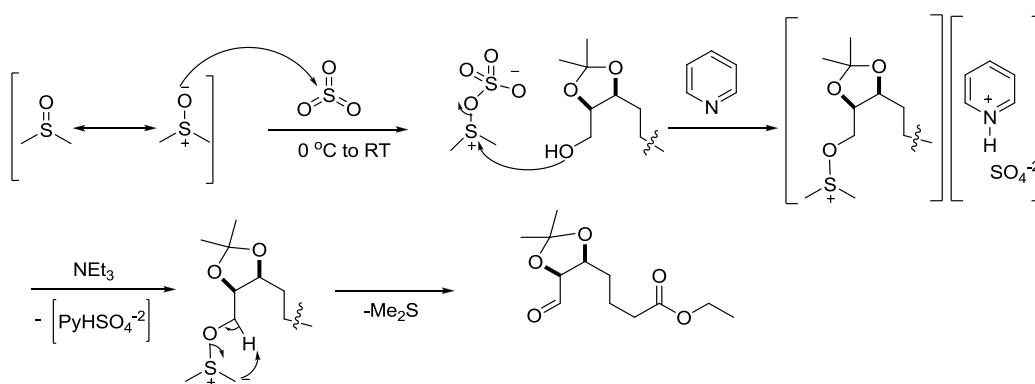
1.4.1.4 Parikh-doering oxidation



Scheme 10. Parikh-Doering oxidation of the 1° alcohol

Parikh-Doering reaction provides a mild oxidation method for primary and secondary alcohols to aldehyde and ketones respectively. This method is based on using DMSO as an oxidizing agent after being activated by sulphur trioxide pyridine complex in the presence of a base, which commonly is triethyl ether. This reaction is performed under mild conditions. The temperature of the reaction varies from 0°C to room temperature. DMSO exists in two-resonance structure it reacts with the Sulfur trioxide in its counter ion structure forming an intermediate. The lone pair of the hydroxyl group will attack this intermediate. The pyridine will then deprotonate the alcohol forming an alkoxysulfonium ion associated with the anionic pyridinium sulfate complex. The base deprotonates the alkoxysulfonium ion providing the sulfur ylid and the pyridinium sulphate counterion. This sulfur ylid goes through a five membered ring transition state before it breaks and provide the desired aldehyde or ketone according to the used alcohol type and dimethyl sulfide as a byproduct. This reaction has been used widely in many applications [144].

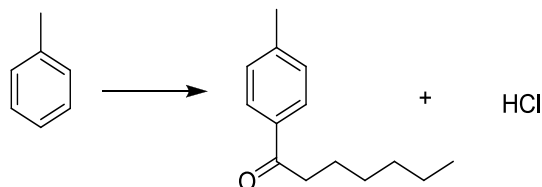
Mechanism



Scheme 11. Mechanism of Parikh-Doering oxidation.

1.4.2 Preparing of the Wittig salts

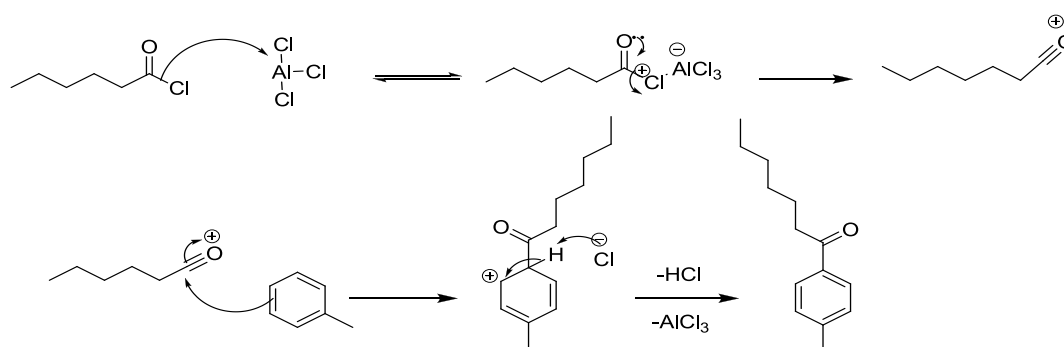
1.4.2.1 Friedel-Crafts acylation



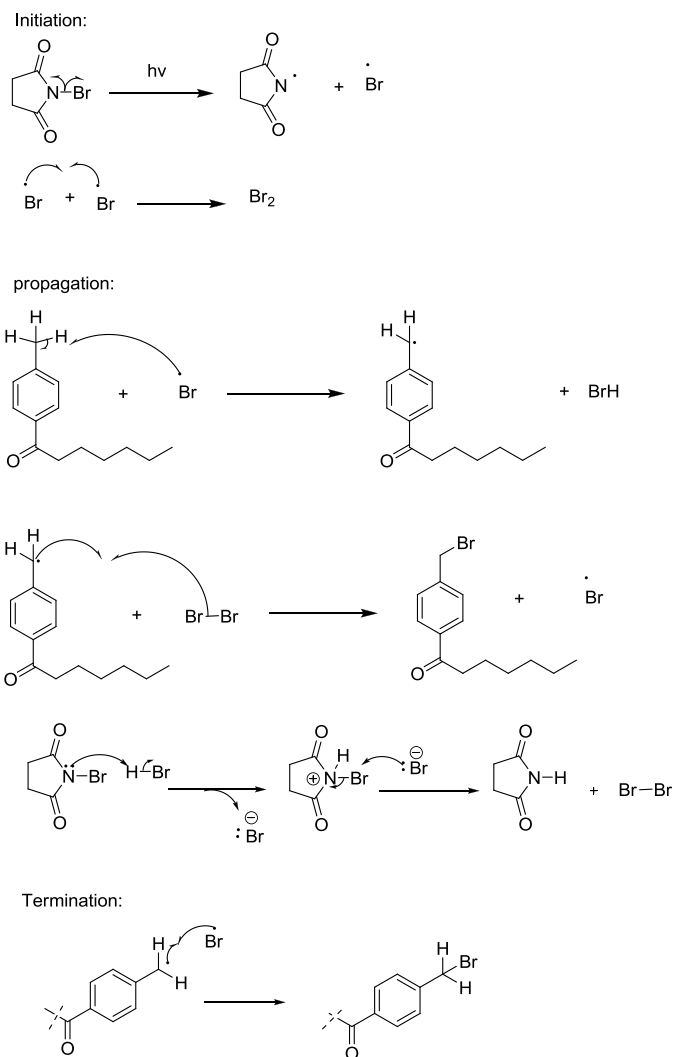
Scheme 12 . Synthesis of the acylated toluene

The reaction is a regular Friedel-Crafts acylation between toluene and heptanoyl chloride. The acylation term refers to the direct formation of compounds containing carbonyl group and attached to the aromatic system. Moreover, the formation of ketones, aldehydes, carboxylic acids, and amides [145]. The aluminum chloride removes chloride from the heptanoyl chloride forming a cation, this cation is a linear acylium ion. This linear ion is stabilized by the adjacent oxygen lone pairs. The acylium ion attacks the benzene ring at ortho and para position because of the CH_3 which acting as e.donating group and activate o, p positions of the benzene ring giving the desired aromatic ketone. Both fridel kraft acylation and alkylation reactions have been widely used in many applications for long time. For example, the acylation of polycyclic aromatic hydrocarbons such as naphthalene and anthracene [146].

Mechanism

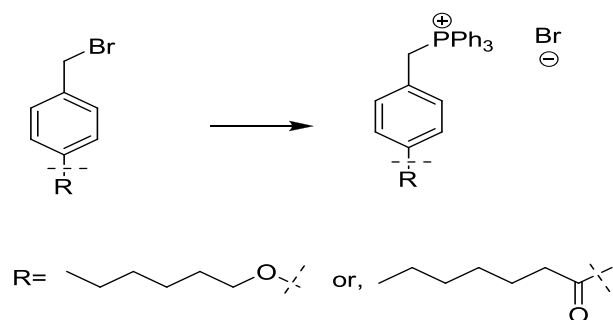


Scheme 13.Friedel-craft acylation mechanism



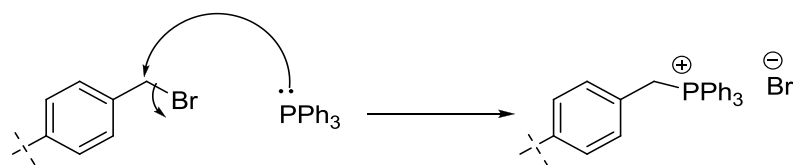
Scheme 15. Mechanism of the benzylic bromination using NBS in visible light.

1.4.2.3 Wittig salts from alkyl halides and triphenylphosphine



Scheme 16. Synthesis of the Wittig salts.

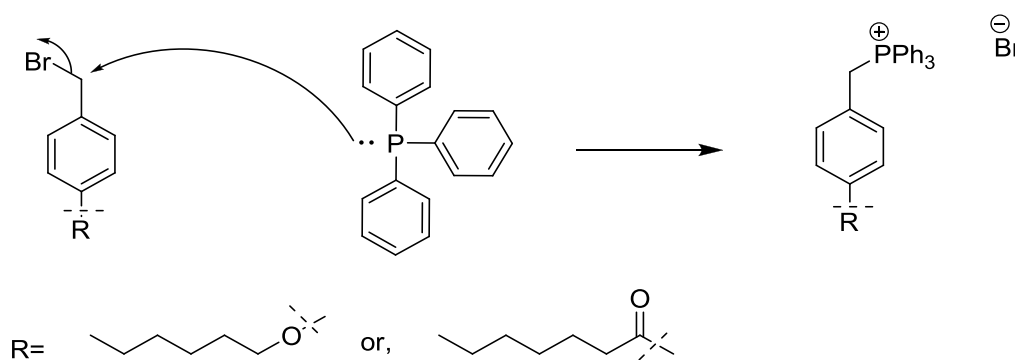
This reaction is a simple nucleophilic substitution reaction. The high-energy lone pair of the phosphorus in the triphenylphosphine reagent attacks on the electrophilic alkyl halide resulting a new C-P bond in the desired tetrahedral phosphonium salt.



Scheme 17. Nucleophilic attack by the triphenyl phosphine on the electrophilic carbon.

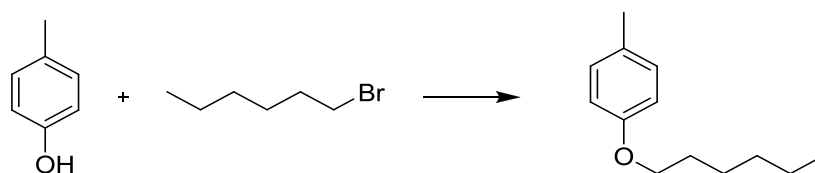
Normally this salt undergoes deprotonation by some kind of base to produce the phosphonium ylid which is the nucleophilic partner in the Wittig reaction. Phosphonium salts are widely used in Solid Phase applications [149] and as co-catalysts in different cases [150].

Mechanism:



Scheme 18. SN2 reaction mechanism

1.4.2.4 The O-alkylation of the para cresol



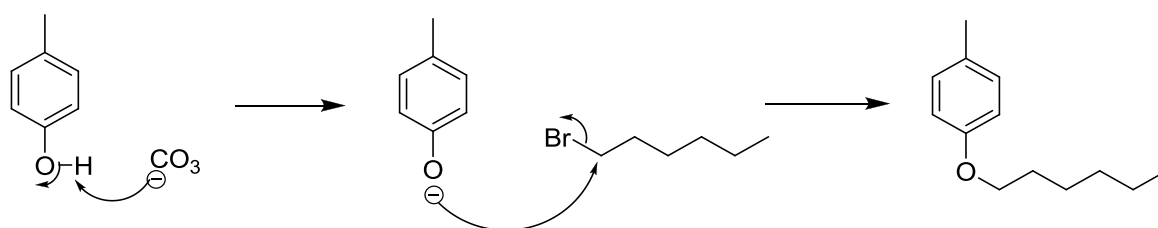
Scheme 19. O-alkylation of para cresol.

This reaction is based on the formation of the phenolate anion. When the proton of the phenolic hydroxyl group is abstracted with a base. The anion reacts with the alkyl halide to alkylate the oxygen or carbons of the aromatic ring due to the possible resonance structures (scheme 20). Although it is usual to get the O-alkylated product, but under certain conditions

it is possible to get the C-alkylated product. In this case the hydroxyl of the phenol is deprotonated by the potassium carbonate base producing the phenolate anion.

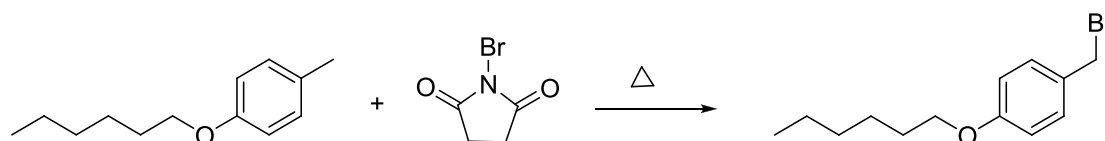
The character of aromaticity will be disturbed during the resonance to get the C-alkylated product. Therefore, the O-alkylation happens via a normal SN2 reaction between the anion and the alkyl halide.

Mechanism



Scheme 20. Benzylic o-alkylation mechanism "SN2"

1.4.2.5 Benzylic bromination "Thermal Approach"

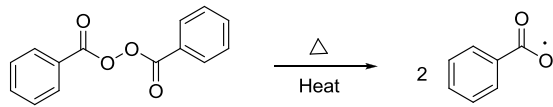


Scheme 21. Benzylic bromination.

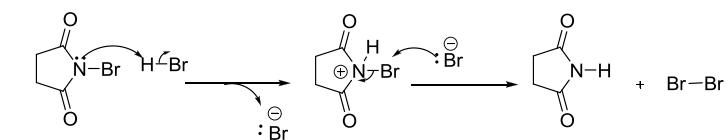
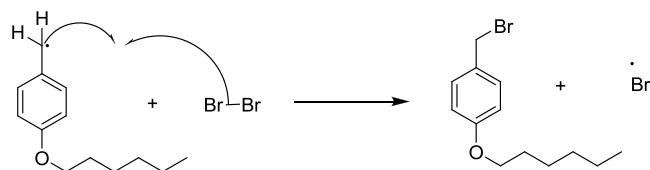
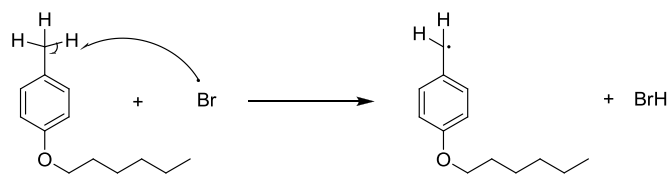
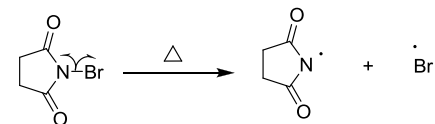
This reaction is another approach for the benzylic bromination by NBS under heating instead of the visible light in presence of benzoyl peroxide as radical initiator. The reaction is considered to have the same degree of regioselectivity as it was mentioned earlier in the visible light case (section 1.4.2.2). Free radical formation by the homogenous cleavage of the N-Br bond was triggered in this case because of the heat and benzoyl peroxide, which is the radical initiator. The Br free radical will abstract a hydrogen from the other molecule leaving a free radical in its place. This free radical will bind with another Br free radical forming the desired benzyl bromide [151].

Mechanism:

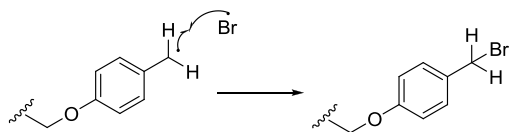
Initiation:



propagation:

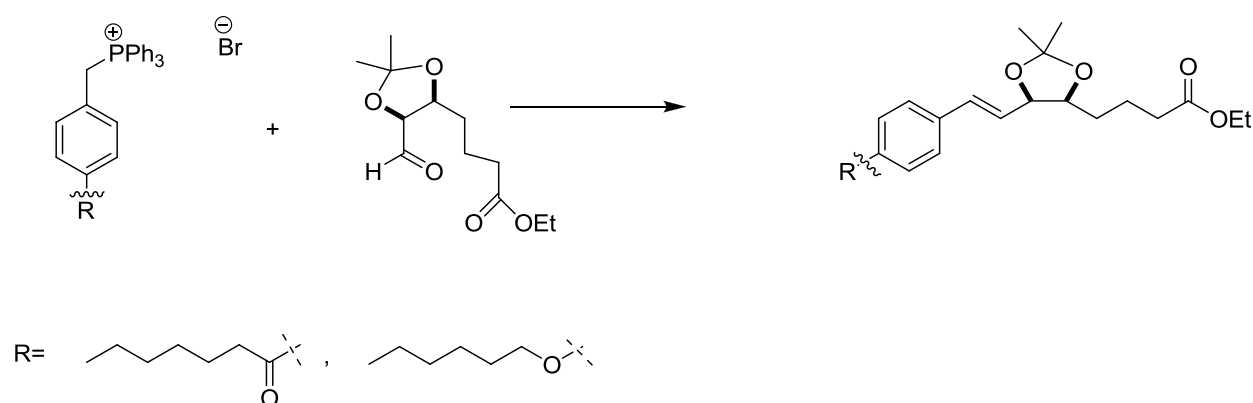


Termination:



Scheme 22. Mechanism of the benzylic bromination by NBS.

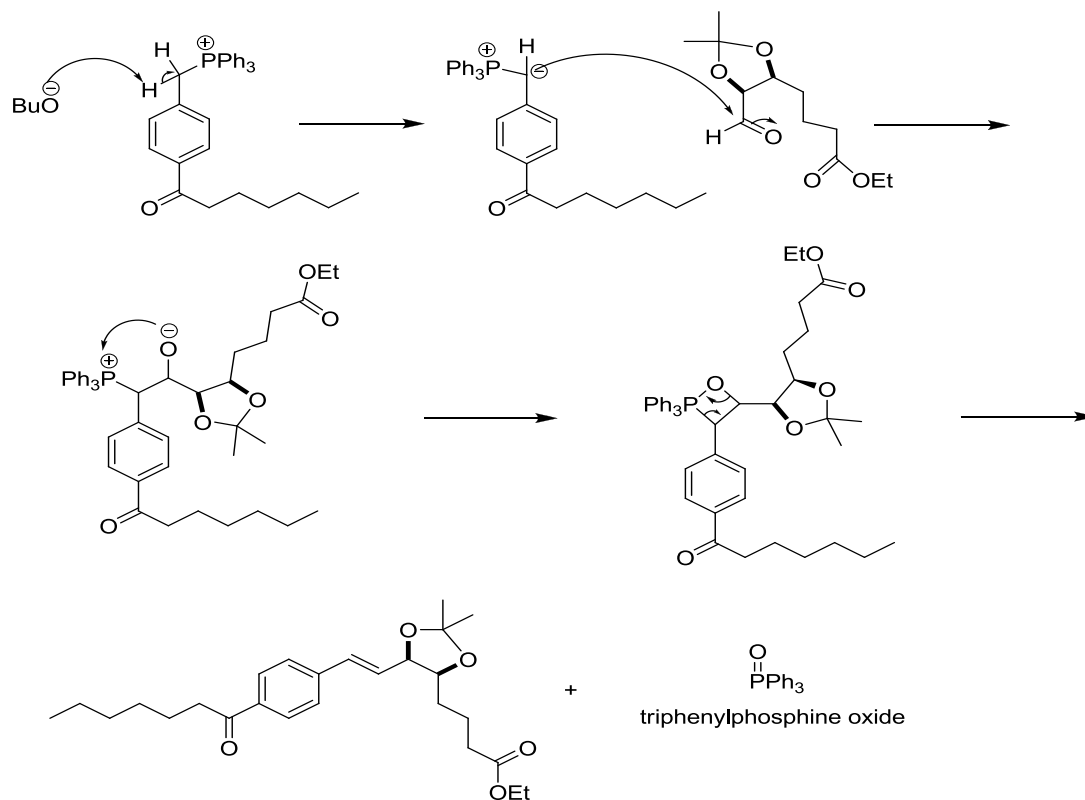
1.4.3 Wittig reaction



Scheme 23. Wittig reaction of the ylid and the aldehyde.

Wittig reaction is one of the premier methods for the alkene synthesis. It proceeds through nucleophilic attack from the phosphorus ylid on the carbonyl group in the other compound. Elimination reactions (E1, E2) are common routes to alkene synthesis from alcohols or alkyl halides. In comparison to Wittig reaction, the carbon skeleton is pre-assembled in case of E1 or E2 within the molecule. Whereas Wittig allows a coupling of two fragments. Moreover, the elimination reactions give mixture of two isomers. In case of Wittig reaction there is no ambiguity about the position of the double bond. On the other hand, Wittig reaction can be compared to the aldol condensation where the carbonyl group is attacked by an enolate instead of the phosphorus ylid. The phosphonium ylid is produced when the phosphonium salt is deprotonated by the base KtBuO . The resulting carbanion is stabilized by the positive phosphorus in addition to the conjugation with the benzene ring. This anion is a strong nucleophile when it is formed, it attacks the carbonyl group of the aldehyde forming an alkoxide. This group rapidly connects to the phosphorus forming a 4-membered ring that cleaves to the desired alkene and triphenylphosphine oxide as a byproduct [152]. Wittig reaction has been widely used in many applications [153, 154].

Mechanism



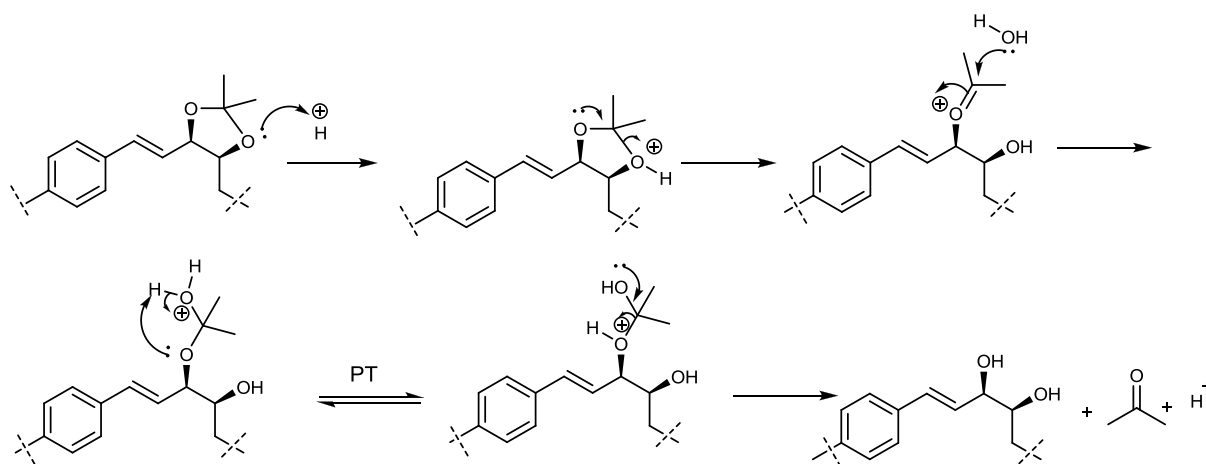
Scheme 24. Mechanism of the Wittig reaction.

1.4.4 De-protection of the acetonide

This reaction is the reverse of the acetonide formation reaction. The 1, 2- diol system can be recovered by hydrolysis of the acetonide in aqueous acidic medium. There are many acids that could be used in this reaction such as acidic resins, acetic acid or acidic workup with 1N HCl. One of the acetonide oxygens will be protonated by the acidic medium, forming an oxonium ion making itself a good leaving group. The other oxygen of the acetonide will attack the electron deficient carbon through its lone pair, which will liberate one hydroxyl group. An unstable oxonium ion will be formed on the other side. The oxonium ion is a powerful electrophile which will be attacked by solvent (H_2O or, methanol) to form a hemiacetal (Scheme25).

Proton exchange between the solvent and the etheric oxygen will lead to another oxonium ion formation. The alcoholic lone pair will attack on the electron deficient carbon leading to a C-O cleavage recovering the 1, 2 diol system and producing acetone as by product [155, 156].

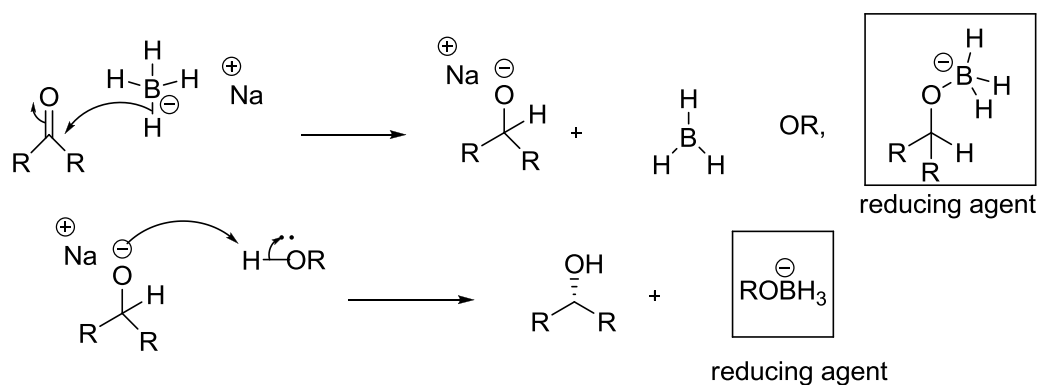
Mechanism



Scheme 25. Deprotection of the diol in acidic medium.

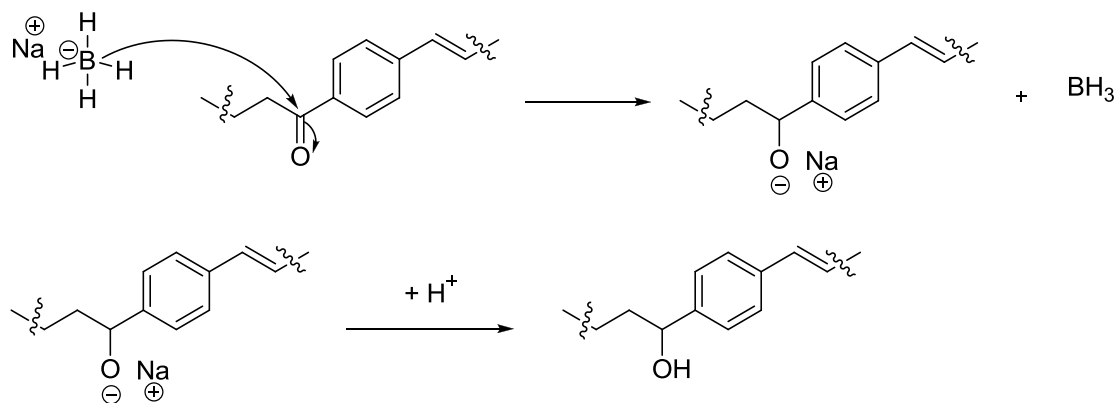
1.4.5 Reduction of benzylic ketone

This reaction is a nucleophilic attack by a hydride on a carbonyl group. Sodium borohydride is the source of the hydride. The nucleophile is the hydrogen atom carrying the pair of electrons from the B-H bond. This hydrogen atom will be transferred to the carbonyl in a nucleophilic attack. The reaction runs in protic solvents such as water and alcohols. These solvents are necessary for the protonation of the alkoxide to give the desired alcohol as a result of the reduction process [157].



Scheme 26. NaBH₄ reduction "general mechanism"

The mechanism proceeds in two steps. In the first step, the hydrogen with the lone pair detaches from the BH_4^- and adds to the carbonyl carbon in a 1, 2 addition forming C-H bond, and breaks the C-O bond forming an alkoxide. In the second step, a proton from water or the protic solvent is added to the alkoxide to form the alcohol [158].

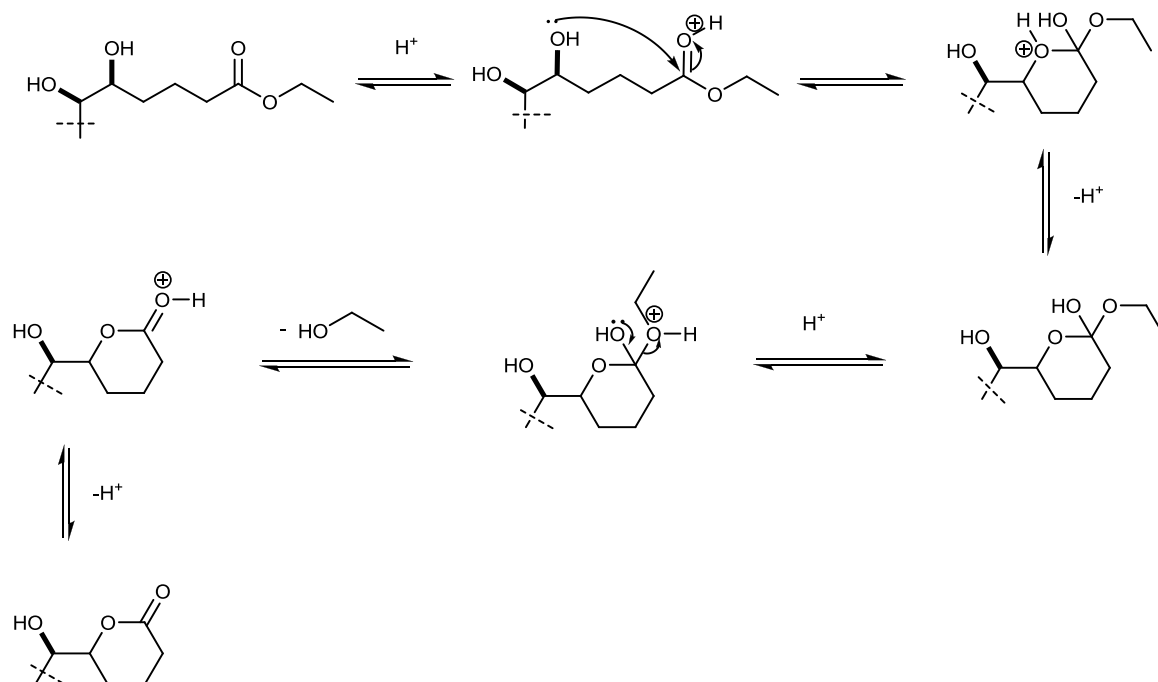


Scheme 27. Carbonyl group reduction mechanism.

1.4.6 Lactone formation

Lactones are internal hydroxycarboxylic acids and esters. They are formed by intramolecular esterification from their corresponding linear forms. The ease of formation depends on the size of the formed ring, it is more likely in case of 5 or 6 membered rings. Those of small ring size or bigger than 6 membered ring are hard to isolate due to their high reactivity [159,160]. In this case the lactone ring is rapidly formed after the deprotection of the diol (Scheme25). The reaction starts in acidic medium when protonation of the carbonyl oxygen take place, which will make the carbonyl group more electron deficient. This will lead the hydroxyl lone pair to attack on the electronegative carbonyl group forming the six membered ring. A proton transfer process followed by loss of the ethanol fraction furnishing the six membered ring lactone (Scheme 28).

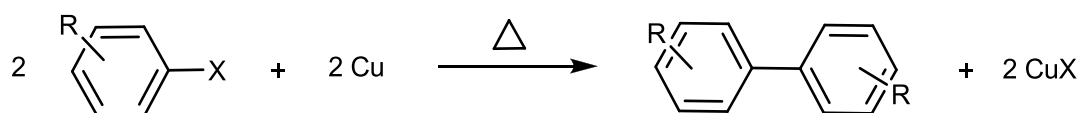
Mechanism



Scheme 28. Lactone formation mechanism.

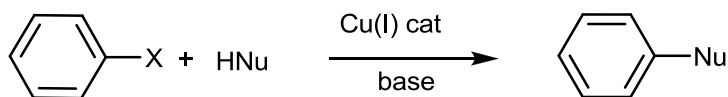
1.4.7 Ullmann approach

There are two classes of Ullmann reactions. The “classic Ullmann reaction” catalyzed by Cu refers to the synthesis of symmetric biaryls through the copper-catalyzed coupling (Scheme 29). The biaryl is accessible through coupling of the aryl halide in excess of the Cu at high temperature (150-200°C). The mechanism includes oxidative addition with a second equivalent of the aryl halide followed by reductive elimination to furnish the desired biaryl. This class of Ullmann reaction has been applied in some studies. The Immobilization of Copper (II) in Organic-Inorganic Hybrid Materials as a Highly Efficient and Reusable Catalyst for the Classic Ullmann Reaction was reported [161].



Scheme 29. Classic Ullman reaction

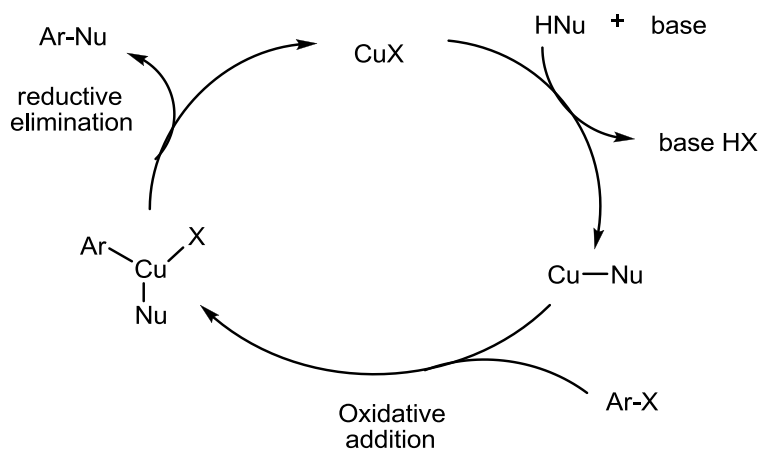
The other class “Ullmann type” reaction refers to copper – catalyzed nucleophilic aromatic substitution between nucleophile and aryl halides as shown below (scheme 30).



Scheme 30. "Ullmann Type" reaction

This class of Ullmann reaction proceed through a catalytic mechanism (Scheme 31). This type is mostly used in Ullmann ether synthesis as it is conducted in our case. Altman et al. reported, the use of this approach to provide an Improved "Cu-Based Catalyst System" for the Reactions of Alcohols with Aryl Halides. In addition, they claimed the improvement of the reaction in presence of a ligands. As a result it reduces the excess of the alcohol needed for the original reaction to proceed and support milder condition for the reaction [175]. Moreover, Ajay B. Naidu et al. postulated a general, mild, and intermolecular " Ullmann-Type" synthesis of diaryl and alkyl aryl ethers catalyzed by diol-copper(I) Complex [162]. Cristau et al. suggested a general and mild Ullmann-type synthesis of diaryl ethers as applications on the Ullmann type reaction [163].

Mechanism

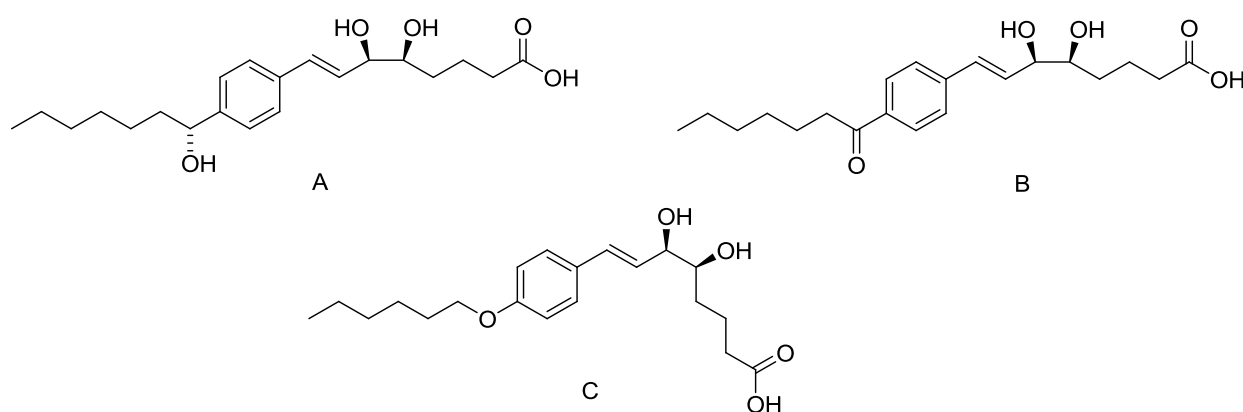


Scheme 31. Catalytic mechanism of Ullmann reaction.

2 RESULT AND DISCUSSION

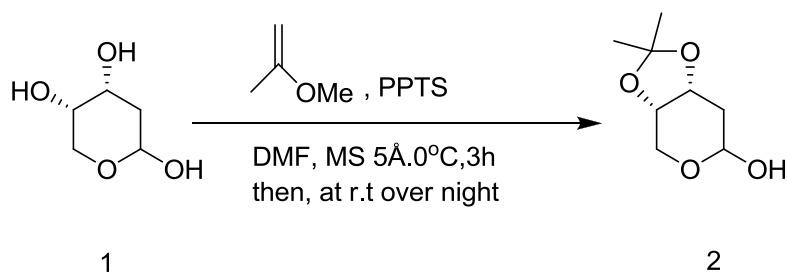
2.1 THE SCOPE OF THE CHAPTER

This chapter describes my contribution towards the synthesis of LXA4 analogues (Scheme 32). It introduces earlier studies in the same field of interest. In addition, discussing results within the performed reaction sequence. Lactone formation (section 2.13, 2.14) is considered to be an interesting intermediate that resulted from the deprotection of the diol **14**, **15** (section 2.12, 2.14). In a later stage of this chapter, we reported a computational study that explain the formation of these intermediates. Moreover, it support the actual mechanism based on the change in free energy values (ΔG) of each step (section 2.17).



Scheme 32. Proposed analogues.

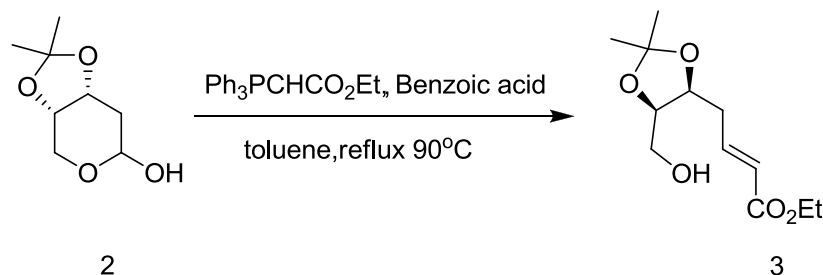
2.2 PROTECTION OF 2-DEOXY-D RIBOSE



Scheme 33. Synthesis of the protected sugar

Klimko et al. reported, the use of 2-methoxypropene as the reactant in the transformation from 2-deoxy-D-ribose to the acetal **2** with PPTS in ethyl acetate [164]. In addition, Colm Duffy and Philips ED reported the same treatment of the sugar at room temperature resulting the product **2** in 43% yield [165,166]. K. C. Nicolaou reported the use of $\text{Me}_2\text{C}(\text{OMe})_2, \text{p-TsOH}$ (cat) in acetone for the protection of same moiety with 87% yield [167]. The conducted treatment in this research is based on the earlier studies [165]. Where the observation showed insolubility of the sugar in ethyl acetate and its selectivity towards some organic solvents. Using DMF solvent showed good solubility of the sugar at room temperature and even at lower temperature. The reaction was performed in very dry conditions and with the use of molecular sieves to capture the water. The crude consisted of the desired product and the methylated alcohol as by product, which could be separated using column chromatography affording 41% pure product **2** which is invisible under UV light. The success of the reaction was confirmed by mass spectrometry. The new two singlets peaks in the $^1\text{H-NMR}$ spectra 1.35(s, 3H), 1.22(s, 3H) clearly identify the formation of the acetal (Section 5.2.1.1).

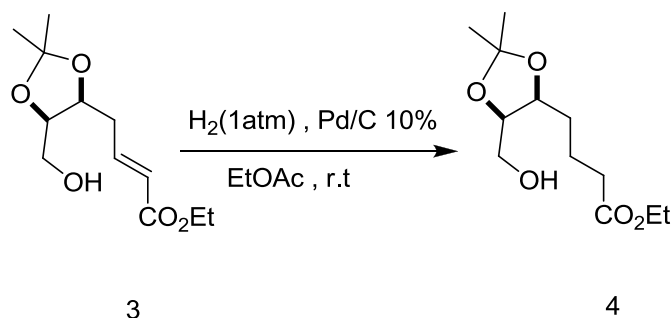
2.3 SYNTHESIS OF THE ALKENE FROM THE SUGAR



Scheme 34. Synthesis of the alkene via Wittig reaction.

Colm Duffy, Klimko, and Philips ED. reported the same treatment of the aldehyde with refluxing in THF resulting 81% of alcohol **3** [164-166]. The reaction conducted in this project based on the earlier studies with minor modifications. The protected sugar **2** treated with the commercially available Wittig salt (1:1.5) mol equivalency respectively in toluene furnished alcohol **3** in 87% yield. The crude contained a big excess of the salt which appeared with the same R_f value as it contain same kind of groups. In this case the crude had to be washed with diethyl ether that showed a good solubility of the product unlick the excess reactant which precipitate in such solvent. The resulted oil submitted for further purification by means of column chromatography furnished a pure colorless oil of compound **2** in 87% yield. The reaction was tested with (1:1) equivalent that gave 80% yield of the alcohol. The success of the reaction confirmed by mass spectrometry and NMR. The visibility of the product under UV light due to the new formed double bond also gives indication on the formation of the alkene. The new two characteristic signals of the double bond and the ester group in the $^1\text{H-NMR}$ spectra clearly indicate the formation of the alkene, 6.97-6.90 (m,1H), 5.89 (d, $J=16$ Hz, 1H), 4.20-4.13(m,3H), 1.25(t,3H), (section 5.2.1.2)

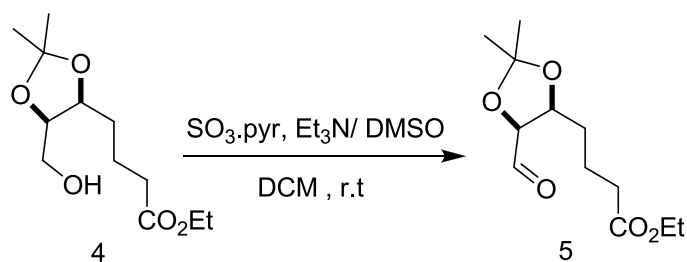
2.4 REDUCTION OF THE ALKENE.



Scheme 35 synthesis of the reduced alcohol.

Adile Duymaz reported the same reduction method for the alkene **3** in MeOH furnished 83% the reduced alcohol **4** [168]. Moreover, Klimko reported the same treatment in iso-propanol [164]. Colm Duffy, and Philips ED et al. reported the catalytic hydrogenation using 10% Pd/C in ethanol furnished 87% yield of the reduced alcohol **4** [165,166]. The same treatment was conducted here in ethanol and gave 93% yield. The success of the reaction was confirmed by mass spectrometry beside the disappearance of the characteristic peaks of the double bond in addition to the invisibility of the product under UV light (section 5.2.1.3).

2.5 OXIDATION OF THE 1^o ALCOHOL TO ALDEHYDE



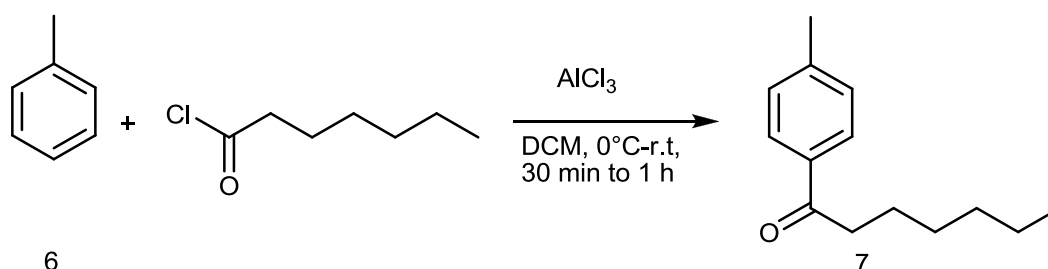
Scheme 36. Synthesis of the aldehyde.

Swern oxidation was the first choice for many research approaches to achieve aldehydes from 1^o alcohols. Adile Duymaz, colm Duffy and Philips ED have reported the use of Swern type of oxidation to obtain the aldehyde **5** from the primary alcohol **4** with a yield ranges from 77% to 86% [165,166, 168]. Parikh-Doering oxidation is another type of oxidation which was conducted in this project furnished 87% yield of the aldehyde **5**. This reaction ran at milder temperature

conditions from 0°C to r.t without formation of very odorous volatile by-products such as dimethyl sulfide and carbon monoxide as in Swern oxidation.

Purification trials by means of automated flash chromatography and column chromatography failed as the product gets lost on the silica. The crude was forward used without further purification. The success of the reaction was confirmed by mass spectrometry and NMR. The new ¹H-NMR signal of the aldehydic hydrogen appears at 9.56 (s, 1H). In addition to, the visibility of the aldehyde under UV light (section 5.2.1.4).

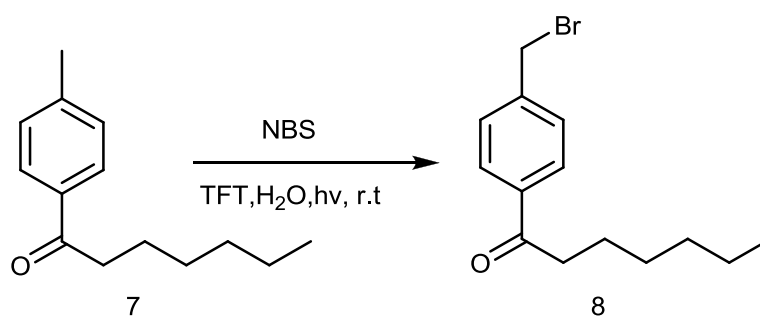
2.6 FRIEDEL-CRAFT ACYLATION OF THE TOLUENE



Scheme 37. Synthesis of the acylated toluene

Friedel craft acylation reaction was assembled by using the commercially available toluene, acyl chloride and aluminum chloride in DCM furnished 73% yield of pure product 7. The success of the reaction was confirmed by ¹³C-NMR and the new characteristic beaks in ¹H-NMR 2.92 (t, 2H), 2.40 (s, 3H), 0.88 (t, 3H) (section 5.2.2.1.1).

2.7 BENZYLIC BROMINATION OF THE ACYLATED TOLUENE.

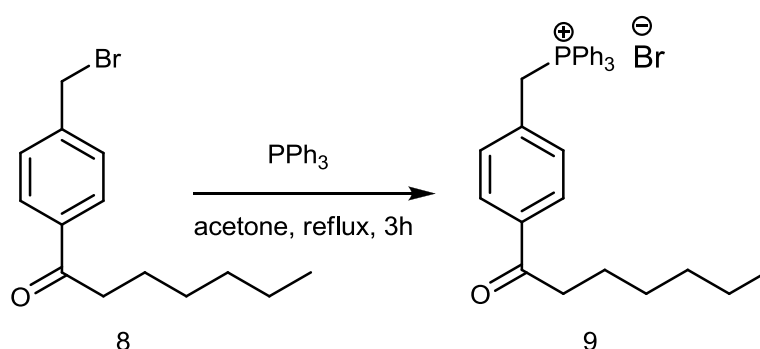


Scheme 38. Synthesis of the brominated acyl.

Ajda Podgorsek et al. reported, the benzylic bromination of various 4-substituted toluenes assembled by NBS in pure water. They have used a 40 W incandescent light-bulb as the radical

initiator of the radical chain process gave 86% yield of bromo-benzylic toluene derivatives [169]. The bromination of the previously synthesized para acylated toluene **7** was conducted following the same principle using NBS, (TFT/ water) as the solvent mixture and illuminated with a 60 W incandescent light bulb at room temperature resulted 83% yield of the mono-brominated product **8**. The success of the reaction was confirmed by ^{13}C NMR and the new characteristic signal of the brominated benzylic $-\text{CH}_2$ ^1H -NMR 4.51 (s, 2H), (section 5.2.2.1.2).

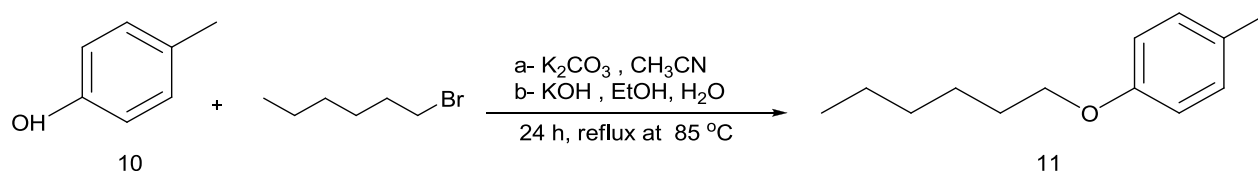
2.8 WITTIG SALT FROM THE BENZYL BROMINATED TOLUENE DERIVATIVE



Scheme 39. Synthesis of the Wittig salt.

The Wittig salt **9** was conducted with refluxing triphenylphosphine and the previously synthesized compound **8** in acetone for 3-5hr at 65°C resulted 82 % yield. The success of the reaction was confirmed by Mass Spectrometry, IR, and NMR. The new characteristic doublet appeared in the ^1H -MNR with the significant J coupling to the phosphorus at 5.64 (d, $J= 16$ Hz, 2H) clearly indicate the formation of the Wittig salt **9**, (section 5.2.2.1.3).

2.9 PREPARATION OF THE O-ALKYLATED P-CRESOL

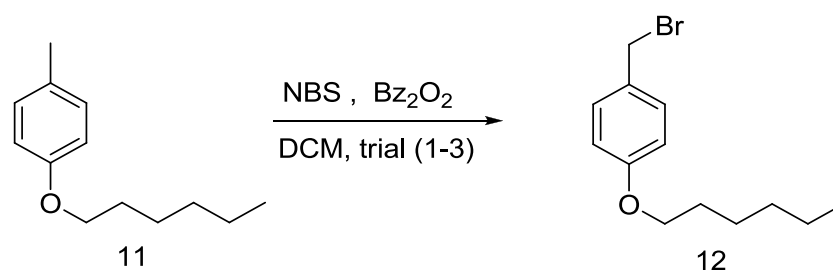


Scheme 40. Synthesis of the benzylic ether

Milhanic et al. reported the success of the O-alkylation of the p-cresol refluxing for 48h in acetonitrile with potassium carbonate gave 88% yield of the ether **11** [170]. In addition, Hong-Cheu Lin et al. reported the same treatment with refluxing for 24 h in a mixture of water/ethanol (1:9) respectively, and potassium hydroxide furnished gave 88% yield of the

ether **11** [171]. Both methods were applied in this project. The reaction was successful in both treatments with a yield ranges from 72%-76% (Table 2). The product was pure and used in the next reaction without further purification. The success of the reaction was confirmed by the mass spectrometry and NMR. The characteristic beaks in $^1\text{H-NMR}$ of the O-CH_2 and the para benzylic methyl group 3.95 (t, 2H), 2.32 (s, 3H), respectively clearly indicated the formation of the desired product (section 5.2.2.2.1).

2.10 BENZYLIC BROMINATION OF THE ETHER



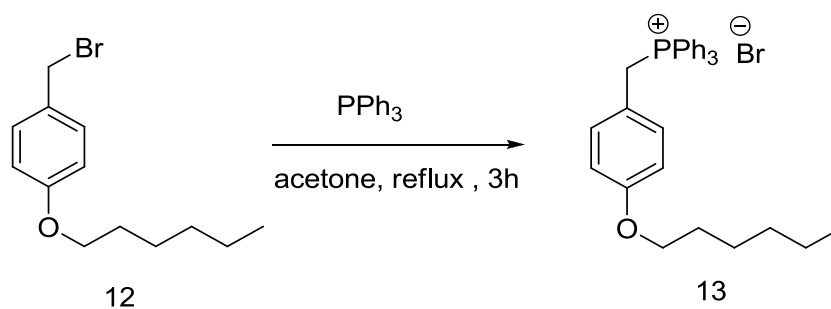
Scheme 41. Synthesis of the brominated benzylic ether.

Bromination of the benzylic ether **11** was reported in earlier studies. The reaction took place by refluxing benzylic ether **11** in carbon tetrachloride with NBS and a catalytic amount of dibenzoyl peroxide resulted 36% yield of the desired product [170]. The reaction was performed based on this study, gave 48% yield of the mono-brominated benzylic alkyl **12**. The observation showed the high possibility of producing mixture of the mono and the di-benzylic brominated products. This problem was indicated by the integration difference of the representing signal of the brominated alkyl in $^1\text{H-NMR}$. The degree of bromination found to be dependent on the mol equivalency of the starting material **11** to the NBS, and the reaction time (Table 1). The success of the reaction was confirmed by NMR. The new beak appeared in the $^1\text{H-NMR}$ at 5.30 (s, 2H) clearly identify the formation of the mono-brominated product (section 5.2.2.2.2).

Table 1. Reaction optimization towards the bromination of the benzylic ether

Trial	Solvent	Reaction time	Equivalency (cpd 11 : NBS)	Yield%	product
1	CHCL3	9h (3*3)	1:3	19 %	Dibromo
2	CHCL3	9h (3*3)	3:1	83 %	mixture
3	DCM	6h (2*3)	3:1	48%	monobromo

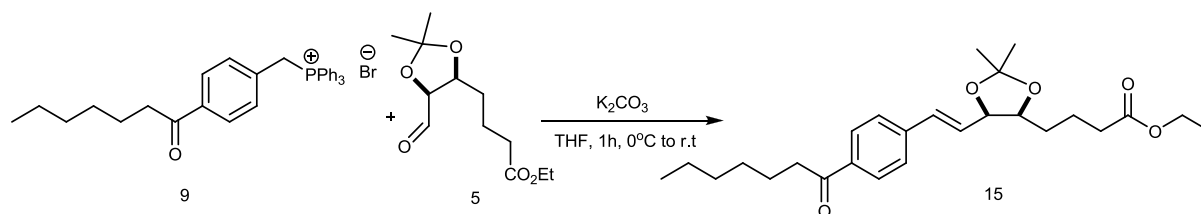
2.11 WITTIG SALT FROM THE BROMO-BENZYLIC ETHER



Scheme 42. Synthesis of the Wittig salt of the benzylic ether

Earlier studies suggested the preparation of the Wittig salt by refluxing the bromide compound **12** in xylene and toluene with triphenyl phosphine for 18h furnished yield ranges from 88% to 69% respectively [170,171]. Based on these studies the reaction was tested in the same solvent systems unsuccessfully. This could be related to instability of the compound in high temperatures or unsuitable reaction conditions. Another mild temperature conditions was conducted in this project. Refluxing the reaction mixture in acetone for shorter time gave 72% yield of the Wittig salt **13**. The success of the reaction was confirmed by mass spectrometry, IR, and NMR. The new characteristic doublet appeared in the $^1\text{H-NMR}$ with the significant J coupling to the phosphorus at 5.23 (d, $J=16$ Hz, 2H) clearly indicate the formation of the Wittig salt **13**, (section 5.2.2.2.3).

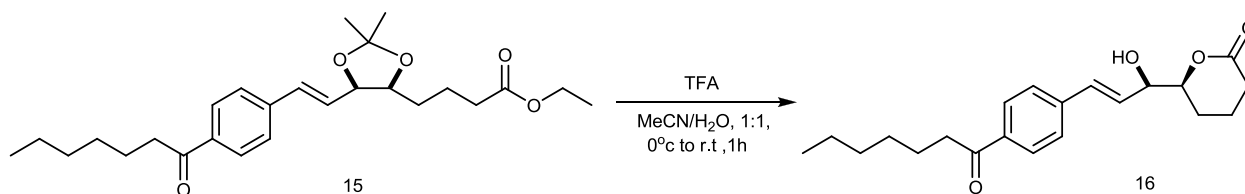
2.12 WITTIG REACTION OF THE ALDEHYDE AND THE KETONIC WITTIG SALT



Scheme 43. Synthesis of the coupled alkene

Wittig reaction was a successful approach to obtain the desired product **15** from the Wittig salt **9** and its aldehyde partner **5** in 47%. The reaction should be preceded under very dry conditions and in dry solvents. The success of the reaction was confirmed by mass spectrometry, IR, and NMR. The new characteristic peaks appeared in the 1H -NMR such as the peak at 6.74 (d, $J = 8$ Hz, 1H) and 5.83 (t, 1H) for the new trans double bond resulted from the Wittig coupling. Similar target compounds were assembled by other approaches in different researches [172], (section 5.2.3).

2.13 HYDROLYSIS OF THE ACETAL IN THE KETONIC MOIETY CONTAINING PRODUCT

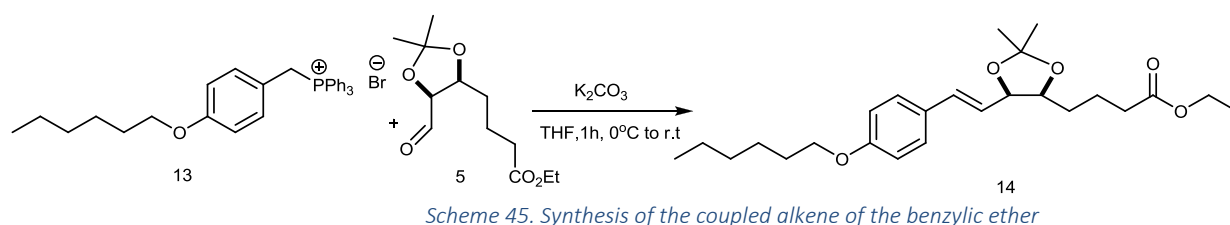


Scheme 44. Hydrolysis of the acetal in the ketone containing compound

The reaction targeted the deprotection of the diol moiety in compound **15**. The lactone formation is commonly reported in many researches that had to deal with such cases. The main theme of these compounds is groups as alcohols or diols and ester or carboxylic acid group in the same side of the compound. The reason behind this could be due to the reactivity of the hydroxyl group in addition to the stability of the six membered ring of the formed lactone. The fact that this lactone formation is an intramolecular reaction, further facilitate the formation. Computational study on the deprotection mechanism followed by the formation of the lactone ring has been conducted in this research in order to fully explain this case. Singh S et al. reported a one-pot esterification and deprotection of another 1, 2- diol system using $ZrCl_4$ that gave 13% lactone formation as by product [173]. In addition, Colm Duffy stated lactone

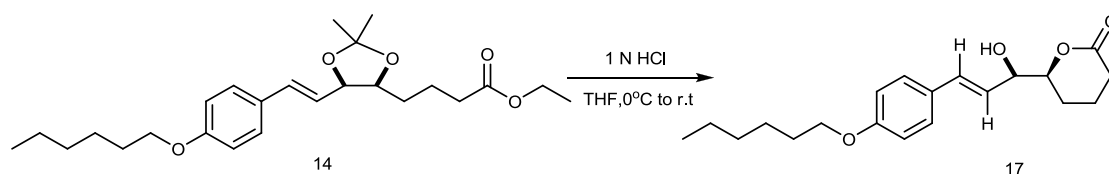
formation in similar case after deprotection of the same diol system using TBAF/THF gave 1:1 yield percent mixture of the deprotected product and the lactone [165]. Pierre van de Weghe postulated similar case during the synthesis of Lipitor where the lactone group was assembled by the deprotection of the acetonid group with HCl in methanol and then treated with calcium acetate to furnish the desired product in a form of calcium salt [174]. Deprotection of the diol **15** was conducted here using TFA in a solvent mixture MeCN/H₂O (1:1) and furnished 70% of the lactone **16**. The lactone formation was confirmed by mass spectrometry, IR and NMR. The new characteristic beaks appeared in the ¹H-NMR 4.40-4.36 (m, 1H), 2.87(t, 2H) indicate the formation of the lactone **16**, (section 5.2.5).

2.14 WITTIG REACTION OF THE ALDEHYDE AND THE ALDEHYDIC WITTIG SALT



The cross coupled product **14** was conducted in the same principle as in case of compound **15** (section 2.12). Wittig reaction was assembled between the Wittig salt **13** and its aldehyde partner **5** and gave 30% of product **14**. The success of the reaction was confirmed by Mass Spectroscopy, IR, and NMR. The new beaks that appeared in the ¹H-NMR at 6.57 (d, J=12, 1H), 5.54 (t, 1H) which represent the new trans double bond resulted from the Wittig coupling (section 5.2.4).

2.15 HYDROLYSIS OF THE ACETAL IN THE ALDEHYDIC MOIETY CONTAINING PRODUCT



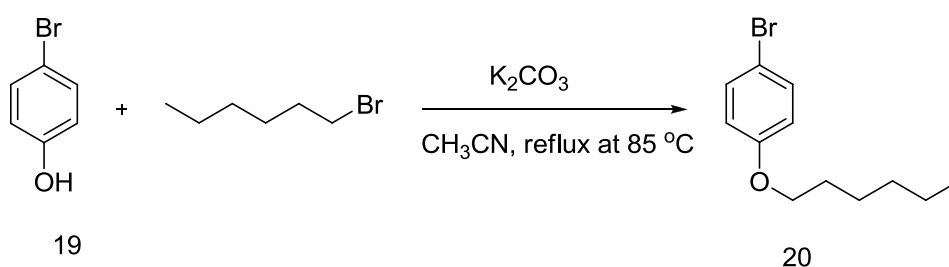
According to the same principles discussed in case of compound **16** it was expected to follow the same observation. The hydrolysis reaction was assembled in the first trial by using TFA in a

solvent mixture of MeCN/H₂O (1:1) at room temperature for 1h. The mass spectroscopy showed the absence of the molecular mass of the expected product.

While the desired compound **17** was assembled using 1N HCl in THF overnight furnished 70% yield. The success of the reaction was confirmed by Mass Spectroscopy, IR (section 5.2.6).

2.16 ULLMANN APPROACH

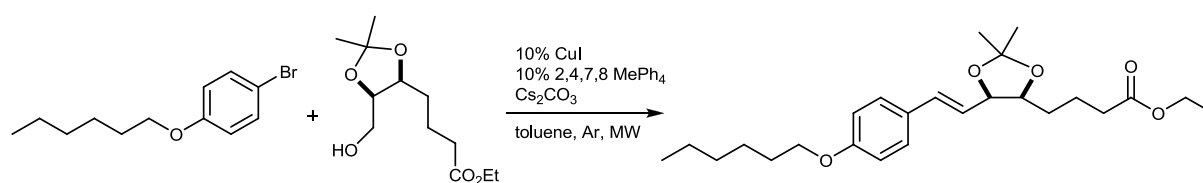
2.16.1 Preparing the O-alkylated phenol derivative.



Scheme 47. Synthesis of the O-alkylated phenol

Compound **20** was conducted according to the same principle used to achieve the benzylic ether **11** (section 2.9). The compound was assembled by the treatment of 4-bromophenol with 1-bromo hexane and potassium carbonate under refluxing for 24h. It furnished the desired product **20** in 85% yield. The success of the reaction was confirmed by the Mass Spectrometry and NMR. The new characteristic signals appeared in the ¹H-NMR at 3.96 (t, 2H), and 0.96 (t, 3H) clearly indicate the formation of the desired product **20**, (section 5.2.7.1).

2.16.2 Preparing the Ullmann ether



Scheme 48. Synthesis of the Ullmann ether

Ryan A. Altman postulated, the use of 3, 4, 7, and 8-tetramethyl-1, 10-phenanthroline as a ligand to improve the Cu-catalyzed cross coupling of alcohols with aryl halides (iodides and bromides) [175]. Similar targeted compounds were assembled by using 5% CuI, 10% Me₄Phen,

and cesium carbonate in toluene at 80-110 °C for 9-24h to give the cross coupled product in 75 % yield. The same treatment has been applied on the aryl halide **20** and the alcohol **4**, but resulted no reaction (Table 2). The reaction was tested by using 1:2 equivalent of the aryl halide and the alcohol respectively, 5% of the catalyst (bis-bipyridyl ligand modified complex), and K₃PO₄ under argon at 110 °C for 24-48 h furnished 61-91% yield.

The reaction could be further optimized for successful reaction conditions. Another reaction system was suggested by Jiajia Niu et al. that could be useful to test, as an efficient O-arylation of aliphatic alcohols with aryl halides using an air-stable copper (I) complex as the catalyst [176],(section 5.2.7.2).

Table 2. Initial optimizations of Ullmann reaction conditions.

Trial	ligand %	Catalyst %	method	Aryl halide: Alcohol	Time	Yield %
1	10	5	Normal heating	1:1.5	2h	-
2	10	5	mw	1:1.5	2h	-
3	15	10	mw	1:1.5	5h	-

2.17 A TOTAL COMPUTATIONAL STUDY ON THE LACTONE CASE

2.17.1 Density functional theory (DFT) calculations

Computational Details

The quantum chemical calculations have been performed using the Gaussian Quantum chemistry program [176]. All the geometries of the molecules studied were optimized using the B3LYP functional [177-179]. The 6-311G (d, p) basis set was used for the optimizations and frequency calculations [180]. All the thermodynamic property calculations were performed at 298.15K and 1.00 atm. Solvent effects were corrected by using the polarizable continuum model (PCM) in its integral equation formalism (IEF) and acetonitrile as a solvent to mimic the experimental conditions [181].

2.17.2 Discussion of the calculated results

The proposed reaction mechanism for the lactone formation based on the DFT calculations is shown in (Figure 12). The change in the standard Gibbs free energy (in kcal/mol) and change in entropy (in cal/mol.K), through each step of the mechanism, gives indication on the spontaneity of the reaction. In addition, it shows to how much extent the reaction is favorable to proceed in the specific direction towards the product, see (Figure 12).

The study on the free energy and the entropy of the reaction showed that the reaction most likely proceed towards the formation of the most stable product that shows the lowest ΔG value, which is the 6-membered ring lactone. The first step which presents the protonation of the acetonide moiety showed spontaneous activity towards the formation of the protonated product **2** with $\Delta G = -4.2$ kcal/mol and $\Delta S = -1.6$ cal/mol.K. While the reaction progresses towards the formation of the oxonium ion intermediate **3** from the intermediate **2** showed also favorable step with $\Delta G = -1.4$ kcal/mol and $\Delta S = +1.72$ cal/mol.K. Then, with the nucleophilic attack on the oxonium ion intermediate **3** by the water molecule the reaction proceed towards the formation of intermediate **4** with $\Delta G = -1.5$ kcal/mol and $\Delta S = -24.3$ cal/mol.K. On the other hand, the proton exchange between the water molecule and the oxygen of the protected hydroxyl towards the formation of intermediate **5** showed $\Delta G = +0.5$ kcal/mol and $\Delta S = -2.9$ cal/mol.K, which means that it is slightly less favorable towards the next intermediate **5**.

Overall, the free energies through intermediates **3-5** supports that the flow of the mechanism through these intermediates is favorable towards intermediate **5** with $\Delta G = -1.0$ kcal/mol and $\Delta S = -27.2$ cal/mol.K.

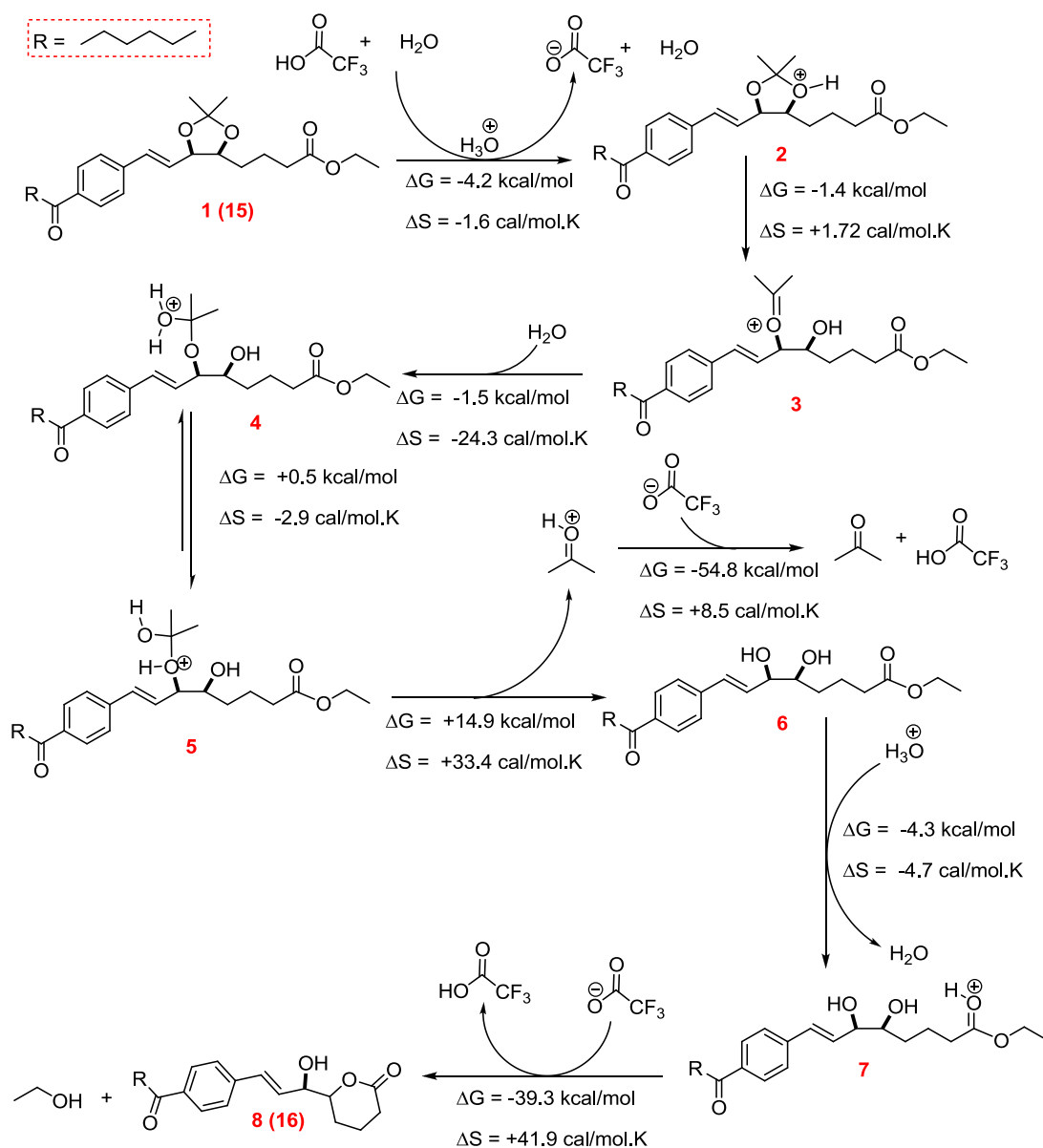


Figure 12. Courtesy of Dr. Taye B. Demissie .B3LYP/6-311G (d, p) calculated change in standard Gibbs free energy (kcal/mol) and change in entropy (cal/mol. K) of the reaction mechanisms leading to the formation of compound **8 (16)**.

Losing the water molecule in a resonance movement towards the formation of product **6** showed $\Delta G = +14.9$ kcal/mol and $\Delta S = +33.4$ cal/mol.K, which may look unfavorable reaction. However, the parallel reaction mechanism for retaining the TFA acid from the anionic TFA and the protonated acetone shows $\Delta G = -54.8$ kcal/mol and $\Delta S = +8.5$ cal/mol.K, which controls the overall reaction at this step and the result would be in favor of proceeding the mechanism towards the formation of product **6** with a net $\Delta G = -39.9$ kcal/mol and $\Delta S = +41.9$ cal/mol.K. Due to the presence of acid in the reaction medium "acidic medium", the carbonyl group in product **6** is easily protonated to form intermediate **7** in a favorable reaction with $\Delta G = -4.3$ kcal/mol and $\Delta S = -4.7$ cal/mol.K. The overall energetics for the last step, the mechanism proceeds in a favorable manner towards the formation of the six member ring lactone in addition to the loss of ethanol molecule plus retaining of the acid catalyst with $\Delta G = -39.3$ kcal/mol and $\Delta S = +41.9$ cal/mol.K.

The last mechanism for the formation of the six member ring lactone is further analyzed based on the potential energy surface (PES) shown in (Figure 13). The PES for the internal cyclization of compound **6** leading to the formation of compound **8** is another explanation element on the preference of lactone formation rather than the corresponding linear ester. In addition, the possible cyclization reaction with and without the protonation of the carbonyl group are also compared in (Figure 13). The (a) model shows that the cyclization reaction do not proceed for the unprotonated carbonyl group, where it shows increase in the energy as the hydroxyl oxygen and the carbonyl carbon distance decreases referring to the instability of the compound with the decrease in the distance. The (b) model shows that the cyclization of compound **7** which has a protonated carbonyl group. The PES clearly shows the favored formation of the six member lactone if the carbonyl group is protonated. This also refers to the essentiality of the protonation of the carbonyl group in order to proceed with the suggested mechanism.

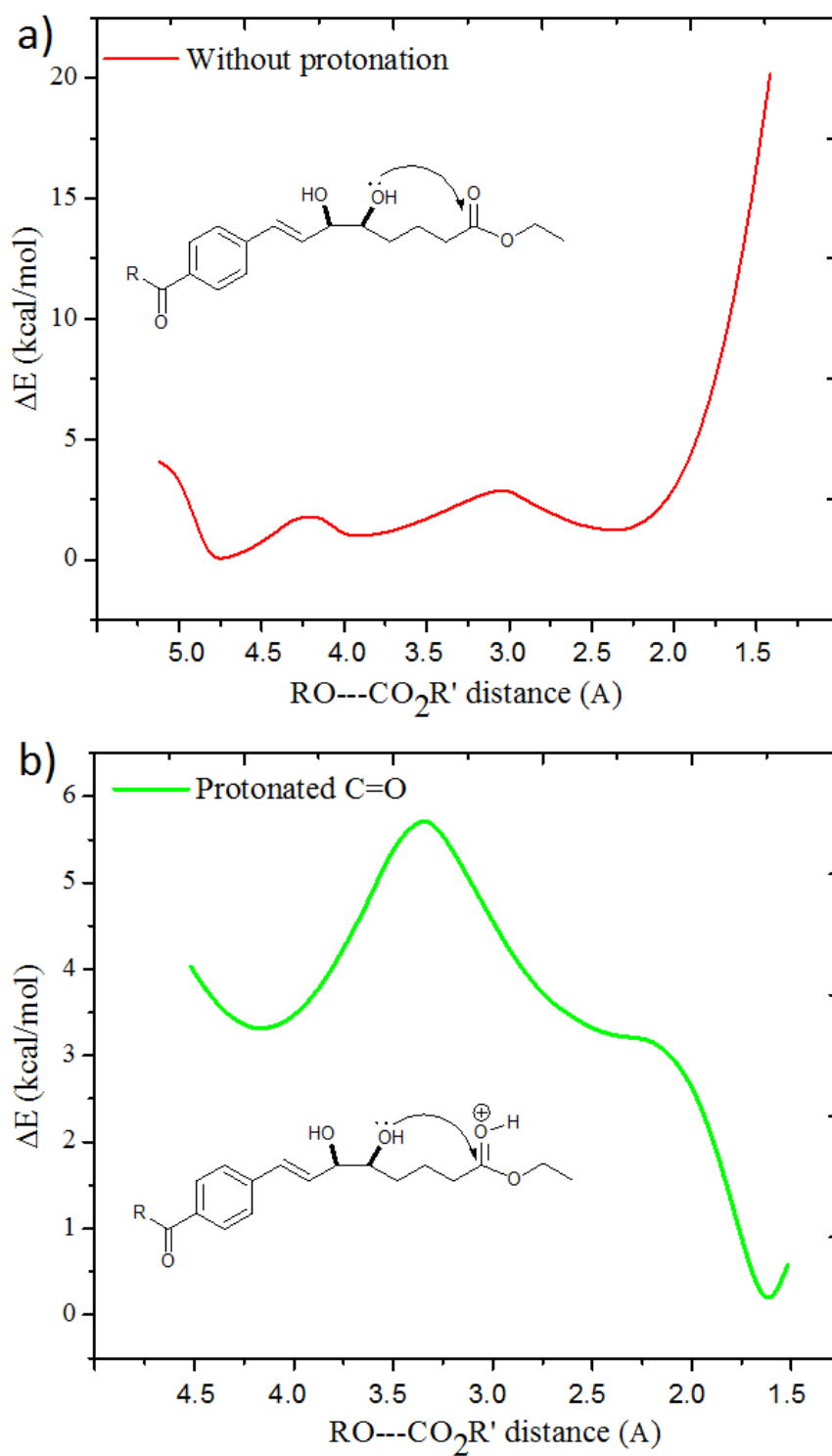
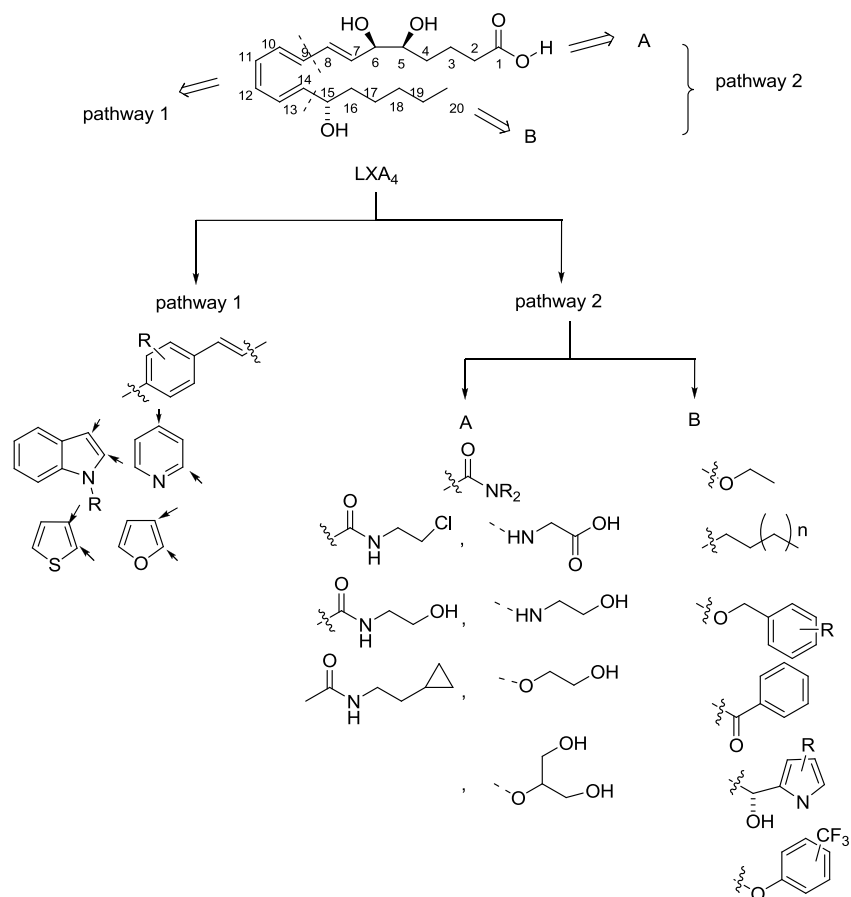


Figure 13. Courtesy of Dr. Taye B. Demissie .Potential energy surface (PES) for the cyclization of compound 6 leading to the formation of compound 8: a) shows the cyclization without protonation of the C=O of the ester group, whereas b) shows the cyclization process after protonation of the C=O group.

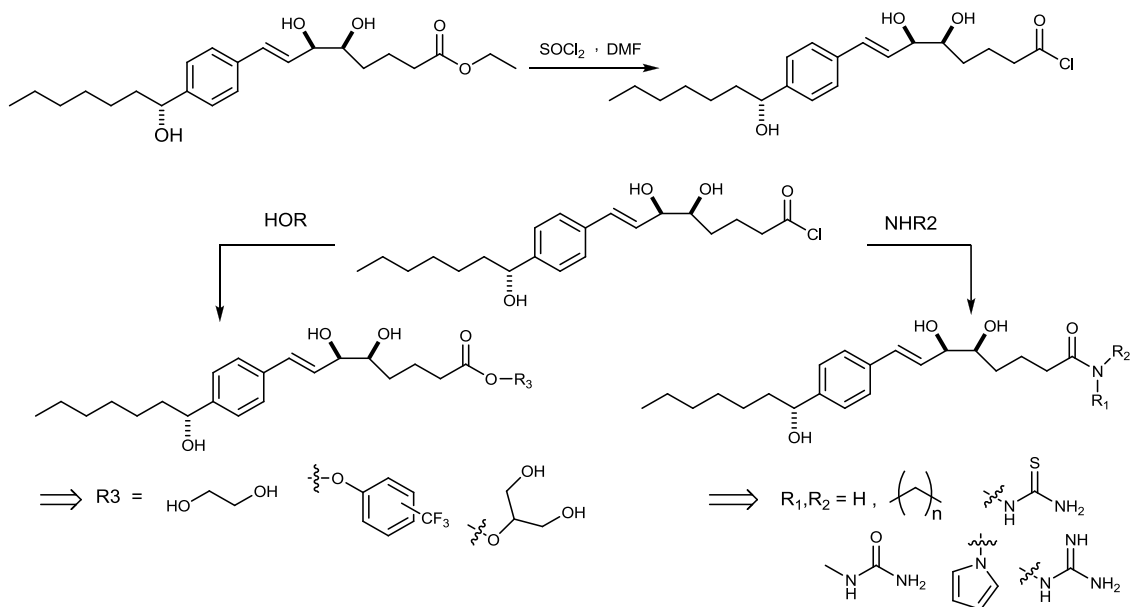
3 FUTURE DIRECTIONS

According to previous studies based on the structure activity relationship of LXA4, wide range of modification and functionalization interest was brought on the way of the research delivered in this thesis. There are two pathways of structure modification of LXA4. These pathways aim at the replacement of some functionalities in the native LXA4 with other chemical stable functionalities in order to retain the potent biological activity. The first pathway is based on the triene moiety to be involved in a stable aromatic, heteroaromatic and the substituted fused benzo systems, see pathway 1 (Scheme 49). Which play an important role of prevention of the reduction at C₁₃-C₁₄ [166]. While the other pathway is based on the structure modification of the side chains at C₁₅₋₂₀ and C₁₋₈, see pathway 2 (scheme 49). Which shows resistance to the oxidation at C₂₀ and prevention of the β oxidation respectively [166, 183, 184]. Through different and wide range of organic synthesis reactions including photochemistry could provide methods for the possible late stage functionalization and modification of the already prepared analogues. Moreover, it could participate in expanding the library of LXA4 analogues that might be interesting for further pharmacological evaluation.



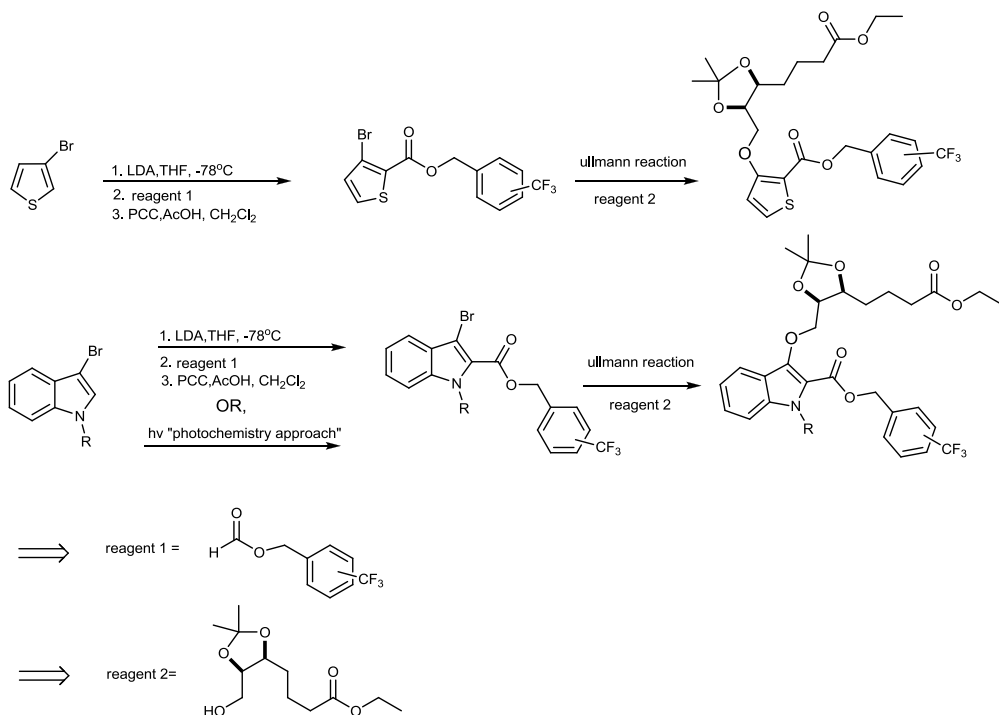
Scheme 49. Strategies for structural diversity of LXA4 analogues library

The late stage functionalization is based on the wide range of the function groups that could be inserted or replaced in the already synthesized analogues. These new structural features would provide a library of the LXA4 analogues to be scanned for biological activity. Some of these novel function groups could participate on enhancing the biological properties of the analogues. Some of these groups have already shown some biological potentialities. For examples the para- fluorophenoxy analogues showed extreme potency for inhibiting the tumor necrosis factor (TNF)- α -induced leukocyte recruitment into the dorsal air pouch. Moreover, it has shown some potentials as anti-cancer agents [185]. All of these ideas could be executed by means of organic chemistry and photochemistry methodologies.



Scheme 50. Late stage functionalization strategy

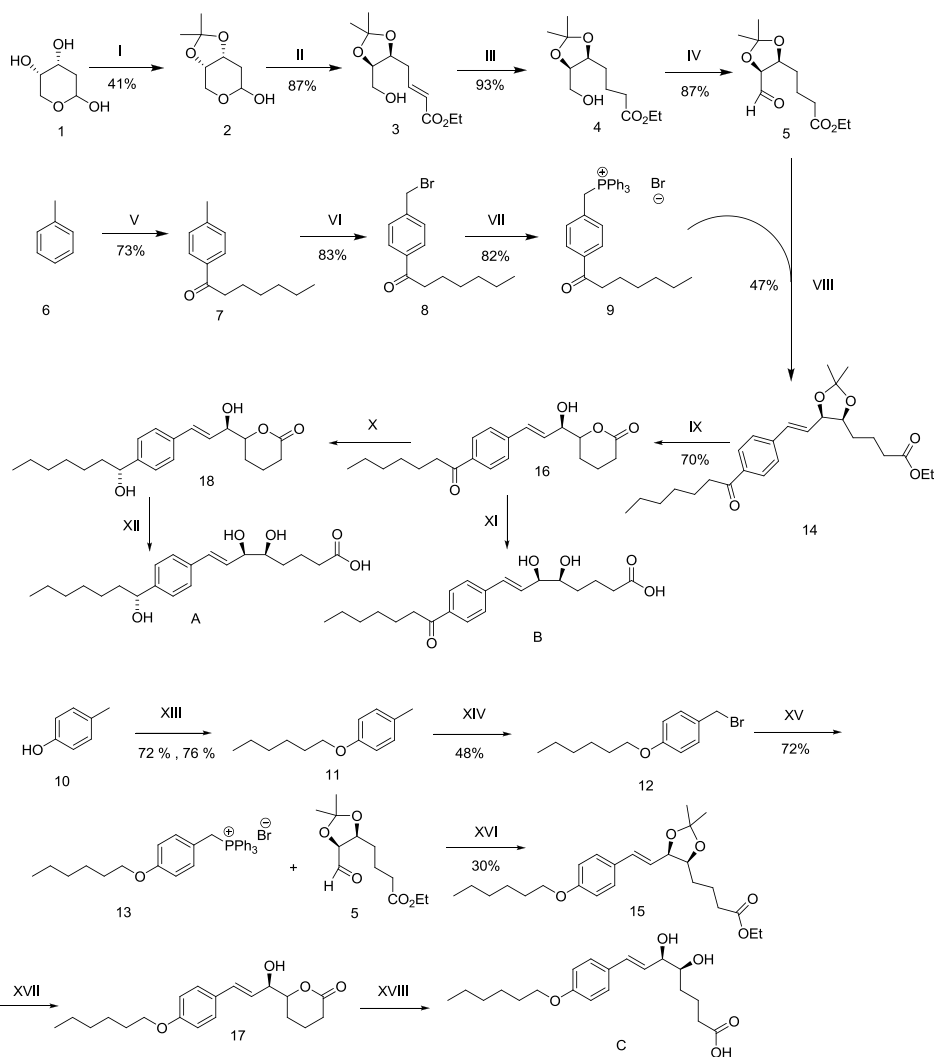
A diversity of synthetic tactics could be developed and applied in order to assemble new stable LXA4 analogues that could be interesting from chemical and biological point of view.



Scheme 51. New proposed analogues with suggested approaches

4 SUMMARY AND CONCLUSIONS

This section describes the synthesis of compounds **16** and **17** through multiple steps. Starting from the commercially available 2-deoxy-D-ribose, toluene, and p-cresol, the desired products were assembled within 14 steps. An overview of the performed reactions with the obtained yields for every intermediate is reported (Scheme 52).



Scheme 52. Summary of Reagents and conditions. (I) 2-methoxy propene, PPTS, acetone at 0 °C; (II) Ph₃PCHCO₂Me, Toluene at 90 °C; (III) H₂/Pd, EtOAc; (IV) SO₃-Pyr NEt₃, DCM at 0 °C to rt; (V) Acyl chloride, AlCl₃, under N₂ gas at 0 °C with stirring; (VI) NBS, H₂O/ trifluoromethyl benzene, hν for 27 h at rt; (VII) PPh₃, acetone, reflux for 3h at 65 °C; (VIII) Wittig reaction under very dry conditions, THF, Potassium tert-butoxide at 0 °C to rt, stirring for 2h under N₂ gas; (IX) TFA, MeCN/H₂O, 1:1; (X) NaBH₄, MeOH, 1h at r.t.; (XI, XII) 4M NaOH, MeOH, 1h at r.t.; (XIII) 1-Bromohexane, K₂CO₃, acetonitrile, protected under N₂ gas, refluxed at 85 °C for 24 h; (XIV) NBS, Bz₂O₂, CHCl₃ reflux at 68 °C; (XV) PPh₃, acetone, reflux for 3h at 65 °C; (XVI) Wittig reaction under very dry conditions, THF, Potassium tert-butoxide at 0 °C to rt, stirring for 2h under N₂ gas; (XVII) 1N HCl, THF, overnight at r.t.

Our results concerning the total synthesis towards LXA4 analogues reflect the diversity of compounds and synthetic tactics which could participate in expanding the synthetic library of LXA4 analogues.

Chapter “1” included the goals and strategy of the thesis in addition to the retro-synthesis study. Moreover, the biological background of the targeted pharmacological agent. Followed by the forward synthesis and theoretical chemical background of the performed reactions.

The first practical part in this thesis (chapter 2) describes my efforts towards the total synthesis of substituted *p*-benzoid LXA4 analogues. The synthesis of the late stage intermediates **16** and **17** was successfully assembled within 14 steps from the commercially available starting materials 2-deoxy-D-ribose, toluene and *p*-cresol in 70% yield. The total suggested strategy was successfully executed except the final lactone hydrolysis and the reduction of the benzylic ketone **16**.

Chapter 3 gives some novel ideas about late stage functionalization of the already prepared analogues. In addition, suggesting new structure that could be interesting stable analogues of LXA4 as future directions.

According to the computational study performed on the lactone formation mechanism, we can conclude that the lactone product should be the expected product from the acetonid hydrolysis step. In addition, Potential energy surface (PES) confirmed that protonation on the carbonyl group could be the driving force for the mechanism to proceed towards the favorable direction of the lactone cyclization.

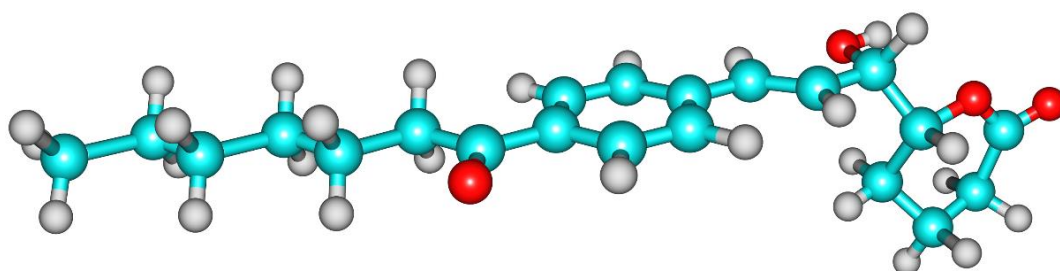


Figure 14. Optimized structure of compound 16, see Figure 12.

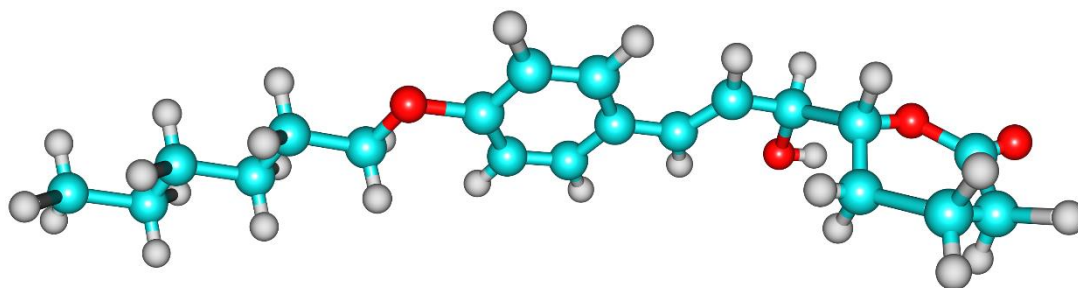


Figure 15. Optimized structure of compound 17, see Figure 12.

Further work on this project could be ongoing. Priority is to complete the total synthesis by the hydrolysis of the lactone moiety in compound **16** and **17**. In addition, optimizing the new Ullmann coupling towards successful conditions. Moreover, submitting the synthesized compound to the biological scanning in order to evaluate these novel analogues towards the pharmacological activity.

5 EXPERIMENTAL SECTION

5.1 GENERAL EXPERIMENTAL CONSIDERATIONS

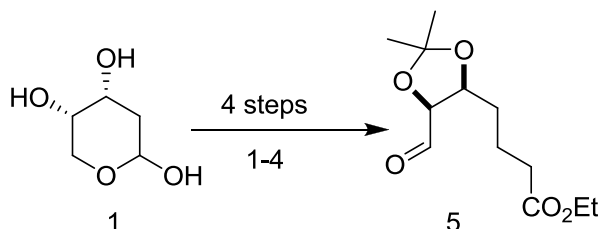
All reactions were carried out under an inert atmosphere of nitrogen using oven dried glassware. All solvents and reagents were purchased commercially from sigma-Aldrich and were utilized without further purification unless specifically noted. Dry solvents were obtained from a sodium/benzophenone still, from water free bottles or dried over molecular sieves before use. Flash chromatography was carried out using silica gel 35-70 micron from DAVISIL. Evaporation in vacuo refers to the removal of volatiles on a Büchi rotary evaporator with an integrated vacuum pump. Thin-layer chromatography (TLC) was performed on Merc KGaA, 60 F254 silica gel plates and visualized with UV and stains. Microwave reactions were carried out using microwave synthesis reactor, monowave 300 from Anton Paar.

NMR spectra were recorded on Varian Mercury-400 Oxford NMR Spectrometers and Oxford NMR 400 MHz and 400 MHz Bruker Avance III HD equipped with a 5 mm SmartProbe BB/1H, using CDCl₃ as the solvent. The reference values used for deuterated chloroform (CDCl₃) were 7.26 and 77.02 ppm for ¹H and ¹³C-NMR spectra, respectively. Deuterated DMSO (DMSO-d₆) reference values were 2.5 and 39.51 ppm for ¹H and ¹³C-NMR spectra, respectively. Chemical shift values (δ) are reported in parts per million (ppm) commensurate to tetramethylsilane (TMS) as standard. Multiplicities are indicated as s (singlet), d (doublet), t (triplet), q (quartet), p (pentet), m (multiplet), bs (broad singlet) and coupling constant *J* were reported in Hz.

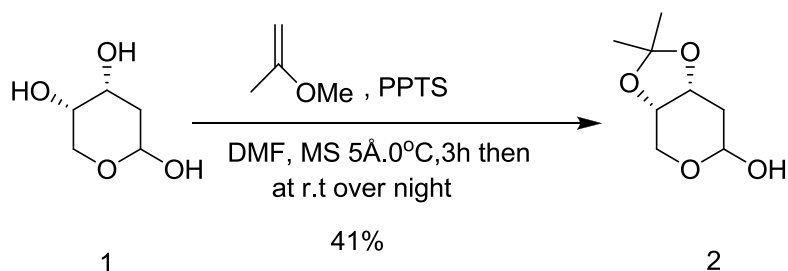
All NMR spectra were processed with MestReNova v7.1.1.1. Some ¹³C-NMR spectra from the early model studies have artifacts in a repeating pattern originated from unknown transmitter. Some ¹H-NMR spectra may contain some of remaining solvents, mainly EtOAc. Infrared spectra were recorded on a Varian 700e FT-IR spectrometer and bands are reported in wavenumber (cm⁻¹). High resolution MS was recorded on a thermos electron LTQ Orbitrap XL +Electrospray ion source (ION/MAX) using methanol as solvent. The melting points was measured with Buchi 535 instrument.

5.2 DETAILED EXPERIMENTAL PROCEDURES AND CHARACTERIZATIONS

5.2.1 Synthesis of the aldehyde



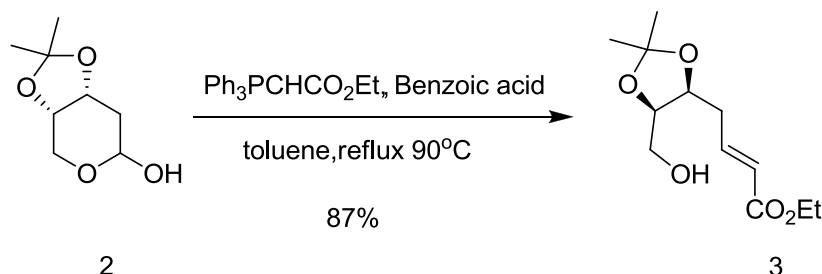
5.2.1.1 Synthesis of the protected 2-deoxy-D-ribose



The commercially available 2-deoxy-D-ribose **1** (3 g, 22.36 mmol) was dissolved in 10ml DMF in a dry and clean round bottomed flask equipped with molecular sieves and stir bar. The mixture stirred under N₂ gas at 0°C before 2-Methoxypropene (3.225 g, 44.72 mmol) was slowly added to it. In another flask, a solution of pyridinium *p*-toluenesulfonate (0.50 g, 20.12 mmol) in minimum amount of DMF was stirring for 5 min before addition to the reaction mixture at 0°C. The reaction continued stirring at 0°C for 3h, then it was left overnight at room temperature. The product was filtered by suction and washed several times with DMF then dried in a high pressure pump. The crude was purified by means of column chromatography (pentane/ethyl acetate, 1:1) affording a colorless oily liquid (1.751 g, 41 %) of the protected sugar **2**. TLC; R_f=0.2 (heptane/ethyl acetate, 1:1); **HRMS** (ESI) *m/z*: [M+Na]⁺ Calcd. for C₈H₁₄O₄Na 197.08, found 197.0800 and [M+MeOH]⁺ 299.1000; ¹H-NMR (DMSO-d₆, 400 MHz) δ =6.24 (d, *J*=8 Hz, 1H), 4.95-4.91 (m, 1H), 4.33 (dd, *J*= 4, 16 Hz, 1H), 4.04 (dd, *J*= 4, 16 Hz, 1H), 3.77 (dd, *J*= 4, 16Hz, 1H), 3.45 (dd, *J*= 4, 16Hz, 1H), 1.95-1.89 (m, *J*= 4, 1H), 1.66-1.59 (m, 1H), 1.35 (s, 3H), 1.22(s, 3H)

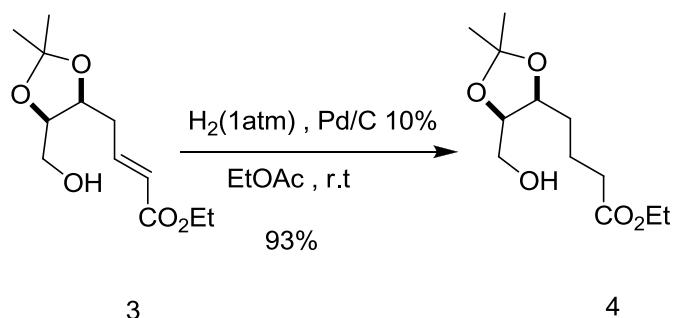
; $^{13}\text{C-NMR}$ (DMSO- d_6 , 100 MHz) δ =108.0, 90.4, 71.3, 70.7, 61.6, 33.2, 27.8, 25.9. The data is consistent with literature [166, 185]. **Appendix 1.**

5.2.1.2 Synthesis of the unsaturated alcohol from the protected sugar



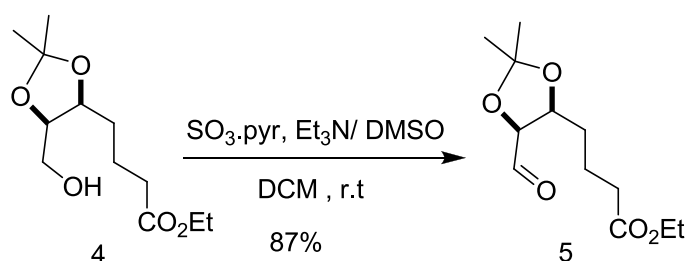
The protected sugar **2** (0.787, 4.51mmol) was dissolved in 10 ml toluene and left under reflux with stirring until it reaches 90°C . Benzoic acid (0.0276, 0.226 mmol) was added to the reaction mixture followed by the slow addition of the Wittig salt solution in toluene to the reaction mixture at 90°C . Reaction was refluxing for 2h and monitored by TLC. Upon completion, the solvent was evaporated in a rotavap and the crude was washed with diethyl ether to remove the excess of the Wittig salt. The resulted oil was purified by means of column chromatography (pentane/ ethyl acetate , 1:1) affording UV active colorless oily liquid (0.96 g, 87%) of the alkene **3** .TLC; R_f = 0.3 ; **HRMS** (ESI) m/z : $[\text{M}+\text{Na}]^+$ Calcd. for $\text{C}_{12}\text{H}_{20}\text{O}_5\text{Na}$ 267.12 found 267.1200; $^1\text{H-NMR}$ (CDCl_3 , 400 MHz) δ =6.97-6.90 (m, 1H), 5.89 (d, J =16 Hz, 1H), 4.29-4.24 (m, 1H), 4.20-4.13 (m, 3H), 3.63 (d, J =8 Hz, 2H), 2.54-2.39 (m, 2H), 2.23(d, J =8, 1H), 1.45 (s, 3H), 1.34 (s, 3H), 1.25 (t, J =8 Hz, 3H) ; $^{13}\text{C-NMR}$ (CDCl_3 , 100 MHz) δ =166.2, 144.5, 123.5, 108.4, 77.5, 75.3, 61.3, 60.3, 32.3, 27.9, 25.2, 14.2. The data is consistent with literature [166].**Appendix 2.**

5.2.1.3 Reduction of the alkene



The previously prepared alkene **3** (0.568, 2.32 mmol) was dissolved in 10 ml ethyl acetate with 10% pd/C. The reaction mixture was stirring at room temperature under H_2 gas (1mp) for 5h. The rection progress was monitored by TLC. Upon completion the reaction mixture was filtered by suction on a Büchner funnel loaded with a celite cake to capture the catalyst. The filtrate was collected and the solvent was evaporated in a rotavap affording (0.55 g, 93%) UV inactive colourless liquid of **4**. TLC; $R_f=0.3$ (heptane/ethylacetate, 1:1); **HRMS** (ESI) m/z : $[\text{M}+\text{Na}]^+$ Calcd. For $\text{C}_{12}\text{H}_{22}\text{O}_5\text{Na}$ 269.14 , found 269.1350; **$^1\text{H-NMR}$** (CDCl_3 , 400 MHz) δ = 4.09-4.04 (m, 5H), 3.54 (d, J = 8 Hz, 2H), 2.29 (q, J = 4Hz, 2H), 2.09 (d, J = 8 Hz, 1H), 1.97 (s, 1H), 1.79-1.75 (m, 1H), 1.66-1.61 (m, 1H), 1.55-1.51 (m, 2H), 1.39 (s, 3H), 1.29 (s, 1H), 1.18 (t, J = 8Hz, 4H); **$^{13}\text{C-NMR}$** (CDCl_3 , 100 MHz) δ =173.3, 108.1, 77.8, 61.6, 60.3, 33.9, 28.1, 25.4, 22.0, 14.2. The data is consistent with literature [166]. **Appendix 3**.

5.2.1.4 Synthesis of the aldehyde

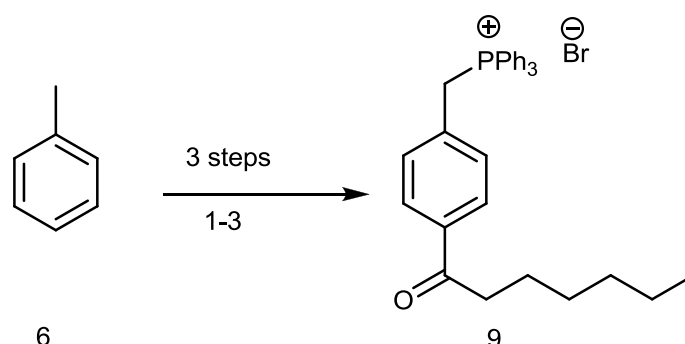


The alcohol **4** (0.2 g, 0.8126) was dissolved in 10 ml DCM with stirring under N_2 gas. (0.45g, 2.82 mmol) of $\text{SO}_3\text{-Pyr}$ was added to the mixture and cooled down to 0°C in an ice bath with stirring. Meanwhile, a solution of (0.40 g, 0.55 ml) triethylamine in 2.07 DMSO was stirring for 5 min before adding to the reaction mixture at 0°C , 5 min after addition the ice bath was removed and the reaction mixture continued to stir at room temperature for 1h .

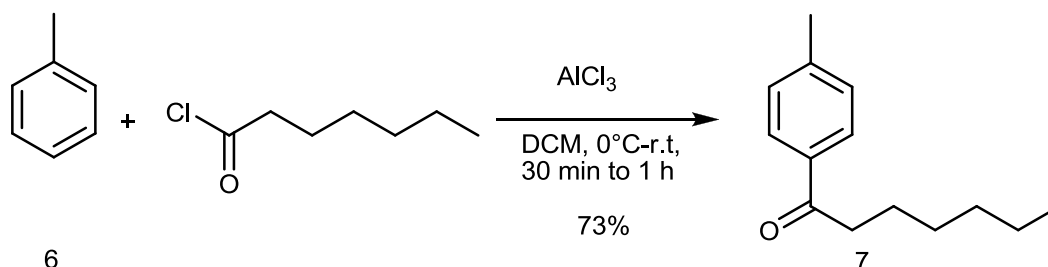
Reaction progress was monitored by TLC, product is UV active. After completion the reaction was quenched by 10 ml distilled water and stirred for 5 min before transferring into a separation funnel. After separation of the two phases. The aqueous phase extracted with DCM the organic phase concentrated in a rotavap. The crude was washed with water, sodium bicarbonate and brine, dried over Na₂SO₄, filtered and concentrated in a rotavap affording brownish orange liquid (1.73, 87%) ethyl 4-(5-formyl-2,2-dimethyl-1,3-dioxolan-4-yl)butanoate **5**. TLC; R_f=0.12 (heptane/ethylacetate, 4:1); HRMS (ESI) m/z: [M+Na]⁺ Calcd. For C₁₂H₂₀O₅Na 267.12, found C₁₂H₂₀O₅Na 267.1200, and [M+MeOH]⁺ 299.1460; ¹H-NMR (CDCl₃, 400 MHz) δ =9.56 (s, 1H), 4.29-4.25 (m, 1H), 4.195 (dd, J= 4, 16 Hz, 1H), 4.05 (q, J= 8, 2H), 2.26 (t, J= 8Hz, 2H), 1.77-1.73 (m, 1H), 1.67-1.62 (m, 1H), 1.59-1.54 (m, 1H), 1.51 (s, 3H), 1.34 (s, 3H), 1.18 (t, J= 8 Hz, 3H); ¹³C-NMR (CDCl₃, 100 MHz) δ= 201.9, 172.9, 110.4, 81.8, 78.1, 60.2, 33.6, 29.0, 27.5, 25.2, 21.8, 14.1. **Appendix 4**.

5.2.2 Synthesis of the Wittig salts

5.2.2.1 Wittig salt of the ketone moiety containing compound



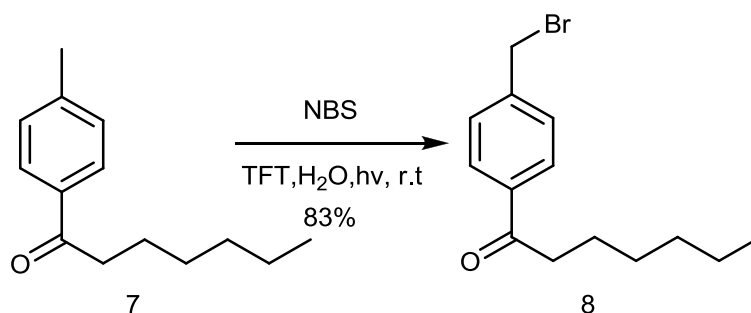
5.2.2.1.1 Synthesis of the acylated toluene



Aluminum chloride (4.42 g, 33.18 mmol) was dissolved in 20 ml of dichloromethane while stirring in an ice bath at 0°C. Heptanoyl chloride (4.896 g, 32.94 mmol) was added dropwise to the reaction mixture followed by dropwise addition of toluene (2.73 g, 29.634 mmol).

After addition, ice bath was removed and the mixture continued stirring for 30 min at room temperature, the reaction was monitored by TLC. The reaction mixture was poured slowly with stirring into a beaker contained 30 g of ice and 10 ml conc HCl, transferred into a separation funnel and extracted with ethyl acetate (2*30 ml). The organic phase was collected and washed with saturated sodium bicarbonate (20 ml), brine (20 ml), dried over Na₂SO₄ then concentrated in rotavap. Crystals collected and purified by recrystallization in ethanol/water (5:1), filtered and dried in vacuo affording white crystals of **7** (4.387 g, 73 %). **m.p.** : 35.5-36.8 °C. TLC; R_f = 0.8 (hexan/ethyl acetate, 9:1); ¹H-NMR (CDCl₃, 400 MHz) δ = 7.85 (d, J = 8 Hz, 2H), 7.24 (d, J = 8 Hz, 2H), 2.92 (t, J = 8 Hz, 2H), 2.40 (s, 3H), 1.74-1.68 (m, 3H), 1.37-1.32 (m, 7H), 0.88 (t, J = 4 Hz, 3H); ¹³C NMR (CDCl₃, 100 MHz) δ = 200.2, 143.5, 134.6, 129.1, 128.1, 38.5, 31.6, 29.0, 24.4, 22.5, 21.5, 14.0. The data is consistent with literature [187]. **Appendix 5.**

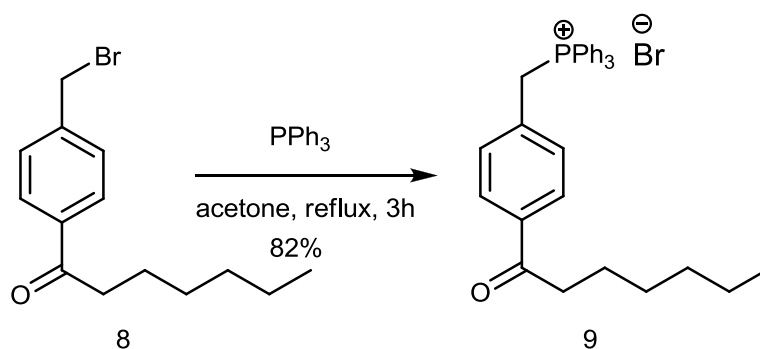
5.2.2.1.2 Synthesis of benzylic brominated *p*-acylated toluene



The previously synthesized acyl toluene **7** (3 g, 14.68 mmol) was dissolved in 12 ml of trifluorotoluene benzene. NBS (2.62 g, 14.72 mmol) was dissolved in 30 ml of H₂O then the mixture was added dropwise to the reaction flask, stirred and illuminated with a 60 W incandescent light bulb for 27 h. Reaction was monitored by TLC. Crude was collected from the reaction flask, extracted with 15 ml ethyl acetate and the organic phase washed with 15 ml brine, dried over Na₂SO₄, filtered, and concentrated on rotavap. Crude underwent purification by means of recrystallization in ethanol/water (5:1). Crystals were filtered, washed with water, and dried in vacuo affording white crystals of **8** (3.46 g, 83 %). **m.p.**: 49-50 °C. TLC ; R_f = 0.2

(hexane/ethyl acetate, 9:1); $^1\text{H-NMR}$ (CDCl_3 , 400 MHz) δ =7.93 (d, J = 8, 2H), 7.48 (d, J = 8, 2H), 4.51 (s, 2H), 2.94 (t, J = 8 Hz, 2H), 1.73 (m, 2H), 1.38-1.31 (m, 6H), 0.89 (t, J = 4 Hz, 3H); $^{13}\text{C-NMR}$ (CDCl_3 , 100 MHz) δ = 195.8, 167.1, 138.5, 132.9, 127.7, 125.2, 124.6, 122.8, 121.1, 56.4, 34.7, 28.2, 27.6, 25.0, 20.3, 18.5, 17.0, 10.0. The data is consistent with literature [169]. **Appendix 6.**

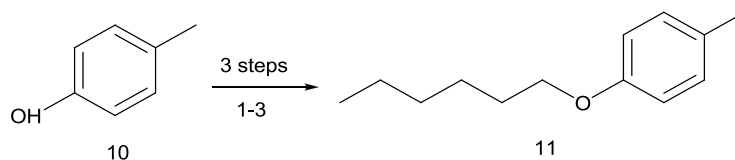
5.2.2.1.3 Synthesis of the Wittig salt



1-(4-(bromomethyl) phenyl) heptan-1-one **8** (1.73 g, 6.1 mmol) was dissolved in 50 ml of acetone followed by addition of triphenylphosphine (1.86 g, 6.58 mmol). The reaction mixture stirred under reflux for 3h at 65°C, the reaction was monitored by TLC. Crude was cooled down forming crystals, filtrated under vacuum filtration, rinsed with diethyl ether, and dried in a desiccator. White clear crystals was obtained (1.58 g, 82 %) of the salt **9**. **m.p.:** 237-236 °C. TLC; R_f = 0.7 (hexane/ethyl acetate, 9:1); **IR** (cm^{-1}) 3044, 2925, 2852, 2771, 1679, 1436, 689; **HRMS** (ESI) m/z : $[\text{M}+\text{H}]^+$ Calcd. For $\text{C}_{32}\text{H}_{34}\text{OP}$ 453.23, found 453.2300 ; $^1\text{H-NMR}$ (CDCl_3 , 400 MHz) δ =7.80-7.75 (m, 10H), 7.68 (d, J =8 Hz, 2H), 7.63 (dd, J = 4, 16 Hz, 5H), 7.60 (d, J =4 Hz, 2H), 7.28 (d, J = 4 Hz, 1H) , 7.26 (d, J =4 Hz, 1H), 5.64 (d, J = 16 Hz, 2H), 2.85 (t, J = 8 Hz, 2H), 1.66 -1.63 (m, 5H), 1.36-1.30 (m, 7H), 0.88 (t, J =4 Hz, 3H); $^{13}\text{C-NMR}$ (CDCl_3 , 100 MHz) δ = 199.8, 142.4, 136.8, 129.1, 128.5, 38.7, 32.1, 31.6, 29.00, 24.2, 22.5, 14.0. The data is consistent with literature [170, 171].

Appendix 7.

5.2.2.2 Wittig salt of the ether moiety containing compound



5.2.2.2.1 Synthesis of O-alkylated p-cresol.

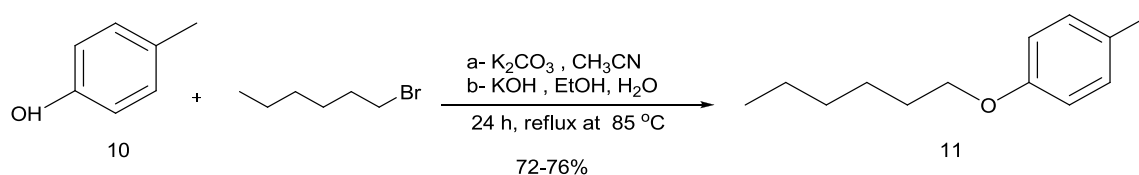


Table 3. The trials towards the O-alkylated product.

Trial	Base	Solvent	Yield %
A	13.6g K_2CO_3	50 ml, CH_3CN	(3.837g, 72%)
b	4.5g KOH	5:45 ml (H_2O , $EtOH$)	(4.071g, 76%)

The commercially available p-cresol (3 g, 2.901 ml, and 27.77 mmol) was dissolved in a certain amount of the solvent with the base under stirring, followed by the addition of 1-bromohexane (4.94 g, 4.25 ml, and 30.547mmol). The reaction mixture refluxed with stirring at $85^\circ C$ under N_2 gas for 24 h, Reaction was monitored by TLC. The reaction mixture removed from heat source and gravity filtered off from the access of the base, rinsed with with DCM and the crude was concentrated in a rotavap. Work up on the crude was done by washing with 100 ml $NaOH$ (2x), H_2O (2x), brine (1x), the organic phase was extracted with DCM and dried over Na_2SO_4 , filtered and finally concentrated on rotavap. The crude was pure no further purification was done to the crude product. TLC; R_f =0.5 (hexane/ ethyl acetate, 9.5: 0.5); ^1H-NMR ($CDCl_3$, 400 MHz) δ =7.11 (d, J = 8 Hz, 2H), 6.84 (d, J = 8 Hz, 2H), 3.95 (t, J = 8 Hz, 2H) , 2.32 (s, 3H), 1.82-1.77 (m, 2H), 1.53-1.48 (m, 2H), 1.39-1.38 (m,4H), 0.95 (t, J = 8Hz, 3H); $^{13}C-NMR$ ($CDCl_3$, 100 MHz) δ

=157.0, 129.8, 129.6, 114.3, 68.0, 31.6, 29.3, 25.7, 22.6, 20.4, 14.0. The data is consistent with literature [170, 171]. **Appendix 8.**

5.2.2.2.2 Synthesis of benzylic brominated *p*-cresol derivative.

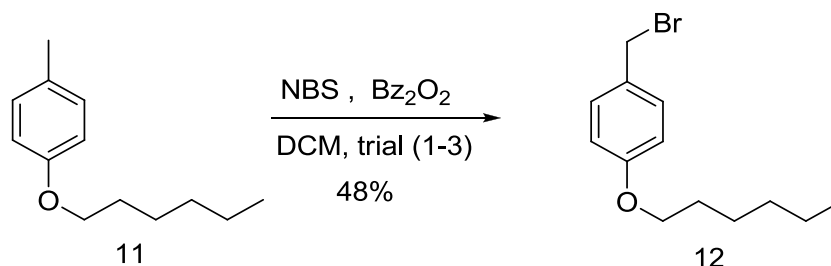


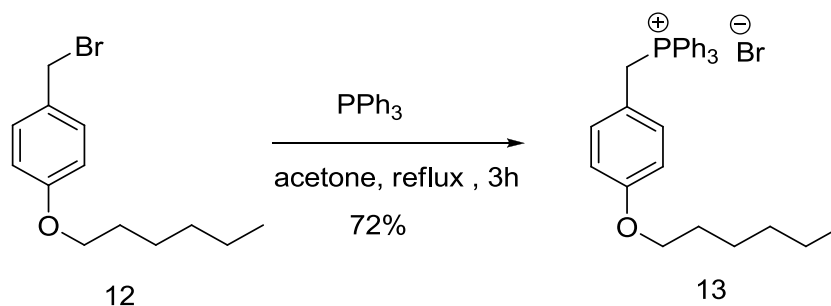
Table 1. Reaction optimization towards the bromination of the benzylic ether

Trial	Solvent	Reaction time	Equivalency (cpd 11: NBS)	Yield%	product
1	CHCL3	9h (3*3)	1:3	19 %	Dibromo
2	CHCL3	9h (3*3)	3:1	83 %	mix
3	DCM	6h (2*3)	3:1	48%	monobromo

1-(hexyloxy)-4-methylbenzene **11** (3.5 g, 18.21 mmol, 3 eq) was dissolved in 121.4 ml chloroform, NBS (3*0.35, 5.95 mmol, 1 eq) was added to the reaction flask in three equal portions in each addition few mg of benzoyl peroxide was also added, refluxed at 68°C for. Upon completion of reaction, the mixture was cooled and filtered. Crude product washed with saturated NaHCO₃ solution (100 ml), brine (100 ml), dried over Na₂SO₄, filtered and concentrated on rotavap. Purification by vacuum distillation ≈4 torr and remaining amount separated using short path distillation (Kugler-distill) affording pure colorless liquid of 1-(bromomethyl)-4-(hexyloxy)benzene **12**. ¹H-NMR (CDCl₃, 400 MHz,) δ = 7.10 (d, *J* = 12 Hz, 2H), 6.83 (d, *J* = 8 Hz, 2H), 5.30 (s, 2H), 3.95 (t, *J* = 4 Hz, 2H), 2.32 (s, 3H), 1.83-1.76 (m, 2H), 1.53-1.46 (m, 2H), 1.39-1.35 (m, 4H),

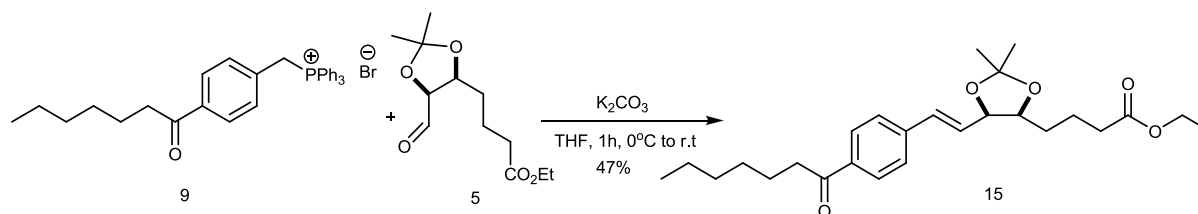
0.94 (t, $J = 8$ Hz, 3H); $^{13}\text{C-NMR}$ (CDCl_3 , 100 MHz) $\delta = 157.0, 129.8, 114.3, 76.6, 68.0, 31.6, 29.3, 25.7, 22.6, 20.4, 14.0$. The data is consistent with literature [170]. **Appendix 9.**

5.2.2.2.3 Synthesis of the Wittig salt



The previously prepared compound **12** (0.565g, 2.07mmol) was dissolved in 20ml acetone, triphenylphosphine (0.58g, 2.25mmol) was added to the reaction mixture and stirred for 3h under reflux at 65°C the reaction was monitored by TLC. After complete reaction, the crude concentrated in a rotavap. The crude washed with ethyl acetate and filtered affording white powder (0.676g, 72%) of 4-(hexyloxy) benzyltriphenylphosphonium bromide **13**. **m.p.:** 360-361°C. **TLC:** $R_f = 0.2$ (hexane/ethyl acetate, 5:1); **IR** (cm^{-1}) 3053, 2926, 2856, 1606, 1508, 1436, 843; **HRMS** (ESI) m/z : $[\text{M}+\text{H}]^+$ Calcd. For $\text{C}_{31}\text{H}_{34}\text{OP}$ 465.23, found 465.2300; $^1\text{H NMR}$ (CDCl_3 , 400 MHz) $\delta = 7.72\text{-}7.63$ (m, 8 H), 7.58 (d, $J = 4$ Hz, 2H), 7.56 (d, $J = 4$, 2H), 7.54 (d, $J = 4$, 1H), 6.92 (dd, $J = 4, 16$ Hz, 2H), 6.57 (d, $J = 8$ Hz, 2H), 5.23 (d, $J = 16$ Hz, 2H), 3.78 (t, $J = 8$ Hz, 2H), 1.69-1.62 (m, 2H), 1.38-1.31 (m, 2H), 1.26-1.23 (m, 4H), 0.82 (t, $J = 8$ Hz, 3H); $^{13}\text{C NMR}$ (CDCl_3 , 100MHz) $\delta = 159.2, 134.9, 134.4, 130.0, 118.4, 117.5, 114.8, 68.0, 31.5, 29.1, 25.6, 22.5, 14.0$. The data is consistent with literature [170, 171]. **Appendix 10.**

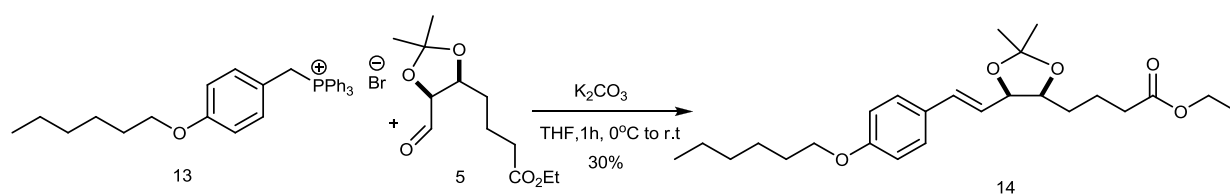
5.2.3 Synthesis of the alkene via Wittig coupling of the ketone partner.



The Wittig salt **9** (0.79g, 1.44 mmol) was dissolved in minimum amount of THF at 0°C in a dry and clean round bottomed flask under N_2 gas. Meanwhile Potassium *t*-butoxide (0.3 g, 2.67 mmol) was dissolved in minimum amount of THF at in another flask, the base solution was

added slowly during 15 min to the reaction flask while stirring at 0°C. After complete addition, cooling source was removed and the reaction mixture was continued stirring for 20 min at room temperature. A solution of the aldehyde **5** (0.27g, 1.105 mmol) in THF was added slowly to the reaction mixture at room temperature. After complete addition the reaction mixture continued stirring for 1-2 hr, reaction progress was monitored by TLC. After complete reaction the solvent was removed in a rotavap, the crude was washed with water and extracted with ethyl acetate, and organic phases was collected, dried over Na₂SO₄, and concentrated on rotavap. The crude was further purified by means of column chromatography (hexane, ethyl acetate, 10:1) affording yellow liquid (0.22 g, 47%). TLC; R_f=0.35 (hexane/ethyl acetate, 5:1); HRMS (ESI) m/z: [M+Na]⁺ Calcd. For C₂₆H₃₈O₅Na 453.26, found 453.2610; IR (cm⁻¹) 2955, 2865, 1732, 1682, 1218, 1030, 856; ¹H-NMR (CDCl₃, 400 MHz) δ =7.94 (d, J= 8 Hz, 2H), 7.43 (d, J= 8 Hz, 1H) 7.33 (d, J= 8 Hz, 1H), 6.74 (d, J= 8 Hz, 1H), 5.83 (t, J= 12 Hz, 1H), 4.92-4.88 (m, 1H), 4.21-4.18 (m, 1H), 4.14-4.11 (m, 3H), 2.95 (t, J= 8 Hz, 2H), 2.34 (t, J= 8 Hz, 2H), 2.04 (s, 2H), 1.72-1.66 (m, 2H), 1.63-1.65 (m, 2H), 1.58-1.22 (m, 18H), 1.25-1.22 (m, 5H), 0.89 (t, J= 8 Hz, 3H); ¹³C-NMR (CDCl₃, 100MHz) δ=199.9, 173.2, 140.6, 135.9, 132.4, 129.5, 128.7, 128.1, 108.46, 78.1, 74.0, 60.2, 38.6, 34.0, 31.6, 29.8, 29.0, 28.3, 25.6, 24.3, 22.5, 21.8, 14.2. **Appendix 11.**

5.2.4 Synthesis of the alkene via Wittig coupling of the ether partner

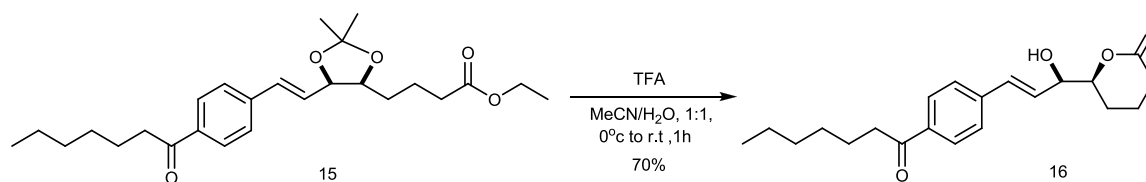


The Wittig salt **13** (0.2g, 0.44 mmol) was dissolved in minimum amount of THF at 0°C in a dry and clean round bottomed flask under N₂ gas. Meanwhile, Potassium t-butoxide (0.11 g, 0.90 mmol) was dissolved in minimum amount of THF at in another flask, the base solution was added slowly during 15 min to the reaction flask while stirring at 0°C. After complete addition, cooling source was removed and the reaction mixture was continued stirring for 20 min at room temperature. A solution of the aldehyde **5** (0.1g, 0.40 mmol) in THF was added slowly to the reaction mixture at room temperature. After complete addition the reaction mixture continued stirring for 1-2 hr, reaction progress was monitored by TLC. After complete reaction the solvent

was removed in a rotavap, the crude was washed with water and extracted with ethyl acetate, and organic phases was collected, dried over Na₂SO₄, and concentrated on rotavap. The crude was further purified by means of column chromatography (pentane, ethyl acetate, 9:1) affording yellow liquid (0.055 g, 30%) of the alkene **14**. TLC; R_f =0.36 (hexane/ethyl acetate, 5:1); IR (cm⁻¹) 2933, 1733, 1510, 1174, 1025, 839; HRMS (ESI) m/z: [M+Na]⁺ Calcd. for C₂₅H₃₈O₅Na 441.26, found 441.2600; ¹H-NMR (CDCl₃,400 MHz) δ=7.08 (d, J= 8 Hz, 2H), 6.79 (d, J= 8 Hz, 2H), 6.57 (d, J= 12 Hz,1H), 5.54 (t, J= 12 Hz, 1H), 4.89 (t, J= 4 Hz, 1H), 4.13-4.09 (m, 2H), 4.06-4.03 (m, 5H), 3.87 (t, J= 8 Hz 2H), 2.26 (t, J= 12 Hz, 2H), 1.96 (s, 5H), 1.72-1.68 (m, 3H), 1.62-1.52 (m, 2H), 1.42 (s, 5H), 1.38-1.35 (m, 2H), 1.26 (s, 6H), 1.19-1.16 (m, 8H), 0.88 (t, J= 8 Hz, 3H); ¹³C-NMR (CDCl₃, 100 MHz) δ=173.3, 171.0, 158.5, 133.1, 129.8, 128.5, 125.7, 114.2, 108.1, 78.2, 74.3, 67.9, 60.3, 34.1, 31.5, 30.0, 29.1, 28.3, 25.6, 22.5, 21.8, 20.9,14.1.

Appendix 12.

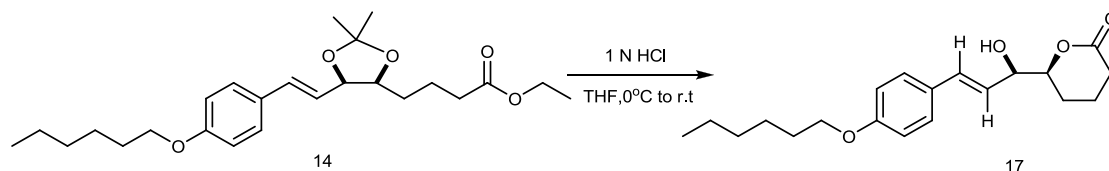
5.2.5 Hydrolysis of the acetonid in the ketone containing analogue



The previously synthesized alkene **15** (0.022g, 0.05mmol) was dissolved in a mixture of acetonitrile and water (1:1) with stirring at 0°C. TFA (0.8 ml) was added dropwise to the stirring mixture at 0°C after complete addition the ice bath was removed and the reaction kept stirring at room temperature for 1h. The reaction progress was monitored by TLC. After complete reaction it was slowly quenched with 2ml sodium bicarbonate and extracted several times with ethyl acetate the combined organic phase was washed with water and brine, dried over sod.sulfate and concentrated in a rotavap affording oily green oily liquid (0.012,70 %) of lactone **16**. TLC; R_f =0.45(CHCl₃/MeOH, 9.8:0.2); IR (cm⁻¹) 2928, 2857, 2248, 2159, 1729, 1679, 1603, 1239, 1049; HRMS (ESI) m/z: [M+Na]⁺ Calcd. for C₂₁H₂₈O₄Na 367.19, found 367.1883; ¹H-NMR (400 MHz, CDCl₃) δ=7.88-7.82 (m, 2H), 7.33 (dd, J=8, 32 Hz,2H), 6.68 (t, J=8 Hz, 1H), 5.83-5.73 (m, 1H), 4.40-4.36 (m, 1H), 4.24-4.21 (m, 1H), 3.49 (bs, 1H), 2.87 (t, J=8 Hz, 2H), 2.58-2.49 (m, 1H), 2.43-2.31 (m, 1H), 1.81-1.72 (m, 2H), 1.69-1.50 (m, 3H), 1.32-1.18 (m, 7H), 0.82 (t, J=8 Hz,

3H); $^{13}\text{C-NMR}$ (CDCl_3 , 100 MHz) δ =200.1, 171.4, 140.5, 136.1, 133.8, 129.7, 128.9, 128.3, 83.1, 69.7, 68.9, 38.7, 31.6, 29.8, 29.0, 24.4, 22.5, 18.3, 14.0. **Appenix 13.**

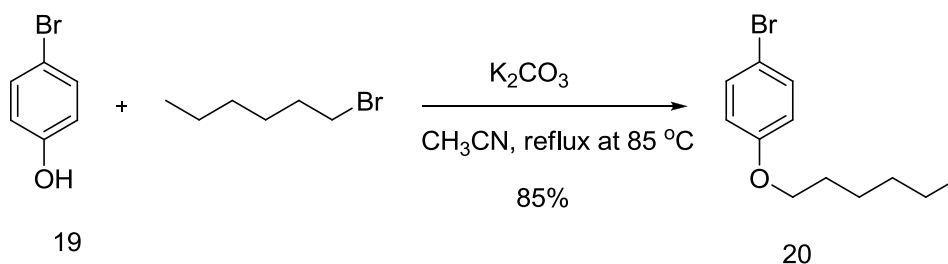
5.2.6 Hydrolysis of acetonid of the ether containing analogue



The previously synthesized alkene **14** (0.022g, 0.05mmol) was dissolved in 2ml THF, 2ml of 1N HCl was added dropwise to the stirring mixture at 0°C after complete addition the ice bath was removed and the reaction kept stirring at room temperature overnight. The reaction progress was monitored by TLC. After complete reaction it was slowly quenched with 2ml NaOH and extracted several times with ethyl acetate the combined organic phase was washed with water and brine, dried over sodium sulfate and concentrated in a rotavap affording colorless liquid. TLC; R_f = 0.45($\text{CHCl}_3/\text{MeOH}$, 9.8:0.2); IR (cm^{-1}) 2927, 2857, 1711, 1606, 1510, 1174, 1049, 839; HRMS (ESI) m/z : $[\text{M}+\text{Na}]^+$ Calcd. for $\text{C}_{21}\text{H}_{28}\text{O}_4\text{Na}$ 355.19 found 355.1884; $^1\text{H-NMR}$ (CDCl_3 , 400 MHz) δ = 7.19 (s, 1H), 7.09 (d, J = 8 Hz, 1H), 6.79 (d, J = 12 Hz, 2H), 6.58 (d, J = 12 Hz, 1H), 5.55 (t, J = 8 Hz, 1H), 4.92-4.88 (m, 1H), 4.14-4.09 (m, 1H), 4.04 (q, J = 8 Hz, 2H), 3.89 (t, J = 8 Hz, 2H), 2.27 (t, J = 4 Hz, 2H), 1.73-1.69 (m, 3H), 1.61-1.53 (m, 2H), 1.43 (s, 3H), 1.41-1.36 (m, 2H), 1.28-1.27 (m, 6H), 1.19-1.15 (m, 3H), 0.84 (t, J = 8 Hz, 3H); $^{13}\text{C-NMR}$ (CDCl_3 , 100 MHz,) δ = 172.3, 157.5, 132.1, 128.8, 127.4, 124.7, 113.2, 107.1, 77.2, 73.3, 67.0, 59.2, 33.1, 30.5, 29.0, 28.1, 27.4, 24.7, 21.5, 20.8, 13.0. **Appenix 14.**

5.2.7 Ullmann approach

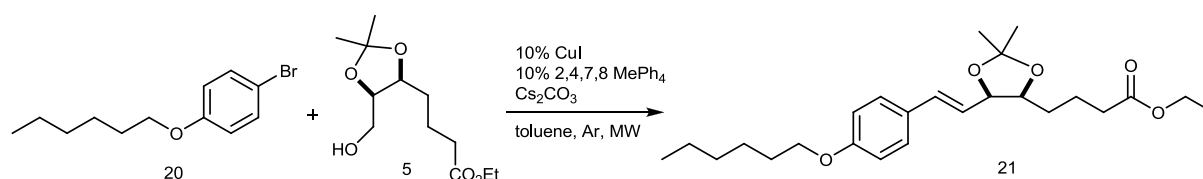
5.2.7.1 Synthesis of the O-alkylated phenol derivative.



The commercially available 4-bromophenol **19** (1g, 5.78 mmol) was dissolved in 20 ml acetonitrile. (1.59g, 11.56mmol) potassium carbonate was added to the reaction mixture under stirring for 5 min before (1.048 g, 6.35 mmol) 1-bromohexane slowly added to the reaction flask and the mixture left refluxing with stirring under N₂ gas for 24h.

The reaction was monitored by TLC. After reaction completion the crude left to cool down and the excess of the base was filtered off and rinsed with acetonitrile. The crude concentrated in rotvap before washing with 1M NaOH to remove the unreacted phenol derivatives, H₂O, and brine and the crude was extracted with ethyl acetate and dried over Na₂SO₄, filtered and concentrated in a vacuo affording colorless oil (1.27g, 85%). The product was quit pure after the workup, no further purification was done on it. TLC; R_f =0.36 (heptane/ethyl acetate, 9.8:0.2); ¹H-NMR (CDCl₃, 400 MHz) δ=7.41 (d, J= 8 Hz ,2H), 6.82 (d, J= 8, 2H), 3.96 (t, J= 4Hz, 2H), 1.85-1.78 (m, 2H), 1.50-1.39 (m, 6H), 0.96 (t, J= 8Hz, 3H); ¹³C-NMR (CDCl₃, 100 MHz) δ=158.2, 132.2, 116.3, 112.5, 68.2, 31.6, 29.1, 25.7, 22.6, 14.0. **Appenix 15.**

5.2.7.2 Synthesis of Ullmann ether.



(10%) CuI, (10%) 2,4,7,8 Me₂Ph₄, and Cs₂CO₃ were added in reaction tube with the (0.0898 g, 0.349 mmol) of the previously synthesized 1-bromo-4-(hexyloxy) benzene **20**. The reaction tube was evacuated from air and backfilled with argon. (0.129 g, 0.523 mmol) of the aldehyde was added with 5ml of toluene through a syringe to the reaction mixture. The reaction tube was submitted to the Microwave apparatus under 160°C for 5h. The reaction was monitored every hour during the reaction time. After 5h the crude was filtered and washed with ethyl acetate. The product couldn't be indicated, the TLC showed the presence of the two starting material and indicated no reaction.

6 REFERENCES

- 1- Chiang N, Arita M, Serhan CN (2005) Anti-inflammatory circuitry: lipoxin, aspirin-triggered lipoxins and their receptor ALX. *Prostaglandins LeukotEssent Fatty Acids* 73:163–177.
- 2- Chiang N, Serhan CN, Dahlen SE, Drazen JM, Hay DW, Rovati GE, Shimizu T, Yokomizo T, Brink C (2006) The lipoxin receptor ALX: potent ligand-specific and stereoselective actions in vivo. *Pharmacol Rev* 58:463–487.
- 3- Mitchell D, O’Meara SJ, Gaffney A, Crean JK, Kinsella BT, Godson C(2007) The Lipoxin A4 receptor is coupled to SHP-2 activation:implications for regulation of receptor tyrosine kinases. *J BiolChem* 282:15606–15618.
- 4- Norel X, Brink C (2004) The quest for new cysteinyl-leukotriene and lipoxin receptors: recent clues. *PharmacolTher* 103:81–94.
- 5- Schaldach CM, Riby J, Bjeldanes LF (1999) Lipoxin A4: a new class of ligand for the Ah receptor. *Biochemistry* 38:7594–7600.
- 6- Pamplona FA, et al. (2012) Anti-inflammatory lipoxin A4 is an endogenous allosteric enhancer of CB1 cannabinoid receptor. *ProcNatlAcadSci USA* 109:21134–21139.
- 7- Pertwee RG (2012) Lipoxin A4 is an allosteric endocannabinoid thatstrengthens anandamide-induced CB1 receptor activationPNAS| vol. 109 | no. 51 | 20781–20782.
- 8- Svensson CI, Zattoni M, Serhan CN (2007) Lipoxins and aspirintriggeredlipoxin inhibit inflammatory pain processing. *J Exp Med* 204:245.
- 9- Mitchell S, Thomas G, Harvey K, Cottell D, Reville K, Berlasconi G et al. Lipoxins, aspirin-triggered epi-lipoxins, lipoxin stable analogues, and the resolution of inflammation: stimulation of macrophage phagocytosis of apoptotic neutrophils in vivo. *J Am Soc Nephrol* 2002, 13: 2497–2507. A paper outlining the effects of LXA4 on macrophage reprogramming
- 10- Ye XH, Wu Y, Guo PP, Wang J, Yuan SY, Shang Y, Yao SL (2010) Lipoxin A4 analogue protects brain and reduces inflammation in a rat model of focal cerebral ischemia reperfusion. *Brain Res* 1323:174–183.
- 11- Colm Duffy (2012) Hetroaromatic Lipoxine A4 Analogues: Synthesis and Biological Evaluation.Springer-Verlag Berlin Heidelberg.
- 12- Clish CB, Levy BD, Chiang N, Tai HH, Serhan CN(2000)Oxidoreductases in lipoxin A4 metabolic inactivation: a novel role for 15-onoprostaglandin 13-reductase/leukotriene B4 12-hydroxydehydrogenase in inflammation. *J Biol Chem.* 275:25372–25380.
- 13- Duymaz,A., U. Nubbemeyer, ORCHEM, 2004, Bad Nauheim, Deustschland: “ Naturstoff-Analoga: Synthesen um das 9,14-Lipoxin A4”
- 14- Chiang, N, Fierro, IM, Gronert, K, Serhan, CN (2000) Activation of lipoxin A4 receptors by aspirin-triggered lipoxins and select peptides evokes ligand-specific responses in inflammation. *J Exp Med.*191:1197–1207.
- 15- Grinspoon L&Bakalar JB (1993) Marihuana, the forbidden medicine. New Haven and London, Yale University Press.
- 16- Peters H&Nahas GG (1999) A brief history of four millennia. (B.C. 2000-A.D. 1974). In: Nahas, G.G., Sutin, K.M., Harvey, D.J. &Agurell, S. Marihuana and Medicine. New Jersey; Humana Press Inc. 1-7.

- 17- Zuardi AW (2006) History of cannabis as a medicine: a review. *Rev Bras Psiquiatr* 28, (2), 153-7.
- 18- Gaoni Y, Mechoulam R (1964) Isolation, structure and partial synthesis of an active constituent of hashish. *Journal of American Chemical Society*. 86:1646.
- 19- Hart C (1999) MARIJUANA: From evil weed to wonder drugs? *Modern Drug Discovery*. 2:39-40, 43, 45.
- 20- Elsohly MA, Slade D (2005) Chemical constituents of marijuana: the complex mixture of natural cannabinoids. *Life Sci*. 78, (5), 539-48.
- 21- Razdan RK (1986) Structure activity relationships in cannabinoids. *Pharmacol Rev* 38 (2): 75-149.
- 22- Agurell S, Hallidin M, Lindgren J.E, Ohlsson A, Widman M, Gillespie & Hollister L (1986) Pharmacokinetics and metabolism of delta-1-tetrahydrocannabinol and other cannabinoids with emphasis on man. *Pharmacol Rev*. 38(1): 21-43.
- 23- Iversen LL (2000) Marijuana and medicine. New York: Oxford University Press.
- 24- Pertwee RG (2006) Cannabinoid pharmacology: the first 66years. *Br J Pharmacol*. 147 Suppl 1: S163-71.
- 25- Mechoulam R, Gaoni Y (1967) recent advances in the chemistry of hashish. *FortschrChemOrgNaturst* 25:175–213.
- 26- ElSohly MA (2002) Chemical constituents of cannabis. In: Grotenhermen F, Russo E (eds) *Cannabis and Cannabinoids Pharmacology, Toxicology and Therapeutic Potential*. Haworth Press, New York, pp 27–36.
- 27- Pate DW (1999) Anandamide structure-activity relationships and mechanisms of action on intraocular pressure in the normotensive rabbit model. Doctoral dissertation. Kuopi University Publications, Kuopio.
- 28- Piomelli D (2003) The molecular logic of endocannabinoid signalling. *Nat Rev Neurosci* 4:873– 884.
- 29- Devane WA, Hanus L, Breuer A, Pertwee RG, Stevenson LA, Griffin G, Gibson D, Mandelbaum A, Etinger A & Mechoulam R (1992a) Isolation and Structure of a Brain Constituent that Binds to the Cannabinoid Receptor. *Science*, 258, 1946-1949.
- 30- Sugiura T, Kondo S, Sukagawa A, Nakane S, Shinoda A, Itoh K, Yamashita A & Waku K (1995) 2-Arachidonoylglycerol – A Possible Endogenous Cannabinoid Receptor Ligand in Brain. *BiochemBiophys.Res.Comm.*, 215, 89-97.
- 31- Wilson RI, Nicoll RA (2001) Endogenous cannabinoids mediate retrograde signalling at hippocampal synapses. *Nature*. 410:588-592.
- 32- Di Marzo, V (2009) The endocannabinoid system: Its general strategy of action, tools for its pharmacological manipulation and potential therapeutic exploitation. *Pharmacological Research*. 60:77-84.
- 33- Di Marzo V, Bifulco M, De Petrocellis L (2004) The endocannabinoid system and its therapeutic exploitation. *Nat Rev Drug Discov* 3:771–84.
- 34- Pertwee RG (2005b) Pharmacological actions of cannabinoids. *Handb Exp Pharmacol* (168): 1-51.
- 35- Pacher P, Bátkai S, and Kunos G (2006) The endocannabinoid system as an emerging target of pharmacotherapy. *Pharmacol Rev* 58:389–462.
- 36- Ahn K, McKinney MK, and Cravatt BF (2008) Enzymatic pathways that regulate endocannabinoid signaling in the nervous system. *Chem Rev* 108:1687–1707.

- 37- Di Marzo V (2008) CB1 receptor antagonism: Biological basis for metabolic effects. *Drug Discovery Today*. 13:1026-1041.
- 38- Sugiura T, Kobayashi Y, Oka S, Waku K (2002) Biosynthesis and degradation of anandamide and 2-arachidonoylglycerol and their possible physiological significance. *Prostaglandins, Leukotrienes and Essential Fatty Acids*. 66:173-192.
- 39- Natarajan V, Schmid PC, Reddy PV, Zuzarte-Augustin ML, and Schmid HHO (1983) Biosynthesis of N-acylethanolamine phospholipids by dog brain preparations. *JNeurochem* 41:1303–1312.
- 40- Di Marzo V, Fontana A, Cadas H, Schinelli S, Cimino G, Schwartz J-C, and Piomelli D (1994) Formation and inactivation of endogenous cannabinoid anandamide in central neurons. *Nature* 372:686–691.
- 41- Blankman JL and Benjamin F Cravatt (2013) Chemical Probes of Endocannabinoid Metabolism. *Pharmacol Rev* 65:849–871.
- 42- Bisogno T, et al (2003) Cloning of the first sn1-DAGlipases points to the spatial and temporal regulation of endocannabinoid signaling in the brain. *J. Cell Biol.* 163, 463–468. (doi:10.1083/jcb.200305129).
- 43- Tanimura A, Yamazaki M, Hashimoto Y, Uchigashima M, Kawata S, Abe M, Kita Y, Hashimoto K, Shimizu T, and Watanabe M, et al (2010) The endocannabinoids 2-arachidonoyl glycerol produced by diacylglycerol lipase α mediates retrograde suppression of synaptic transmission. *Neuron* 65:320–327.
- 44- Hashimoto Y, Ohno-Shosaku T, Tsubokawa H, Ogata H, Emoto K, Maejima T, Araishi K, Shin H-S, and Kano M (2005) Phospholipase C β serves as a coincidence detector through its Ca^{2+} dependency for triggering retrograde endocannabinoids signal. *Neuron* 45:257–268.
- 45- Di Marzo V, Bisogno T, Sugiura T, Melck D, De-Petrocellis L (1998) The novel endogenous cannabinoid 2-arachidonoylglycerol is inactivated by neuronal- and basophil-like cells: Connections with anandamide. *Biochemical Journal*. 331:15–19.
- 46- Blankman JL, Simon GM, and Cravatt BF (2007) A comprehensive profile of brain enzymes that hydrolyze the endocannabinoid 2-arachidonoylglycerol. *Chem Biol* 14:1347–1356.
- 47- Howlett AC and Fleming RM Howlett AC and Fleming RM (1984) Cannabinoid inhibition of adenylate cyclase. *Pharmacology of the response in neuroblastoma cell membranes*. *Mol Pharmacol* 26(3): 532-538.
- 48- Howlett AC (1985) Cannabinoid inhibition of adenylate cyclase. *Biochemistry of the response in neuroblastoma cell membranes*. *Mol Pharmacol* 27 (4): 429-436.
- 49- Devane WA, Dysarz FA III, Johnson MR, Melvin LS, Howlett AC (1988) Determination and characterization of a cannabinoid receptor in rat brain. *Mol. Pharmacol.* 34, 605–613.
- 50- Matsuda LA, Lolait SJ, Brownstein MJ, Young AC and Bonner TI (1990) Structure of a cannabinoid receptor and functional expression of the cloned cDNA. *Nature* 346(6284):561-564.
- 51- Munro S, Thomas KL and Abu-Shaar M (1993) Molecular characterization of a peripheral receptor for cannabinoids. *Nature* 365(6441): 61-65.
- 52- Howlett AC, Barth F, Bonner TI, Cabral G, Casellas P, Devane WA, Felder CC, Herkenham M, Mackie K, Martin BR, Mechoulam R, Pertwee RG (2002) International

- Union of Pharmacology. XXVII. Classification of Cannabinoid Receptors. *Pharmacol Rev*54:161–202. [PubMed: 12037135].
- 53- Mirzadegan T, Benko G, Filipek S and Palczewski K (2003) Sequence analyses of G-protein coupled receptors: similarities to rhodopsin. *Biochemistry* 42(10): 2759-2767.
 - 54- Shim J, Welsh WJ, Howlett AC (2003) Homology model of the C cannabinoid receptor: Sites critical for nonclassical cannabinoid agonist interaction. *Biopolymers*. 71:169-189.
 - 55- Stadel R, Ahn K H, and Kendall D A (2011) The cannabinoid type-1 receptor carboxyl-terminus, more than just a tail. *J. Neurochem*. 117, 1–18.
 - 56- Jin W, Brown S, Roche JP, Hsieh C, Celver JP, Kovoov A, Chavkin C, Mackie K (1999) Distinct domains of the CB1 cannabinoid receptor mediate desensitization and internalization. *J Neurosci*.19:3773–3780. [PubMed: 10234009]
 - 57- Daigle TL, Kearns CS, Mackie K (2008) Rapid CB1 cannabinoid receptor desensitization defines the time course of ERK1/2 MAP kinase signaling. *Neuropharmacology* 54:36–44[PMC free article] [PubMed].
 - 58- Leff P (1995) The two-state model of receptor activation. *Trends PharmacolSci*16 (3): 89-97. Lefkowitz RJ (1998) G protein-coupled receptors. III. New roles for receptor kinases and betaarrestins in receptor signaling and desensitization. *J BiolChem*273 (30): 18677-186.
 - 59- Kenakin T (2001) Inverse, protean, and ligand-selective agonism: matters of receptor conformation. *FASEB J* 15:598–611.
 - 60- Tate C G A (2012) Crystal Clear Solution for Determining G-Protein-Coupled Receptor Structures. *Trends in Biochemical Sciences*37, 343–352.
 - 61- Kobilka BK and Deupi X (2007) Conformational complexity of G-protein-coupled receptors. *Trends PharmacolSci*28:397–406.
 - 62- De Lean A, Stadel JM and Lefkowitz RJ (1980) A ternary complex model explains the agonist specific binding properties of the adenylatecyclase-coupled beta-adrenergic receptor. *JBiolChem*255 (15): 7108-7117.
 - 63- Szabo B and Schlicker E (2005) Effects of cannabinoids on neurotransmission. *HandbExpPharmacol*168:327–365.
 - 64- Elphick MR, Egertová M (2001) The neurobiology and evolution of cannabinoid signalling. *Philos Trans R SocLond B* 356:381.
 - 65- Picone, Robert P. Kendall, Debra A (2015) Minireview: From the Bench, Toward the Clinic: Therapeutic Opportunities for Cannabinoid Receptor Modulation *MolEndocrinol*, 29(6):801–813.
 - 66- Pagotto U, Marsicano G, Cota D, Lutz B, Pasquali R (2006) The emerging role of the endocannabinoid system in endocrine regulation and energy balance. *Endocr Rev* 27: 73–100.
 - 67- Jenkin KA, McAinch AJ, Grinfeld E, Hryciw DH(2010) Role for cannabinoid receptors in human proximal tubular hypertrophy. *Cell PhysiolBiochem* 26: 879–886.
 - 68- Scotter EL, Abood ME, Glass M (2010) The endocannabinoid system as a target for the treatment of neurodegenerative disease. *Br J Pharmacol*160:480–498.
 - 69- Walsh D, Nelson KA, Mahmoud FA (2003) Established and potential therapeutic applications of cannabinoids in oncology. *Support Care Cancer* 11:137–143. [PubMed: 12618922].

- 70- Rahn EJ and Hohmann AG (2009) Cannabinoids as pharmacotherapies for neuropathic pain: from the bench to the bedside. *Neurotherapeutics* 6:713–737.
- 71- Pertwee RG, A C Howlett, M E Abood, S P H Alexander, V Di Marzo, M R Elphick, P J Greasley, H S Hansen, G Kunos, K Mackie, R Mechoulam, and R A Ross (2010) International Union of Basic and Clinical Pharmacology. LXXIX. Cannabinoid Receptors and Their Ligands: Beyond CB1 and CB2. *Mol. Pharmacol Rev* 62:588–631.
- 72- Martin BR, Compton DR, Thomas BF, et al (1991) Behavioral, biochemical, and molecular modeling evaluations of cannabinoid analogs. *Pharmacol Biochem Behav* 40:471.
- 73- Compton DR, Aceto MD, Lowe J, Martin BR (1996) In vivo characterization of a specific cannabinoid receptor antagonist (SR141716A): inhibition of Δ^9 -tetrahydrocannabinol-induced responses and apparent agonist activity. *J Pharmacol Exp Ther* 277:586.
- 74- Rinaldi-Carmona M, Barth F, Héaulme M, et al (1994) SR141716A, a potent and selective antagonist of the brain cannabinoid receptor. *FEBS Lett* 350:240.
- 75- <http://www.fundacion-canna.es/en/endocannabinoidsystem>.
- 76- Abadji V, Lucas-Lenard JM, Chin C & Kendall DA (1999) Involvement of the carboxyl terminus of the third intracellular loop of the cannabinoid CB1 receptor in constitutive activation of Gs. *Journal of Neurochemistry* 72 2032–2038.
- 77- Calandra B, Portier M, Kerneis A, Delpech M, Carillon C, Le Fur G, Ferrara P & Shire D (1999) Dual intracellular signalling pathways mediated by the human cannabinoid CB1 receptor. *European Journal of Pharmacology* 374 445–455.
- 78- CHILDERS S R & DEADWYLER S R (1996) Role of cyclic AMP in the actions of cannabinoid receptors. *Biochemical Pharmacology* 52, 819–827.
- 79- Caulfield MP & Brown DA (1992) Cannabinoid receptor agonists inhibit Ca current in NG108-15 neuroblastoma cells via a pertussis toxin-sensitive mechanism. *British Journal of Pharmacology* 106 231–232.
- 80- Mackie K, Lai Y, Westenbroek R & Mitchell R (1995) Cannabinoids activate an inwardly rectifying potassium conductance and inhibit Q-type calcium currents in AtT20 cells transfected with rat brain cannabinoid receptor. *Journal of Neuroscience* 15 6552–6561.
- 81- McAllister SD, Griffin G, Satin LS & Abood ME (1999) Cannabinoid receptors can activate and inhibit G protein-coupled inwardly rectifying potassium channels in a *Xenopus* oocyte expression system. *Journal of Pharmacology and Experimental Therapeutics* 291: 618–626.
- 82- Gebremedhin D, Lange AR, Campbell WB, Hillard CJ & Harder DR (1999) Cannabinoid CB1 receptor of cat cerebral arterial muscle functions to inhibit L-type Ca²⁺ channel current. *American Journal of Physiology* 276 H2085–H2093.
- 83- Ga'bor Turu and La'szlo' Hunyady (2010) Signal transduction of the CB1 cannabinoid receptor. *Journal of Molecular Endocrinology* 44, 75–85.
- 84- Howlett AC (2005) Cannabinoid receptor signalling. *Handbook of Experimental Pharmacology* 168 53–79.
- 85- Rueda D, Galve-Roperh I, Haro A & Guzman M (2000) The CB (1) cannabinoid receptor is coupled to the activation of c-Jun N-terminal kinase. *Molecular Pharmacology* 58 814–820.

- 86- Paradisi A, Pasquariello N, Barcaroli D & Maccarrone M (2008) Anandamide regulates keratinocyte differentiation by inducing DNA methylation in a CB1 receptor-dependent manner. *Journal of Biological Chemistry* 283 6005–6012.
- 87- Galve-Roperh I, Rueda D, Gomez DP, Velasco G & Guzman M (2002) Mechanism of extracellular signal-regulated kinase activation by the CB(1) cannabinoid receptor. *Molecular Pharmacology* 62:1385–1392.
- 88- Hillard CJ, Muthian S, Kearn CS (1999) Effects of CB (1) Cannabinoid receptor activation on cerebellar granule cell nitric oxide synthase activity. *FEBS Lett* 459:277–281. [PubMed: 10518035]
- 89- Jones JD, Carney ST, Vrana KE, Norford DC, Howlett AC (2008) Cannabinoid receptor-mediated translocation of NO-sensitive guanylyl cyclase and production of cyclic GMP in neuronal cells. *Neuropharmacology* 54:23–30. [PubMed: 17707868]
- 90- Nussler A K, Rénia L, Pasquetto V, Miltgen F, Matile H, Mazier D (1993) In vivo induction of the nitric oxide pathway in hepatocytes after injection with irradiated malaria sporozoites, malaria blood parasites or adjuvants. *Eur. J. Immunol.* 23, 882–887. 10.1002/eji.1830230417
- 91- Pertwee RG (1999a) Pharmacology of cannabinoid receptor ligands. *Curr Med Chem* 6:635–664.
- 92- Mechoulam R, Fride E, Di Marzo V (1998) Endocannabinoids. *Eur J Pharmacol* 359:1–18.
- 93- Thakur A, Spyros P, and Makriyannis A (2005) CB1 Cannabinoid Receptor Ligands. *Mini-Reviews in Medicinal Chemistry* Vol. 5, No. 7, 631-640.
- 94- Little PJ, Compton DR, Johnson MR, Melvin LS, Martin B R (1988) Pharmacology and stereoselectivity of structurally novel cannabinoids in mice. *J. Pharmacol. Exp. Ther.* 247, 1046–1051.
- 95- Huffman JW, Yu S, Showalter V, Abood ME, Wiley JL, Compton DR, Martin BR, Bramblett RD and Reggio ph (1996) Synthesis and pharmacology of a Very potent Cannabinoid lacking a phenolic Hydroxyl with High Affinity for the CB2 Receptor. *J Med Chem.* 39:3875-3877.
- 96- Eissenstat MA, Bell MR, D'Ambra TE, Alexander EJ, Daum SJ, Ackerman JH, Grueett MD, Kumar V, Estep KG, Olefirowicz EM, Wetzel JR, Alexander MD, Weaver JD, Haycock DA, Luttinger DA, Casiano FM, Chippari SM, Kuster JE, Stevenson JI, Ward SJ (1995) Aminoalkylindoles: structure-activity relationships of novel cannabinoid mimetics *J Med chem.* 38: 3094-105.
- 97- Wiley JL, Compton DR, Dai D, Lainton JA, Phillips M, Huffman JW, and Martin BR (1998) Structure-activity relationships of indole- and pyrrole-derived cannabinoids. *J Pharmacol Exp Ther* 285:995–1004.
- 98- Showalter VM, Compton DR, Martin BR, Abood ME (1996) Evaluation of binding in a transfected cell line expressing a peripheral cannabinoid receptor (CB2): identification of cannabinoid receptor subtype selective ligands. *J Pharmacol Exp Ther* 278:989–999.
- 99- Lin S, Khanolkar AD, Fan P, Goutopoulos A, Qin C, Papahadjis D, Makriyannis A (1998) Novel analogues of arachidonyl ethanolamide (anandamide): affinities for the CB1 and CB2 cannabinoid receptors and metabolic stability. *J Med Chem* 41:5353–5361.
- 100- Khanolkar AD, Makriyannis A (1999) Structure/activity relationships of anandamide, an endogenous cannabinoid ligand. *Life Sci.* 65, 607–616.

- 101- Abadji V, Lin S, Taha G, Griffin G, Stevenson LA, Pertwee RG, Makriyannis A (1994) (R)-methanandamide: a chiral novel anandamide possessing higher potency and metabolic stability. *J Med Chem* 37:1889–1893.
- 102- Khanolkar AD, Abadji V, Lin S, Hill WAG, Taha G, Abouzid K, Meng Z, Fan P, Makriyannis A (1996) Head group analogs of arachidonylethanolamide, the endogenous cannabinoid ligand. *J Med Chem* 39:4515–451.
- 103- Tius MA, Makriyannis A, Zou XL, Abadji V (1994) Conformationally restricted hybrids of CP-55,940 and HHC: stereoselective synthesis and activity. *Tetrahedron* 50, 2671–2680.
- 104- Tius MA, Hill WAG, Zou XL, Busch-Petersen J, Kawakami JK, Fernandez-Garcia MC, Drake DJ, Abadji V, Makriyannis A (1995) Classical/non-classical cannabinoid hybrids; stereochemical requirements for the southern hydroxyalkyl chain. *Life Sci.* 56, 2007–2012.
- 105- Harrington PE, Stergiades IA, Erickson J, Makriyannis A, Tius MA (2000) Synthesis of functionalized cannabinoids. *J. Org. Chem.* 65, 6576–6582.
- 106- Palmer SL, Thakur GA, Makriyannis A (2002) Cannabinergic ligands. *Chemistry and Physics of Lipids* 121, 3–19.
- 107- Kendall D (2000) Sr-141716a sanofi-synthelabo. *Curr. Opin. Centr. Periph. Nervous Sys. Investigat. Drugs* 2, 112–122.
- 108- Pertwee RG (1997) Pharmacology of cannabinoid CB1 and CB2 receptors. *Pharmacol Ther* 74:129–180.
- 109- Muccioli GG and DM Lambert (2005) Current Knowledge on the Antagonists and Inverse Agonists of Cannabinoid Receptors. *Current Medicinal Chemistry* 12, 1361–1394.
- 110- Gatley SJ, Lan R, Volkow ND, Pappas N, King P, Wong CT, Gifford AN, Pyatt B, Dewey SL, Makriyannis A (1998) Imaging the brain marijuana receptor: development of a radioligand that binds to cannabinoid CB1 receptors in vivo. *J Neurochem* 70:417–423.
- 111- Lan R, Gatley J, Lu Q, Fan P, Fernando SR, Volkow ND, Pertwee R, Makriyannis A (1999a) Design and synthesis of the CB1 selective cannabinoid antagonist AM281: a potential human SPECT ligand. *AAPS PharmSci* 1:U13–U24.
- 112- Felder CC, Joyce KE, Briley EM, Glass M, Mackie KP, Fahey KJ, Cullinan GJ, Hinde DC, Johnson DW, Chaney MO, Koppel GA, Brownstein M (1998) LY320135, a novel cannabinoid CB1 receptor antagonist, unmasks coupling of the CB1 receptor to stimulation of cAMP accumulation. *J Pharmacol Exp Ther* 284:291–297.
- 113- Monod J, Changeux JP, and Jacob F (1963) Allosteric proteins and cellular control systems. *J Mol Biol* 6:306–329.
- 114- May L T, Leach K, Sexton P M and Christopoulos A (2007) Allosteric modulation of G protein-coupled receptors. *Annu. Rev. Pharmacol. Toxicol.* 47, 1–51.
- 115- Christopoulos A, Jean-Pierre Changeux, William A. Catterall, Doriano Fabbro, Thomas P Burris, John A Cidlowski, Richard W Olsen, John A Peters, Richard R Neubig, Jean Philippe Pin, Patrick M Sexton, Terry P Kenakin, Frederick J Ehlert, Michael Spedding, and Christopher J Langmead (2014) Recommendations for the Nomenclature of Receptor Allosterism and Allosteric Ligands. *Pharmacol Rev* 66:918–947.
- 116- KENAKIN, TERRY P (2010) Ligand Detection in the Allosteric World. *J Biomol Screen* 15: 119.
- 117- Price M R, Baillie G L, Thomas A, Stevenson L A, Easson M Goodwin R, McLean A, McIntosh L, Goodwin G, Walker G, Westwood P, Marrs J, Thomson F, Cowley P,

- Christopoulos A, Pertwee R G and Ross R A (2005) Allosteric modulation of the cannabinoid CB1 receptor. *Mol. Pharmacol.* 68, 1484–1495.
- 118- Ahn K H, Mariam M and Debra A Kendall (2012) Allosteric Modulator ORG27569 Induces CB1 Cannabinoid Receptor High Affinity Agonist Binding State, Receptor Internalization and Gi Protein-independent ERK1/2 Kinase Activation. *J. Biol. Chem.* 287:12070-12082.
- 119- Ross RA (2007) Allosterism and cannabinoid CB1 receptors: The shape of things to come. *Trends PharmacolSci* 28(11):567–572.
- 120- Fay J F and Farrens DL (2012) A Key Agonist-induced Conformational Change in the Cannabinoid Receptor CB1 Is Blocked by the Allosteric Ligand .Org 27569. *J. Biol. Chem.* 287:33873-33882.
- 121- Horswill J G, Bali U, Shaaban S, Keily J F, Jeevaratnam P, Babbs A J, Reynet C and Wong Kai in P (2007) PSNCBAM-1, a novel allosteric antagonist at cannabinoid CB1 receptors with hypophagic effects in rats. *Br. J. Pharmacol.* 152, 805–814.
- 122- Wang X, Horswill JG, Whalley BJ and Stephens GJ (2011) Effects of the Allosteric Antagonist 1-(4-Chlorophenyl)-3-[3-(6-pyrrolidin-1-ylpyridin-2-yl)phenyl]urea (PSNCBAM-1) on CB1 Receptor Modulation in the Cerebellum. *Mol. Pharmacol* 79:758–767, 2011.
- 123- Navarro HA , Howard JL, Pollard GT , Carroll FI (2009) Positive allosteric modulation of the human cannabinoid (CB) receptor by RTI -371, a selective inhibitor of the dopamine transporter. *Br J Pharmacol* 156:1178-1184.
- 124- Serhan CN, Hamberg M, and Samuelsson B (1984) Lipoxins: novel series of biologically active compounds formed from arachidonic acid in human leukocytes. *Proc Natl Acad Sci USA* 81: 5335–5339.
- 125- Serhan CN, Hamberg M, Samuelsson B, Morris J, and Wishka DG (1986) On the stereochemistry and biosynthesis of lipoxin B. *Proc Natl Acad Sci USA* 83: 1983–1987.
- 126- Edenius C, Haeggstrom J, and Lindgren JA (1988) Transcellular conversion of endogenous arachidonic acid to lipoxins in mixed human platelet-granulocyte suspensions. *Biochem Biophys Res Commun* 157: 801–807.
- 127- Serhan CN and Sheppard KA (1990) Lipoxin formation during human neutrophil-platelet interactions. Evidence for the transformation of leukotriene A4 by platelet 12-lipoxygenase in vitro. *J Clin Invest* 85:772–780.
- 128- Claria J, Titos E, Jimenez W, Ros J, Gines P, Arroyo V, Rivera F, and Rodes J (1998) Altered biosynthesis of leukotrienes and lipoxins and host defense disorders in patients with cirrhosis and ascites. *Gastroenterology* 115: 147–156.
- 129- Lawrence W, Willoughby DA, and Gilroy DW (2002) Anti-inflammatory lipid mediators and insights into the resolution of inflammation. *Nat Rev Immunol* 2: 787–795.
- 130- Dahlen SE, Franzen L, Raud J, Serhan CN, Westlund P, Wikstrom E, Bjorck T, Matsuda H, Webber SE, Veale CA, Puustinen T, Haeggstrom J, Nicolau KC, and Samuelsson B (1988) Actions of lipoxin A4 and related compounds in smooth muscle preparations and on the microcirculation in vivo. *Adv Exp Med Biol* 229: 107–130.
- 131- Serhan CN (1994) Lipoxin biosynthesis and its impact in inflammatory and vascular events. *Biochim Biophys Acta* 1212: 1–25.
- 132- Sun T, Yu E, Yu L, Luo J, Li H, Fu Z (2012b) Lipoxin A(4) induced antinociception and decreased expression of NF-kappaB and proinflammatory cytokines after chronic dorsal

- root ganglia compression. *Eur J Pain.* 2012 Jan; 16(1):18-27. Doi: 10.1016/j.ejpain.2011.05.005.
- 133- Whitaker Sinclair, Whitaker, D.Todd, e-EROS Encyclopedia of Reagents for Organic SynthesisK, Published Online: 15 APR 2001.
- 134- Clayden J, Nick G, Stuart W(2001)Organic Chemistry;2nd ed. Oxford University Press Inc., New York: USA, 23:529-560
- 135- Reitz AB, Nortey SO, Jordan AD, et al (1986) Dramatic Concentration Dependence of Stereochemistry in the Wittig Reaction. Examination of the Lithium-Salt Effect, *J. Org. Chem.*, 51, 3302–3308.
- 136- Norcross BE (1993) Advanced Organic Chemistry: Reactions, Mechanisms, and Structure, 4th ed. (March, Jerry). *Journal of Chemical Education [Internet]. American Chemical Society (ACS)* 70(2):A51.
- 137- Pommer H, (2003) The Wittig Reaction in Industrial Practice, DOI: 10.1002/anie.197704233.
- 138- Shoji Eguchi, Keizo Yamashita, Yuji Matsushita, Akikazu Kakehi (1995) Facile Synthesis of 1,4-Benzodiazepin-5-one Derivatives via Intramolecular Aza-Wittig Reaction. Application to an Efficient Synthesis of O-Benzyl DC-81, *J. Org. Chem.*, 60 (13), pp 4006–4012.
- 139- List G, Jackson M, Eller F, Adlof R (2007) Low trans spread and shortening oils via hydrogenation of soybean oil. *Journal of the American Oil Chemists* 84: 609-612.
- 140- Singh D, Rezac M and Pfromm P (2009) Partial Hydrogenation of Soybean Oil with Minimal Trans Fat Production Using a Pt-Decorated Polymeric Membrane Reactor.*Journal of the American Oil Chemists Society* 86: 93-101.
- 141- Fraaije MW, Christian S, et al (2007) Reduction of Carbon-Carbon Double Bonds Using Organocatalytically Generated Diimide, *J. Org. Chem.* 73, 9482–9485.
- 142- Kwesi Amoa (2007) `Catalytic Hydrogenation of Maleic Acid at Moderate Pressures A Laboratory Demonstration, *Journal of Chemical Education* , Vol. 84 No. 12.
- 143- Rylander A (1979) Catalytic Hydrogenation in organic synthesis, ACADEMIC PRESS, Elsevier Inc.
- 144- Flamme EM, Roush WR (2005) Synthesis of the C (1) –C (25) Fragment of Amphidinol 3: Application of the Double-Allylboration Reaction for Synthesis of 1, 5-Diols, *Organic Letters.* 7(7):1411-4. DOI: 10.1021/ol050250q.
- 145- GORE PH (1955) The Friedel-Crafts Acylation Reaction and its Application to Polycyclic Aromatic Hydrocarbons, *Chem. Rev.*55 (2), pp 229–281. DOI: 10. 1021/cr50002a001
- 146- Nordlander EJ, Balk MA, et al (1984) Friedel-Crafts acylation with N-(trifluoroacetyl)-.alpha.-amino acid chlorides. Application to the preparation of .beta.-arylalkylamines and 3-substituted 1, 2, 3, 4-tetrahydroisoquinolines, *J. Org. Chem.*, 49 (22), pp 4107–4111.
- 147- Tanko JM, Blackert JF (1994) Free-radical side-chain bromination of alkylaromatics in supercritical carbon dioxide.*Science.*263(5144):203-5.
- 148- Liu R, Zhang P, Gan T, Cook JM (1997)A regiospecific bromination of substituted 3-methylindoles, Synthesis of Optically Active Unusual Tryptophans Present in Marine Cyclic Peptides(1), *J Org Chem.*62(21):7447-7456.

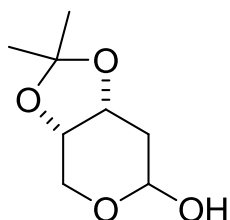
- 149- Hughes I (1996) Application of polymer-bound phosphonium salts as traceless supports for solid phase synthesis. *Tetrahedron Letters* [Internet]. Elsevier BV; 37(42):7595–8.
- 150- Johnson CL, Donkor RE, et al (2004) Novel application of phosphonium salts as co-catalysts for the Baylis–Hillman reaction, *Tetrahedron Letters* Volume 45, Issue 39, Pages 7359–736.
- 151- Flaherty PT (2009) Book Review of *Organic Synthesis: The Disconnection Approach*. Second Edition *Organic Synthesis: The Disconnection Approach*. Second Edition. By Stuart Warren and Paul Wyatt Wiley, Hoboken, NJ. *Journal of Medicinal Chemistry* [Internet]. American Chemical Society (ACS); 2009 Sep 24; 52(18):5768–9.
- 152- Boyd D (1993) *Advanced organic chemistry*. Endeavour [Internet]. Elsevier BV 17(2):96. Available from: [http://dx.doi.org/10.1016/0160-9327\(93\)90217-q](http://dx.doi.org/10.1016/0160-9327(93)90217-q)
- 153- Davies S B, Anthony M., et al (1999) Convenient in situ synthesis of nonracemic N-protected β -amino aldehydes from β -amino acids, *Tetrahedron Letters* Volume 40, Issue 6, pp 1229–1232.
- 154- Ernest I , Main A J , Menassé R (1982) Synthesis of the 7-cis isomer of the natural leukotriene d4 , *Tetrahedron Letters* Volume 23, Issue 2, pp167-170.
- 155- <http://abacus.bates.edu/~jkoviach/218/ps/Th3.13.pdf>
- 156- Kocieński PJ (1994) 3.2.2: Diol Protecting Groups—Acetals—Isopropylidene Acetals, Thieme. p. 103.
- 157- Holden MS. *Organic Chemistry* (Sorrell, Thomas N.). *Journal of Chemical Education* [Internet]. American Chemical Society (ACS); 2000 Jan; 77(1):31.
- 158- <http://www.masterorganicchemistry.com/2011/08/12/reagent-friday-sodium-borohydride-nabh4/>.
- 159- Carey F A, et al (2011) *Organic Chemistry*; 8th ed, McGraw-Hill, pp. 798–799.
- 160- Bombarelli RG, Calle E and Casado J (2013) Mechanisms of Lactone Hydrolysis in Neutral and Alkaline Conditions, [dx.doi.org/10.1021/jo400258w](https://doi.org/10.1021/jo400258w) | *J. Org. Chem.* 78, 6868–6879.
- 161- Wu Q , Wang L (2008) Immobilization of Copper(II) in Organic-Inorganic Hybrid Materials as a Highly Efficient and Reusable Catalyst for the Classic Ullmann Reaction, *Thieme* 13; 2007-2012; j.SYNTHESIS –STUTT GART.
- 162- Naidu AB, Jaseer EA, Sekar G. General, Mild, and Intermolecular Ullmann-Type Synthesis of Diaryl and Alkyl Aryl Ethers Catalyzed by Diol–Copper (I) Complex. *J Org Chem* [Internet]. American Chemical Society (ACS); 2009 May 15; 74(10):3675–9.
- 163- Cristau HJ, Cellier PP, Hamada S, Spindler JF (2004) A General and Mild Ullmann-Type Synthesis of Diaryl Ethers, *Org. Lett.*, Vol. 6, No., 6, 2004.
- 164- Klimko et al (2011) 5, 6, 7-Trihydroxyheptanoic Acid and Analogs for The Treatment of Ocular Diseases and Diseases Associated with Hyperproliferative and Angiogenic Responses, Patent No: US 7, 879,905 B2.
- 165- Colm Duffy (2012) *Heteroaromatic Lipoxin A4, synthesis and biological evaluation*, Springer-Verlag Berlin Heidelberg.
- 166- Phillips ED, Chang H-F, Holmquist CR, McCauley JP (2003) Synthesis of methyl(5S,6R,7E,9E,11Z,13E,15S)-16-(4-fluorophenoxy)-5,6,15-trihydroxy-7,9,11,13-hexadecatetraenoate, an analogue of 15R-Lipoxin A4, *Bioorganic & Medicinal Chemistry Letters*, Volume 13, Issue 19, 16 October 2003, Pages 3223-3226.
- 167- Nicolaou KC, et al (2009) Total Synthesis and Biological Evaluation of Cotistatins A and J and Analogues Thereof, *J. AM. CHEM. SOC.*, 131, 10587-10597.

- 168- Adile Duymaz (2007) Doctoral dissertation. Gutenberg university publications, Germany.
- 169- Ajda Podgorsek, et al (2006) Visible Light Induced `on water` Benzylic Bromination with N-bromosuccinimide, *Tetrahedron Letters* 47:1097-1099.
- 170- Milhanic S, et al (2005) Photoinduced Gelation by Stilbene Oxalyl Amide Compounds, *Langmuir*, 21(7), 2754-2760.
- 171- HONG-CHEU LIN et al (2009) Self-Assembly of H-Bonded Side-Chain and Cross-Linking Copolymers Containing Diblock-Copolymeric Donors and Single/Double H-Bonded Light-Emitting Acceptors, *Journal of Polymer Science: Part A: Polymer Chemistry*.
- 172- O'Sullivan TP, Vallin KSA, Shah STA, Fakhry J, Maderna P, Scannell M, Sampaio ALF, Perretti M, Godson C, Guiry PJ (2007) Aromatic Lipoxin A4 and Lipoxin B4 Analogues Display Potent Biological Activities, *J Med Chem* 50:5894.
- 173- Singh S, Duffy CD, Shah STA, Guiry PJ (2008) ZrCl₄ as an Efficient Catalyst for a Novel One-Pot Protection/Deprotection Synthetic Methodology . *J Org Chem [Internet]. American Chemical Society (ACS);* 73(16):6429–32.
- 174- Pierre van de Weghe (2011) Synthesis of Commercial Drugs, Université de Rennes 1 – Vietnam National University, Hanoi.
- 175- Altman R A, Shafir A, Choi A, Lichtor PA, Buchwald S L (2008) An improved cu-based catalyst system for the reactions of alcohols with aryl halides, *J. Org. Chem.* 2008, 73, 284-286.
- 176- Niu J, Zhou H, Li Z, et al (2008) An efficient Ullmann-Type C-O bond formation catalyzed by an air-stable copper(I)-bipyridyl complex, *J. Org. Chem.* 73, 7814-7817.
- 177- Frisch M J G , Trucks W, Scalmani G, Schlegel HB, Iyengar S S, et al (2009) Gaussian 09 Revision A.02, Gaussian, Inc., Wallingford CT.
- 178- Becke A.D (1993) Density-functional thermochemistry. III. The role of exact exchange, *J. Chem. Phys.* 98, 5648-5652.
- 179- Lee C, Yang W, Parr RG (1988) Development of the Colle-Salvetti correlation-energy formula into a functional of the electron density. *Physical Review B [Internet]. American Physical Society (APS);* 37(2):785–9.
- 180- Stephens P. J, Devlin F. J, Chabalowski C. F, Frisch M. J (1994) Ab Initio Calculation of Vibrational Absorption and Circular Dichroism Spectra Using Density Functional Force Fields *J. Phys. Chem.*, 1994, 98 (45), pp 11623–11627.
- 181- Krishnan R, Binkley J S, Seeger R, Pople J A (1980) Self-consistent molecular orbital methods. XX. A basis set for correlated wave functions, *J. Chem. Phys.* 72, 650-654.
- 182- Tomasi J, Mennucci B, Cammi R (2005) Quantum Mechanical Continuum Solvation Models. *Chem. Rev.* 105, 2999-3094.
- 183- Guilford WJ, Bauman JG, Skuballa W, Bauer S, Wei GP, Davey D, et al (2004) Novel 3-oxa lipoxin A4 analogues with enhanced chemical and metabolic stability have anti-inflammatory activity in vivo. *J Med Chem.* 47:2157-2165.
- 184- Petasis NA, Keledjian R, Sun YP, Nagulapalli KC, Tjonahen E, Yang R, Serhan CN (2008) Design and synthesis of benzo-lipoxin A4 analogs with enhanced stability and potent anti-inflammatory properties. *Bioorg. Med. Chem. Lett.* 18:1382-1387.

- 185- Clish CB, O'Brien JA, Gronert K, Stahl GL, Petasis NA, Serhan CN (1999) Local and systemic delivery of a stable aspirin-triggered lipoxin prevents neutrophil recruitment in vivo. *Proc Natl Acad Sci U S A* 96:8247.
- 186- Moretti, Jared D, Wang, Xiao, Curran, Dennis P (2012) Minimal Fluorous Tagging Strategy that Enables the Synthesis of the Complete Stereoisomer Library of SCH725674 Macrolactones. *Journal of the American Chemical Society*. Vol 134. Issue 18. P 7963-7970.
- 187- Tseng M, Kan H, Chu Y (2007) Reactivity of Trihexyl (tetradecyl) Phosphonium Chloride, A Room-Temperature Phosphonium Ionic Liquid. *Tetrahedron Letters* 48 (2007) 9085-9089.

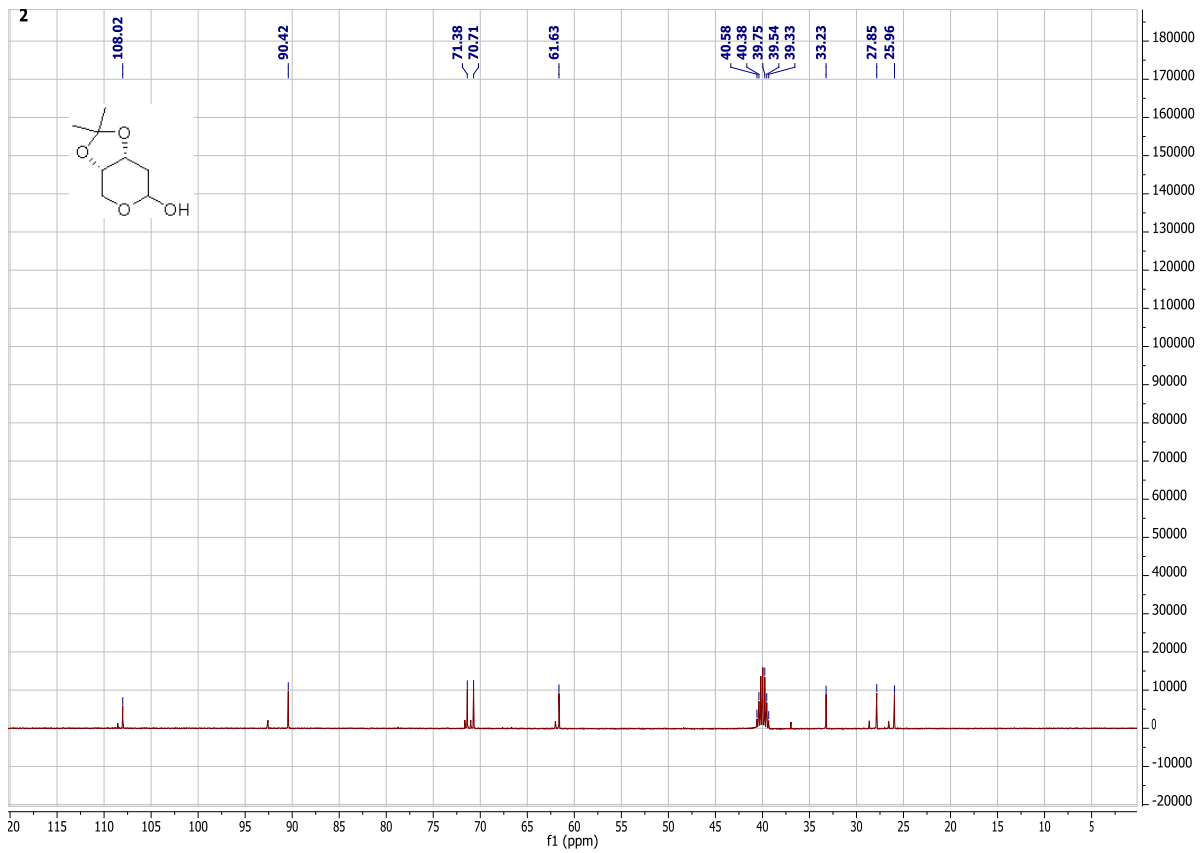
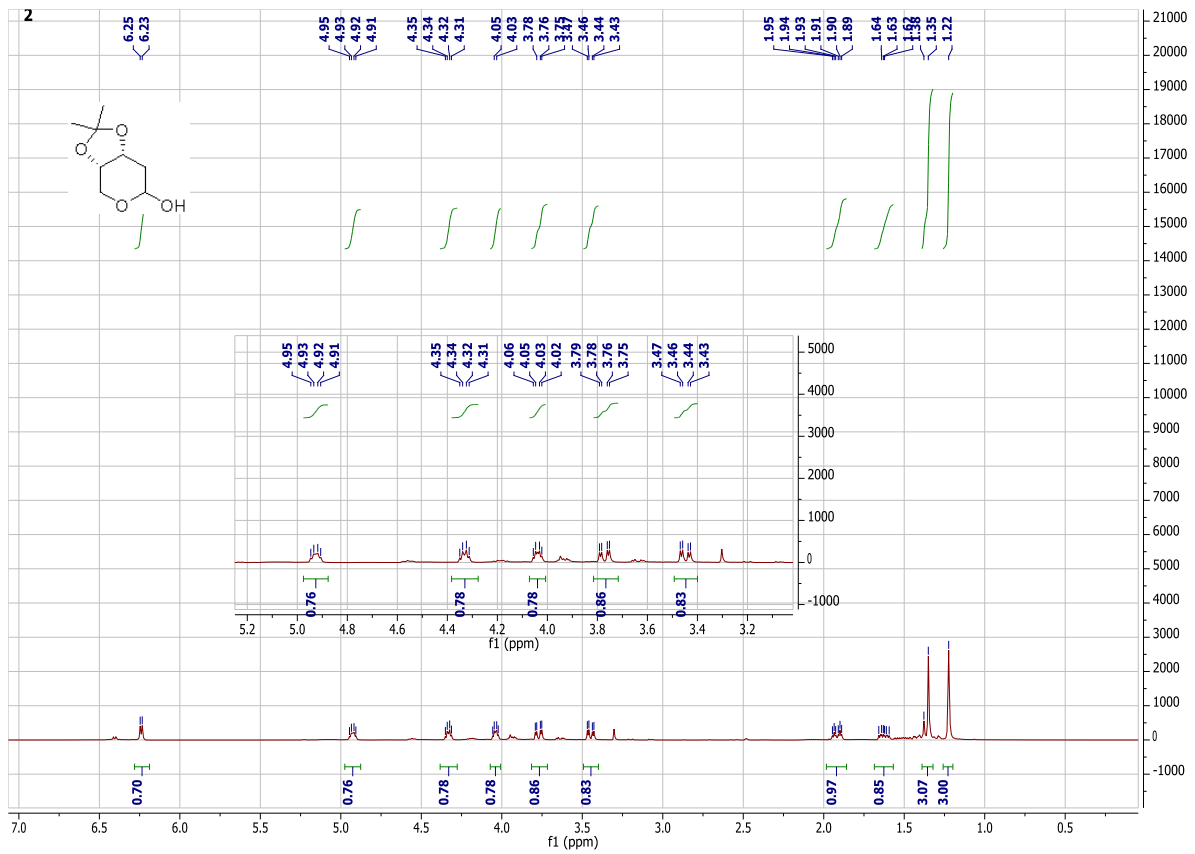
7 APPENDICES

Appendix1

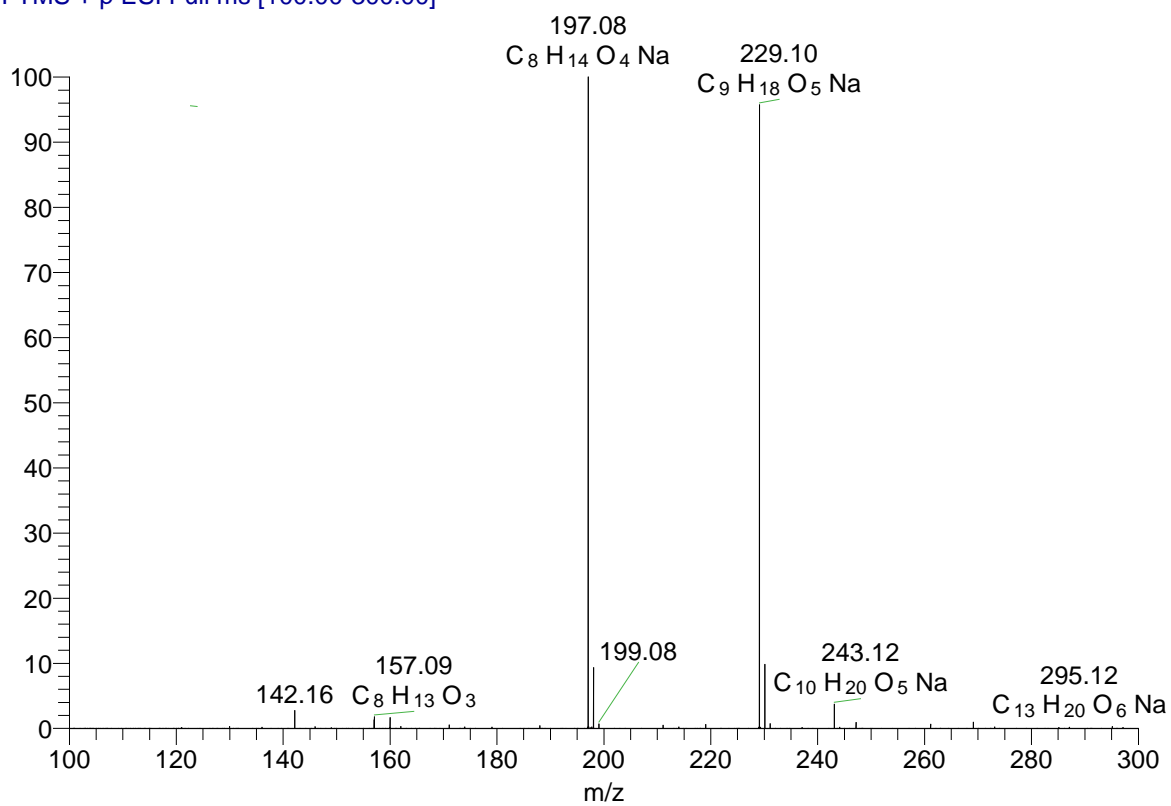


(3a*S*,7a*R*)-2,2-dimethyltetrahydro-3a*H*-[1,3]dioxolo[4,5-*c*]pyran-6-ol

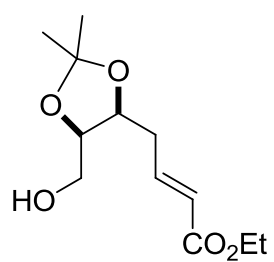
2



JHAI-2-5_4 #1 RT: 0.02 AV: 1 NL: 1.65E7
T: FTMS + p ESI Full ms [100.00-300.00]

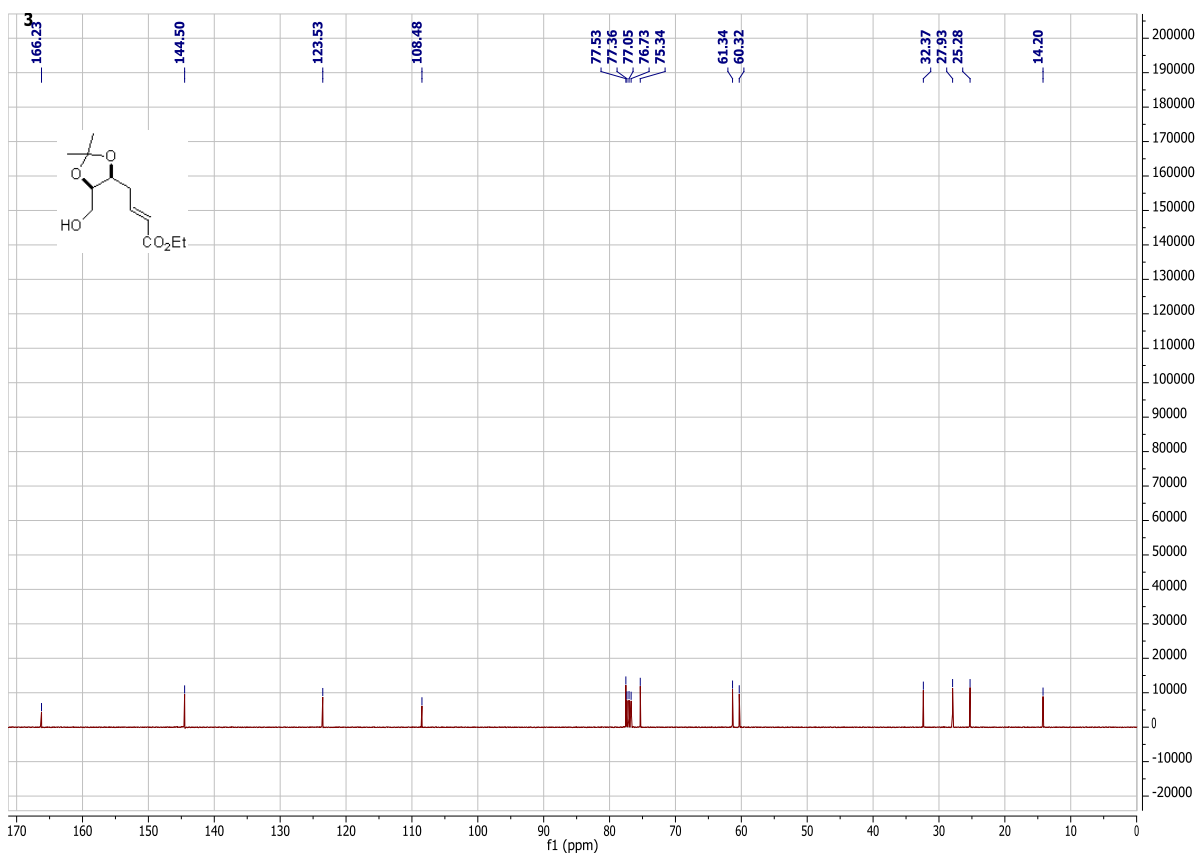
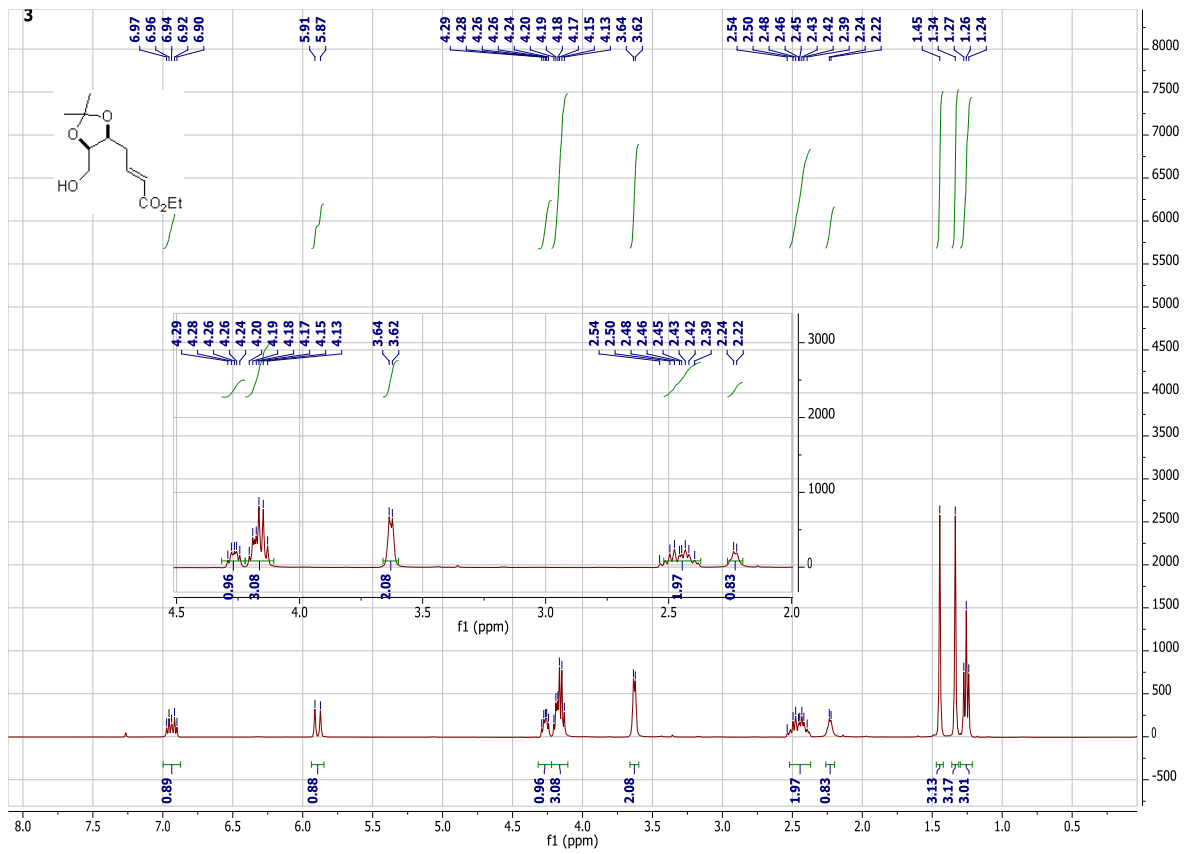


Appendix 2

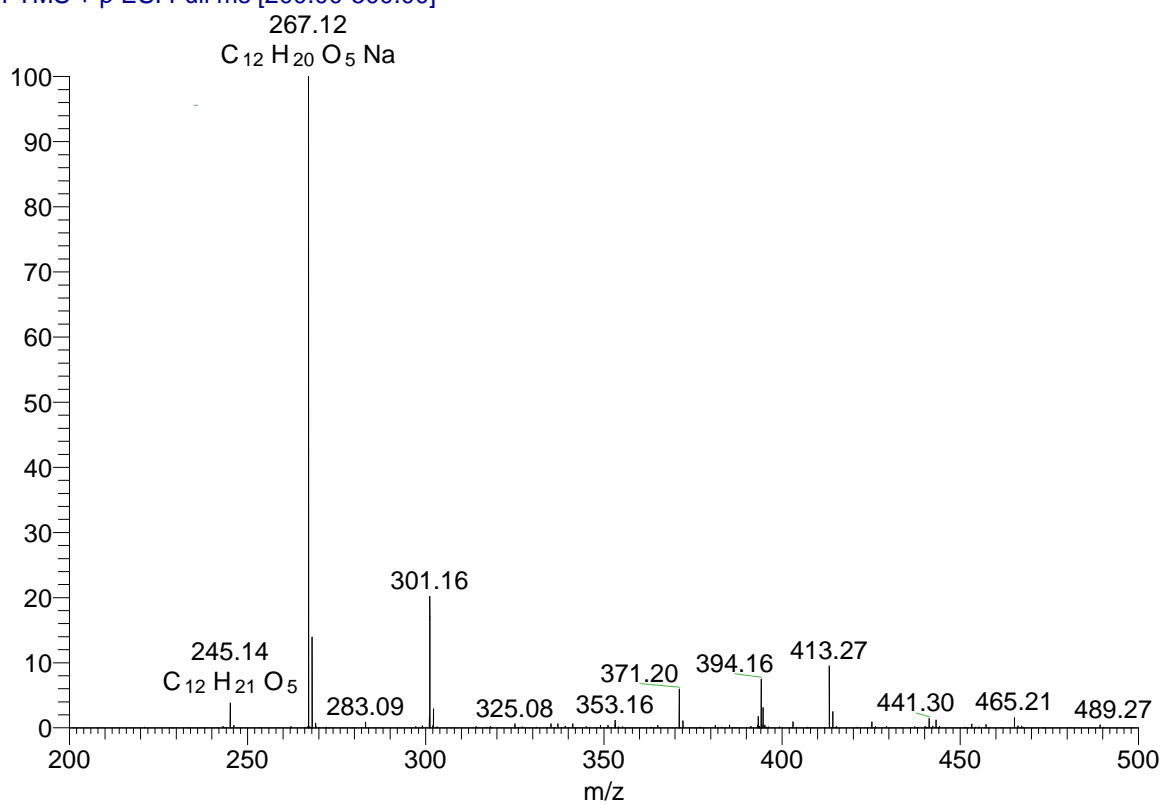


(*E*)-ethyl 4-((4*S*,5*R*)-5-(hydroxymethyl)-2,2-dimethyl-1,3-dioxolan-4-yl)but-2-enoate

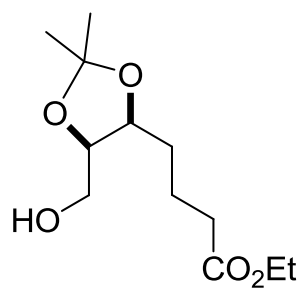
3



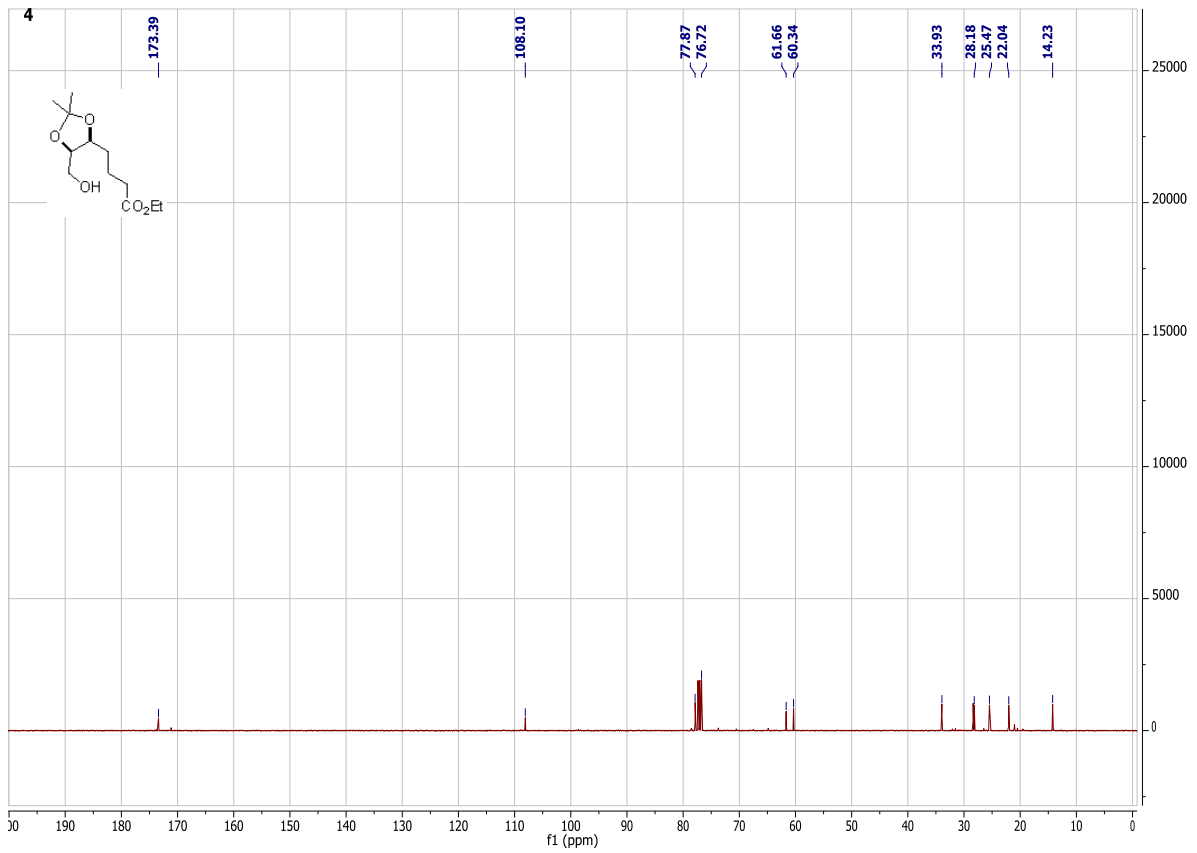
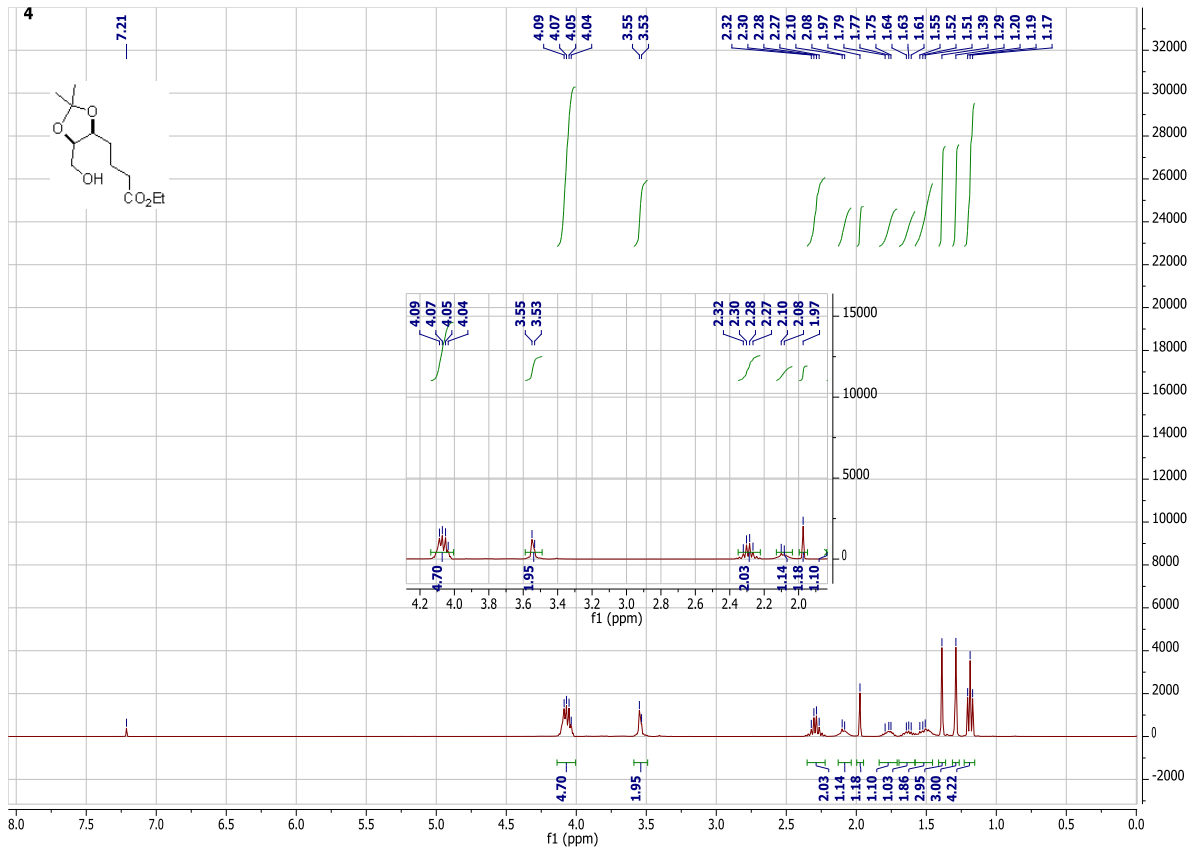
UNALK_151002103248 #1 RT: 0.01 AV: 1 NL: 6.36E7
T: FTMS + p ESI Full ms [200.00-500.00]



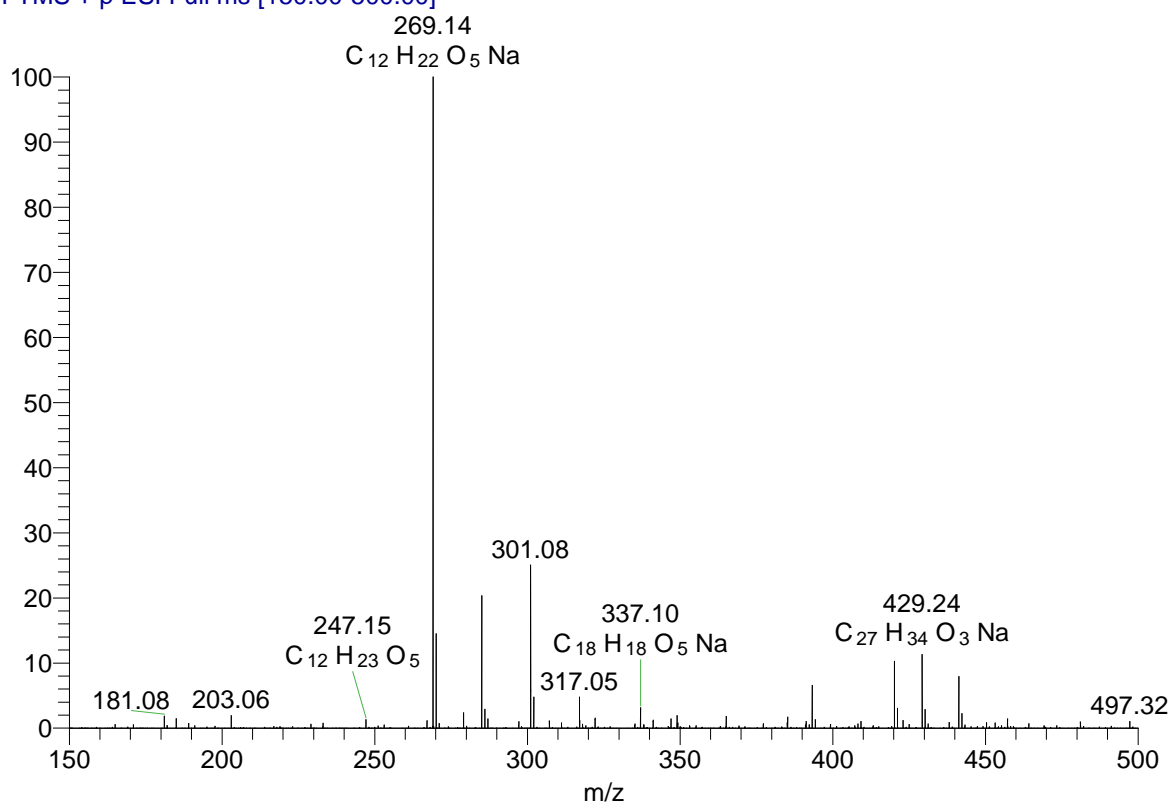
Appendix 3



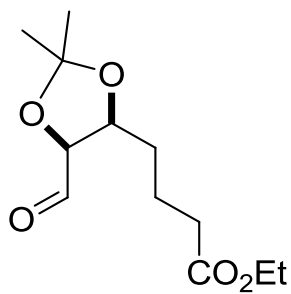
ethyl 4-((4*S*,5*R*)-5-(hydroxymethyl)-2,2-dimethyl-1,3-dioxolan-4-yl)butanoate
4



red #1 RT: 0.01 AV: 1 NL: 8.14E7
T: FTMS + p ESI Full ms [150.00-500.00]

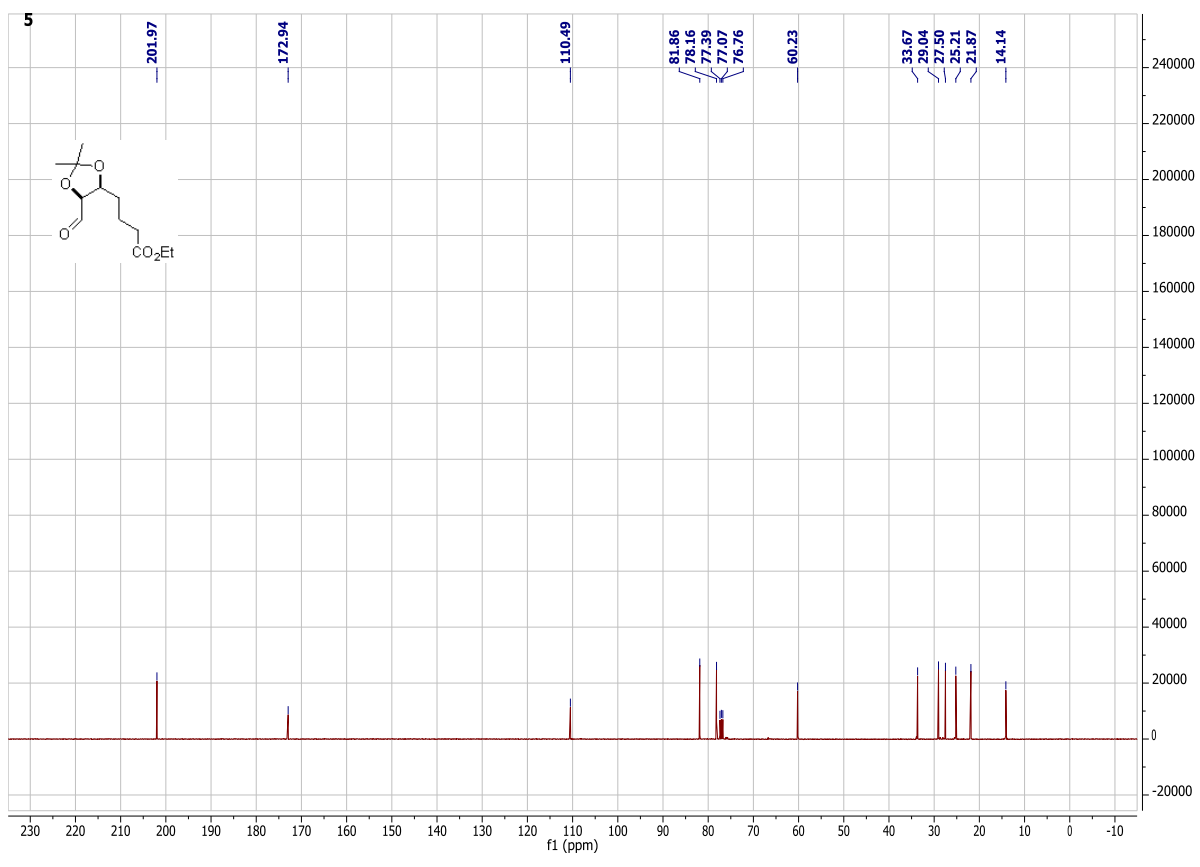
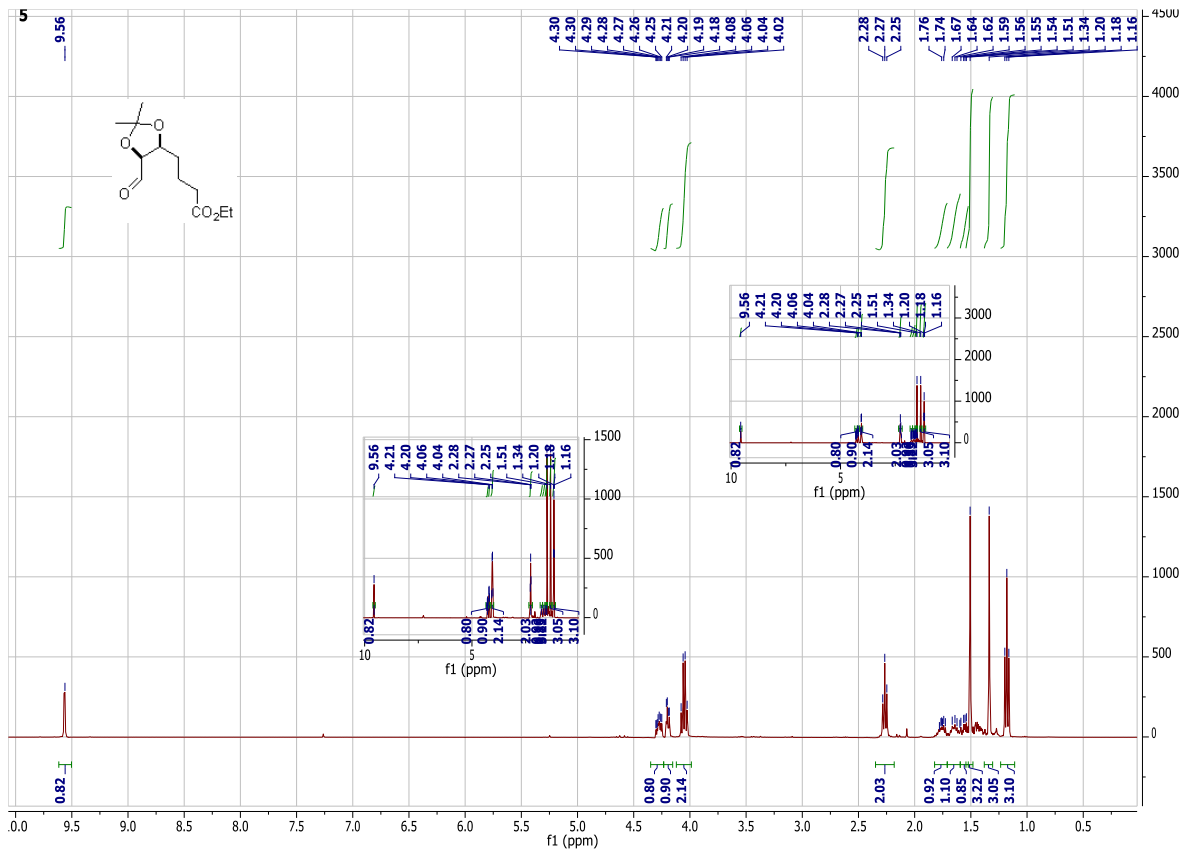


Appendix 4

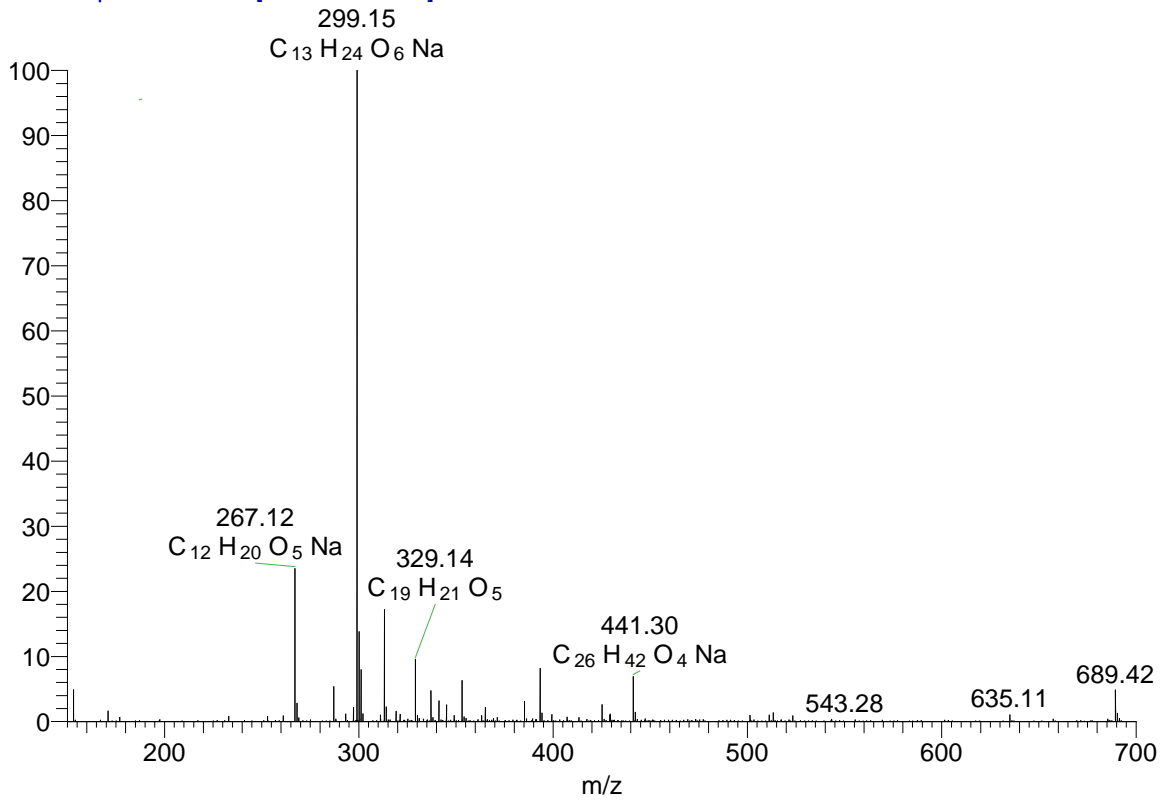


ethyl 4-((4S,5S)-5-formyl-2,2-dimethyl-1,3-dioxolan-4-yl)butanoate

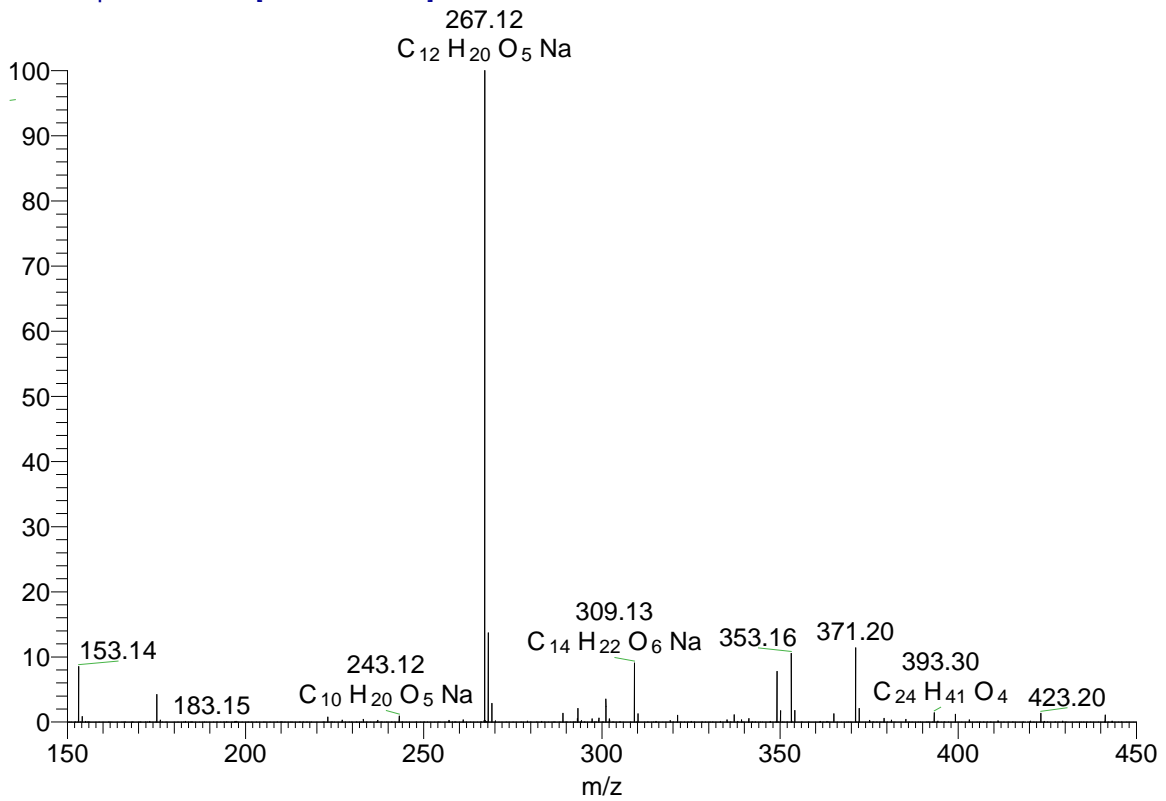
5



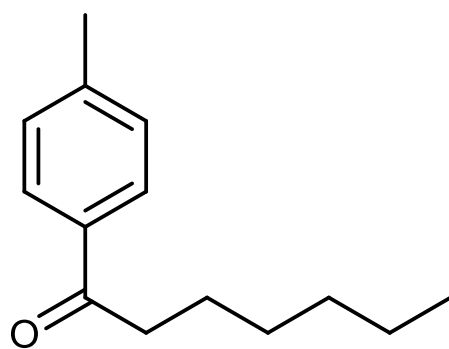
JHAI-2-10-2 #1 RT: 0.01 AV: 1 NL: 2.57E7
T: FTMS + p ESI Full ms [150.00-700.00]



JHAI-2-7-2_pos #1 RT: 0.00 AV: 1 NL: 2.45E7
T: FTMS + p ESI Full ms [150.00-450.00]

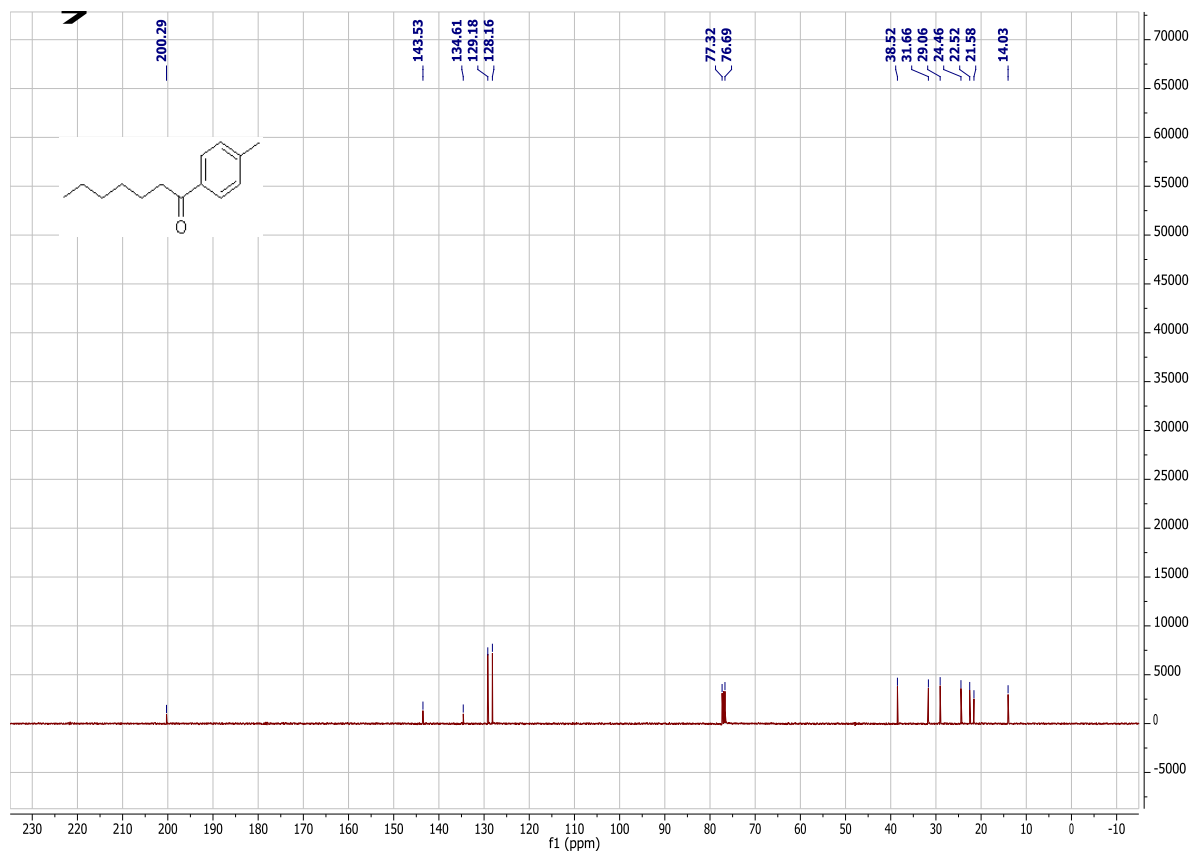
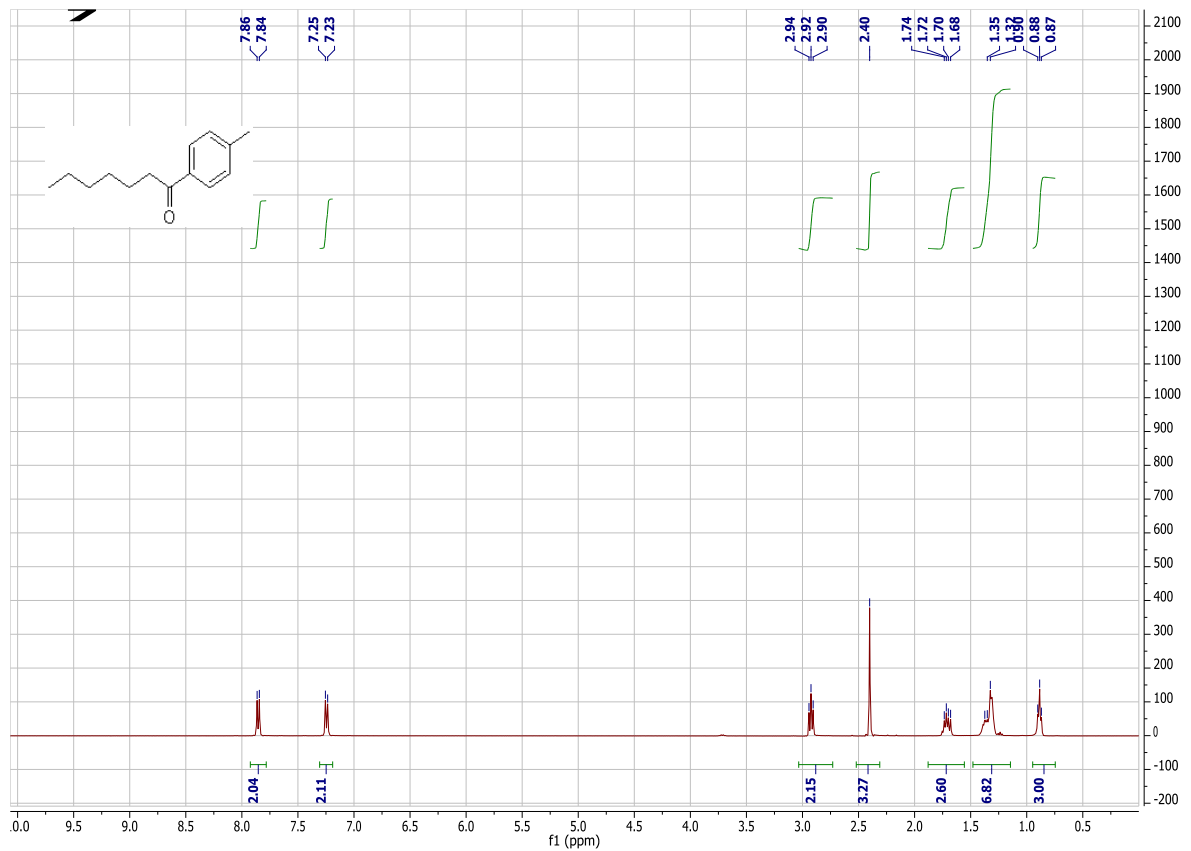


Appendix 5

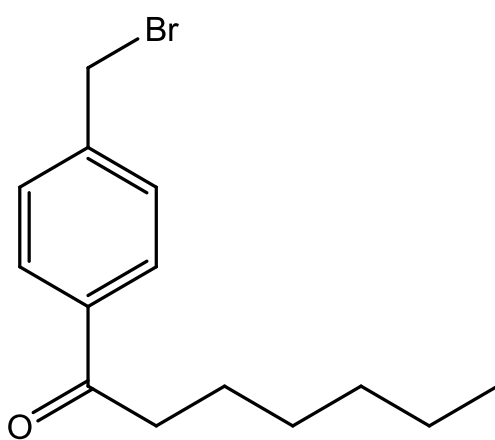


1-*p*-tolylheptan-1-one

7

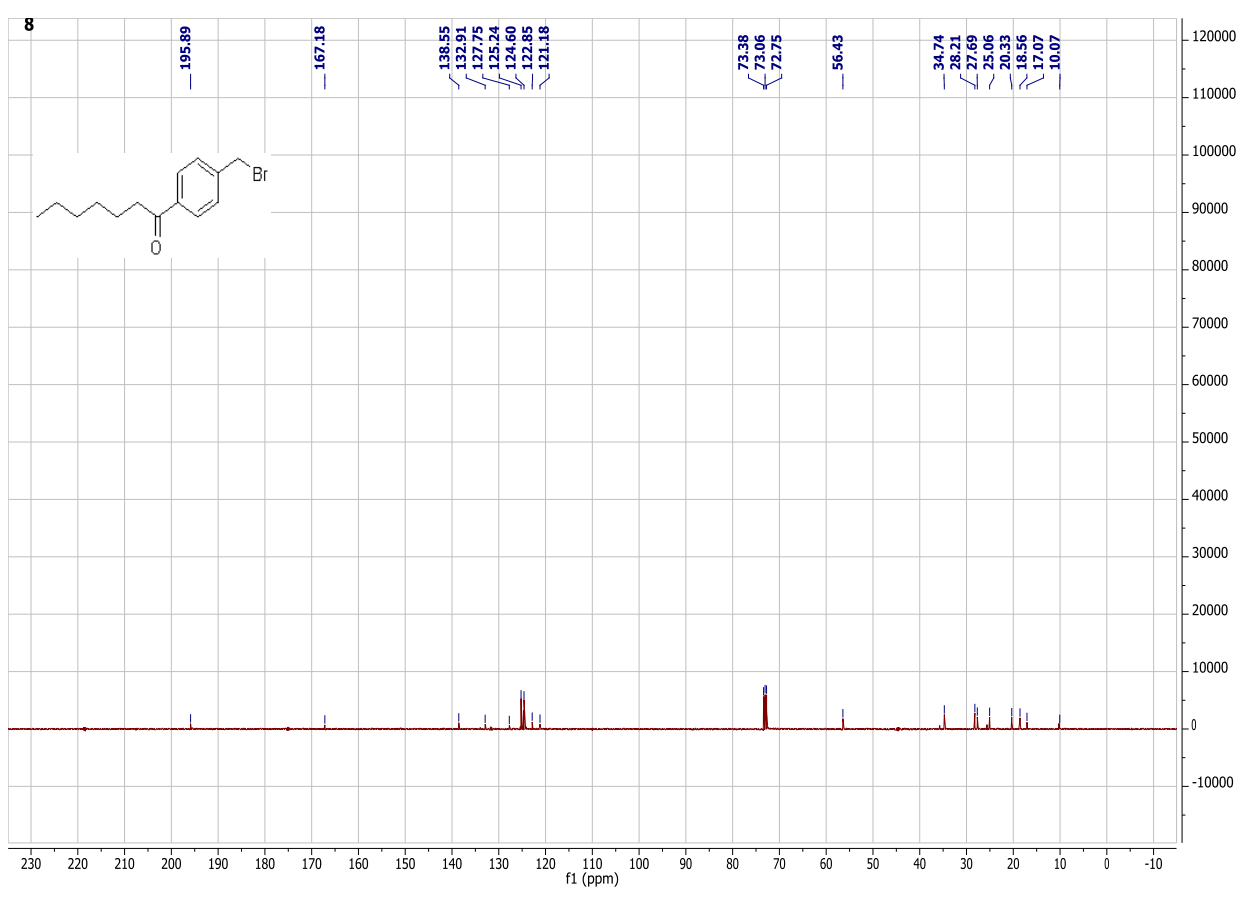
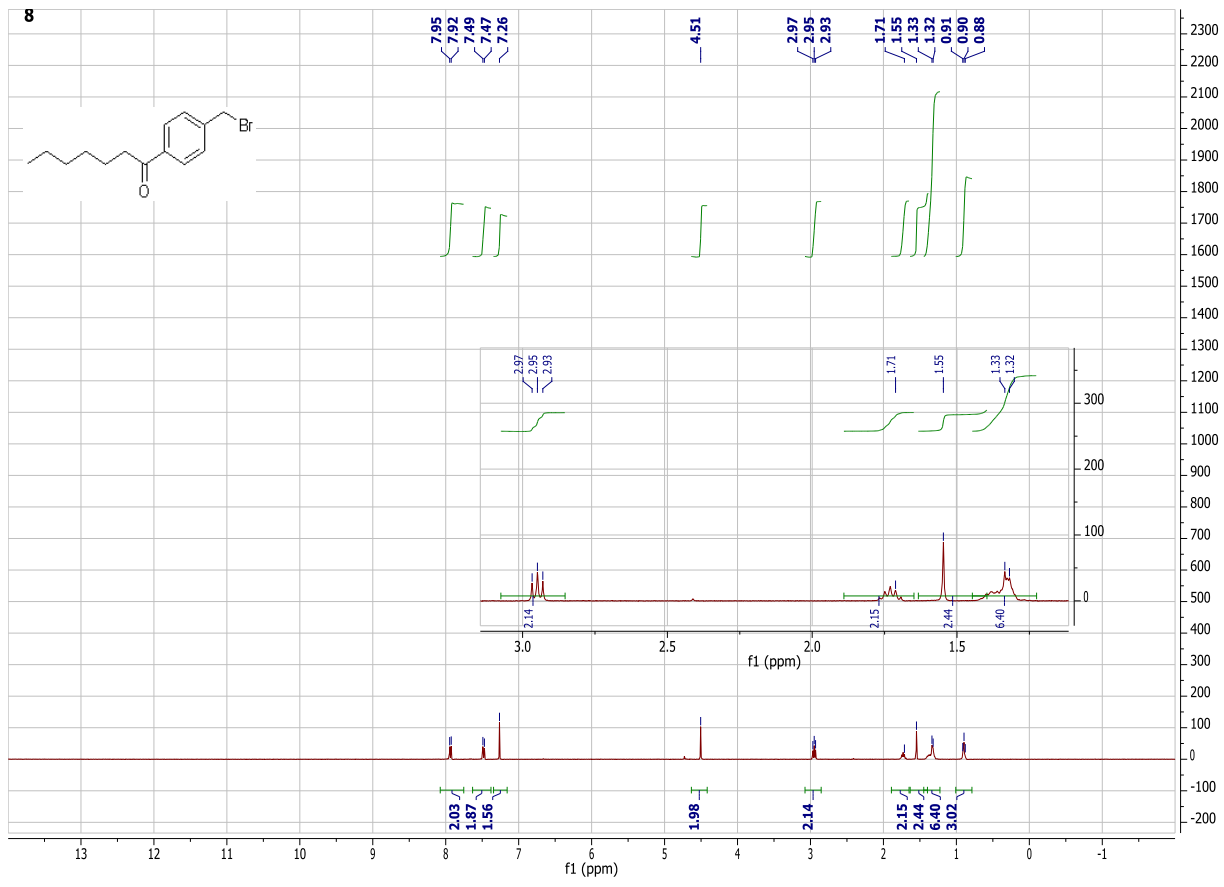


Appendix 6

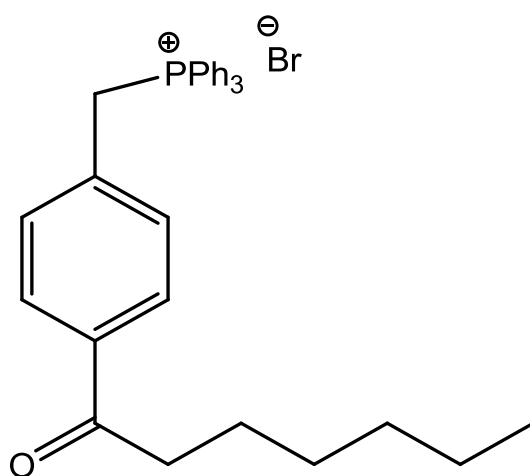


1-(4-(bromomethyl)phenyl)heptan-1-one

8

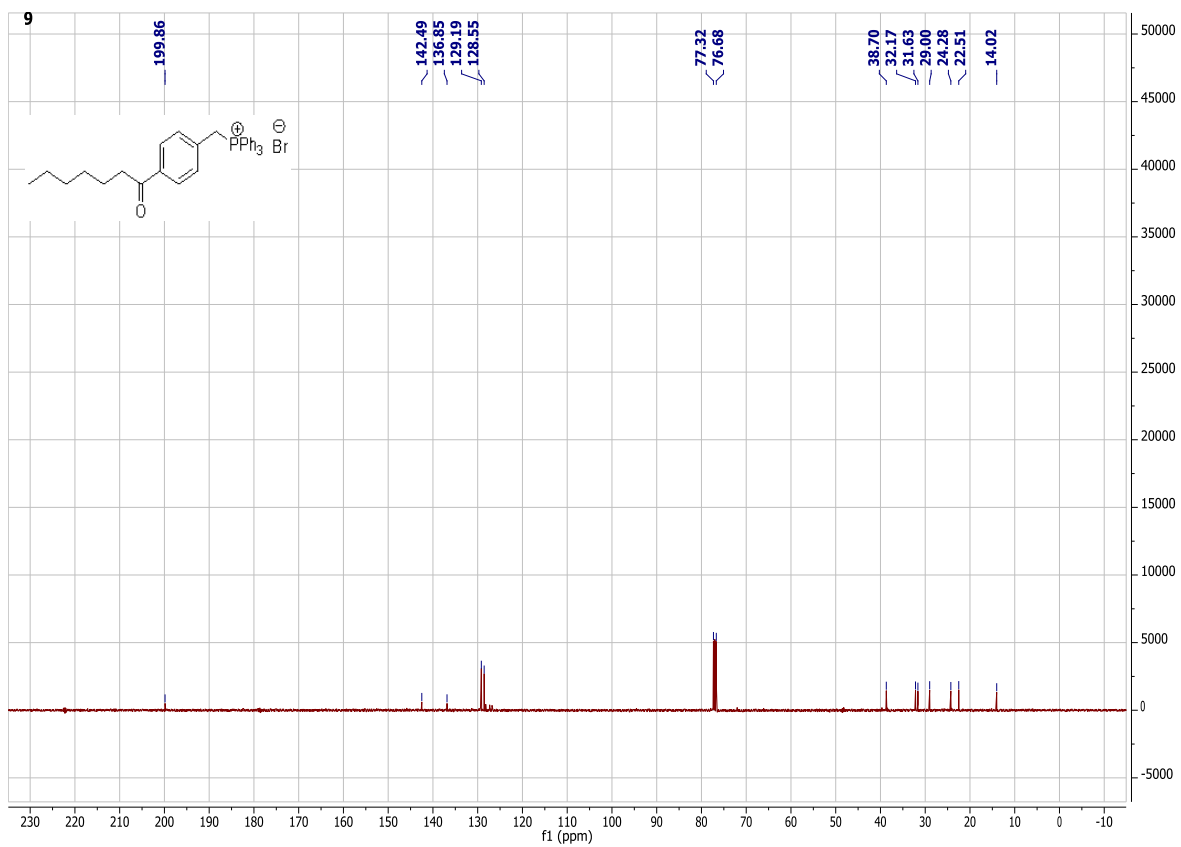
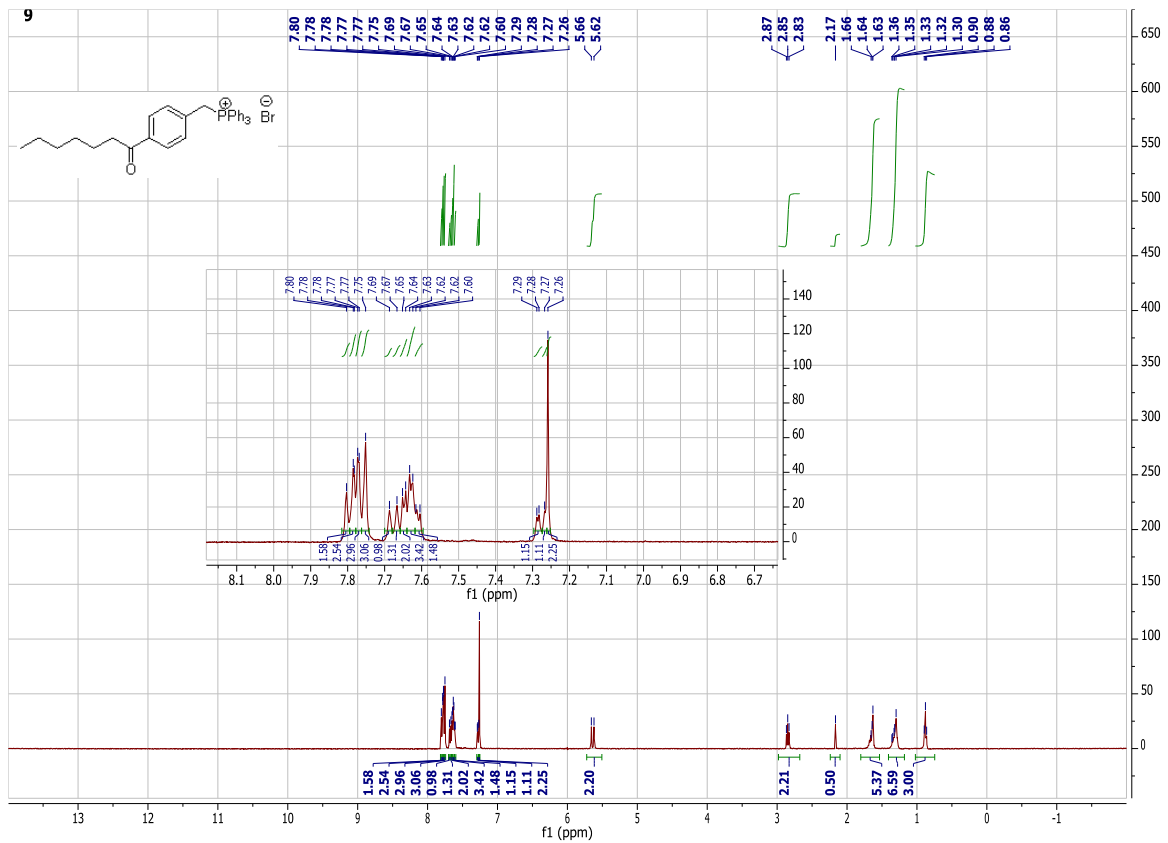


Appendix 7

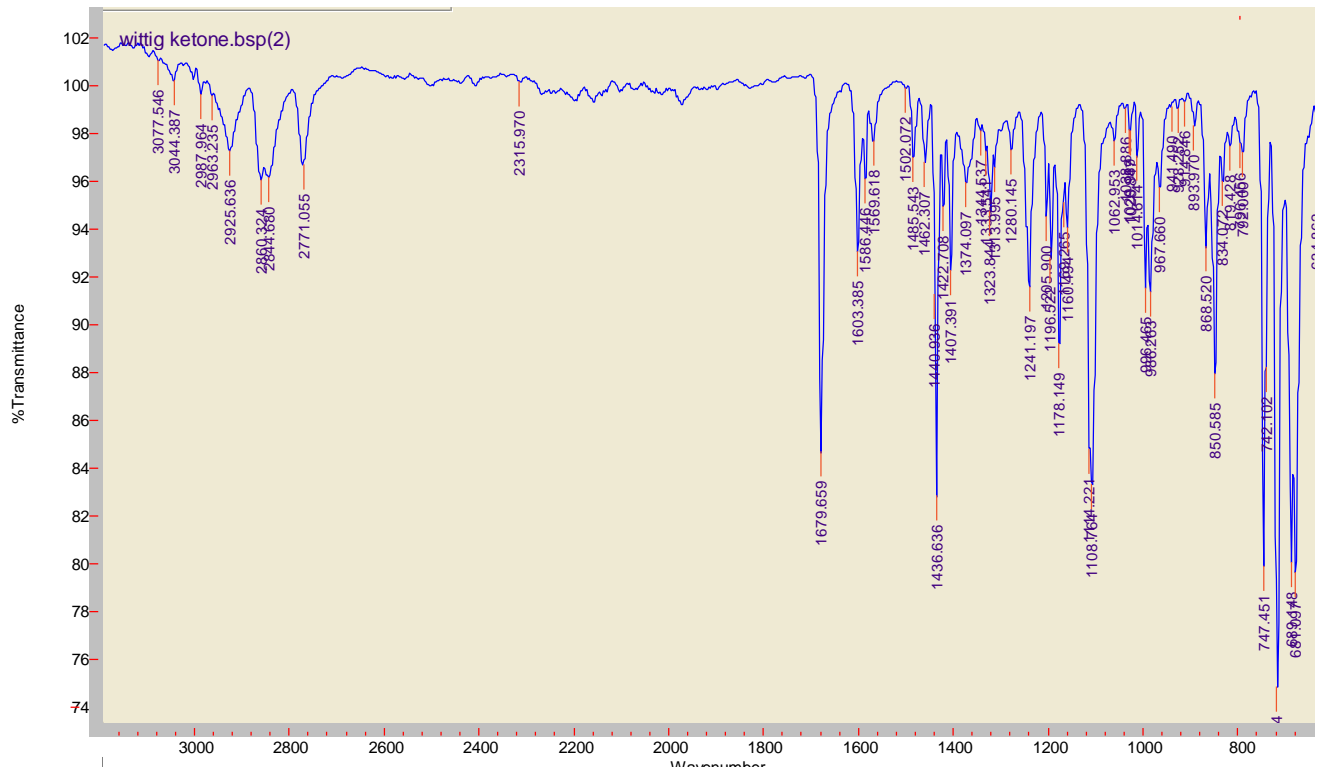
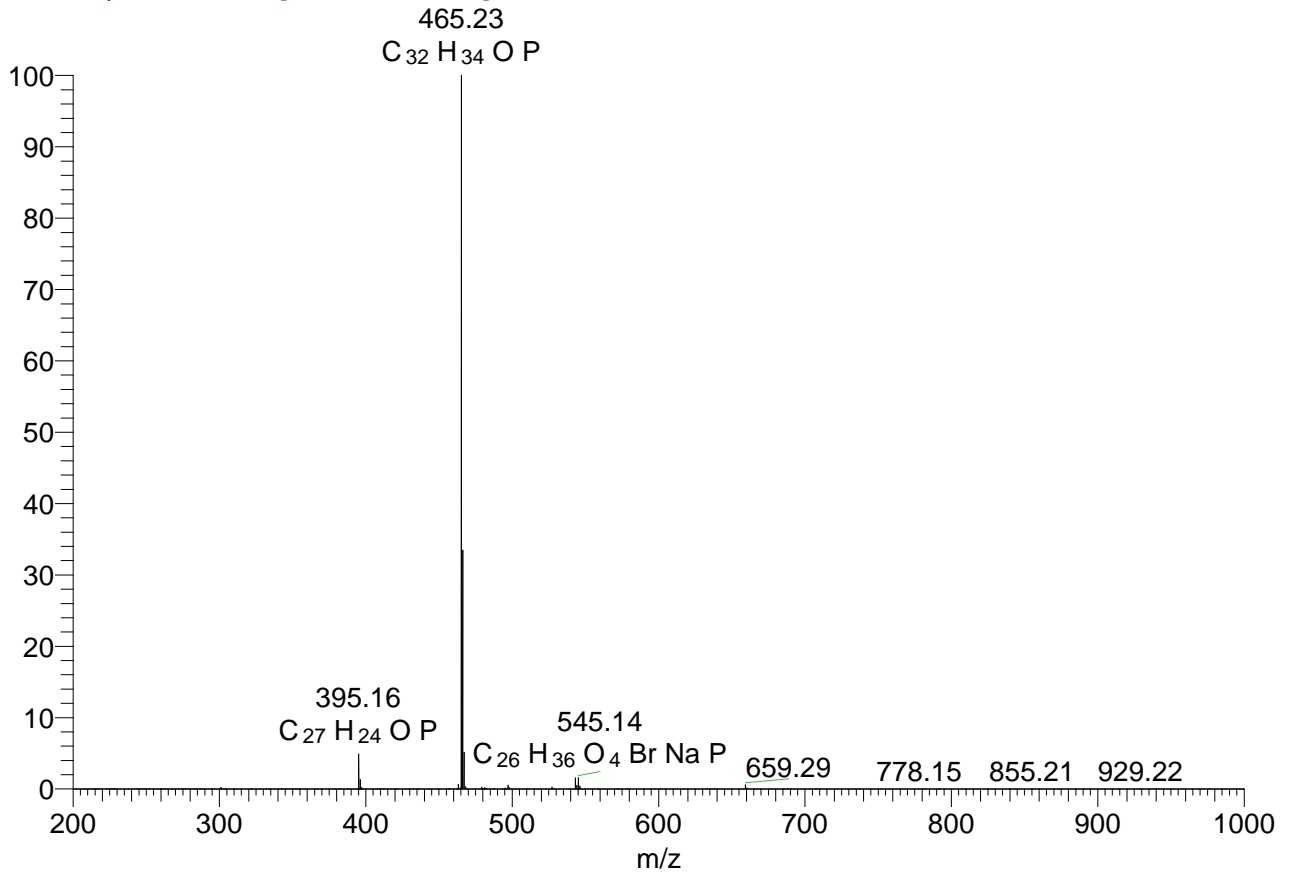


(4-heptanoylbenzyl)triphenylphosphonium bromide

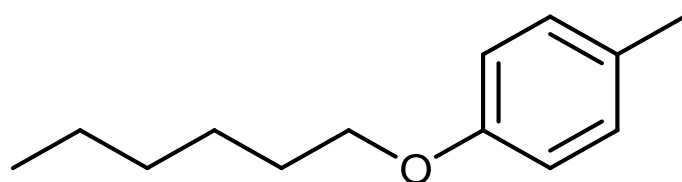
9



JHAI-1-20wit_MeOH #1 RT: 0.01 AV: 1 NL: 3.22E8
T: FTMS + p ESI Full ms [200.00-1000.00]

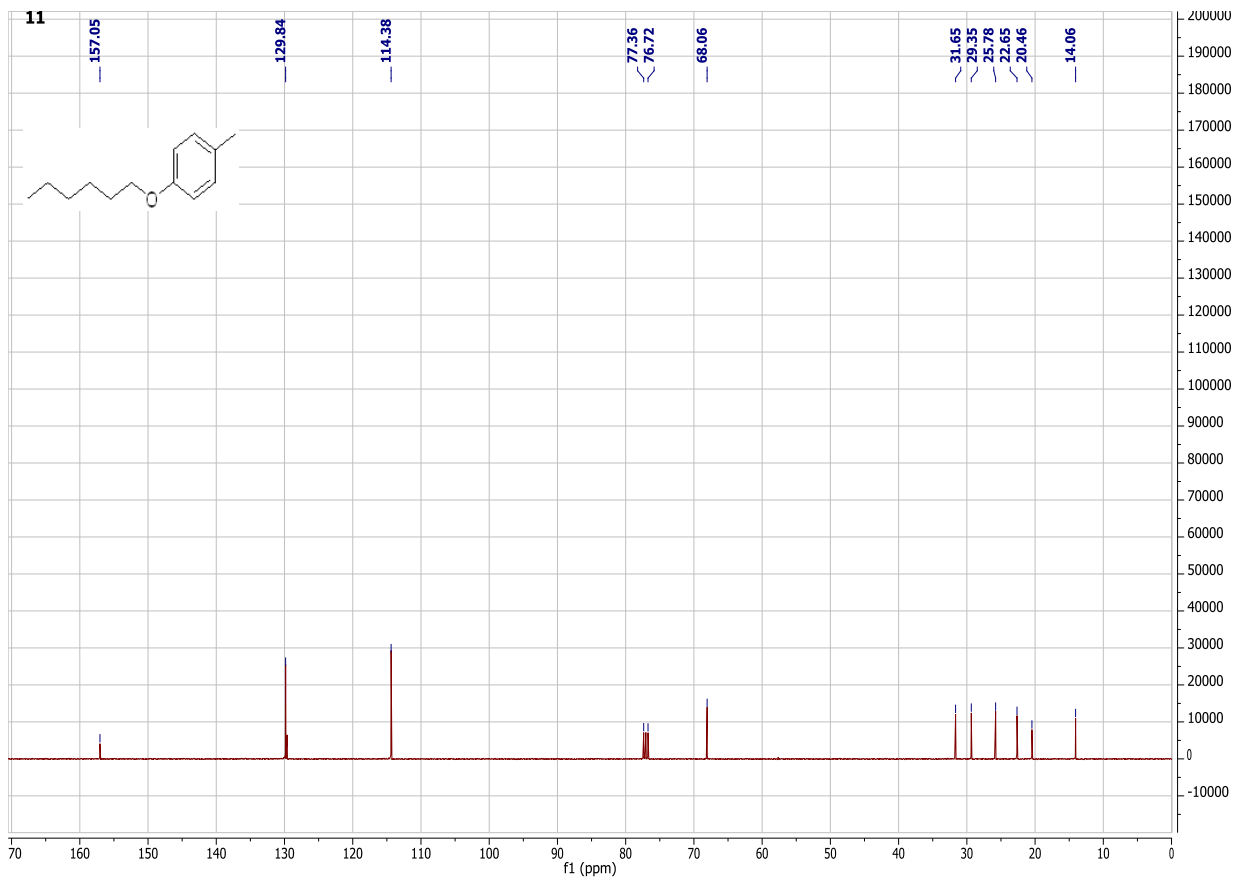
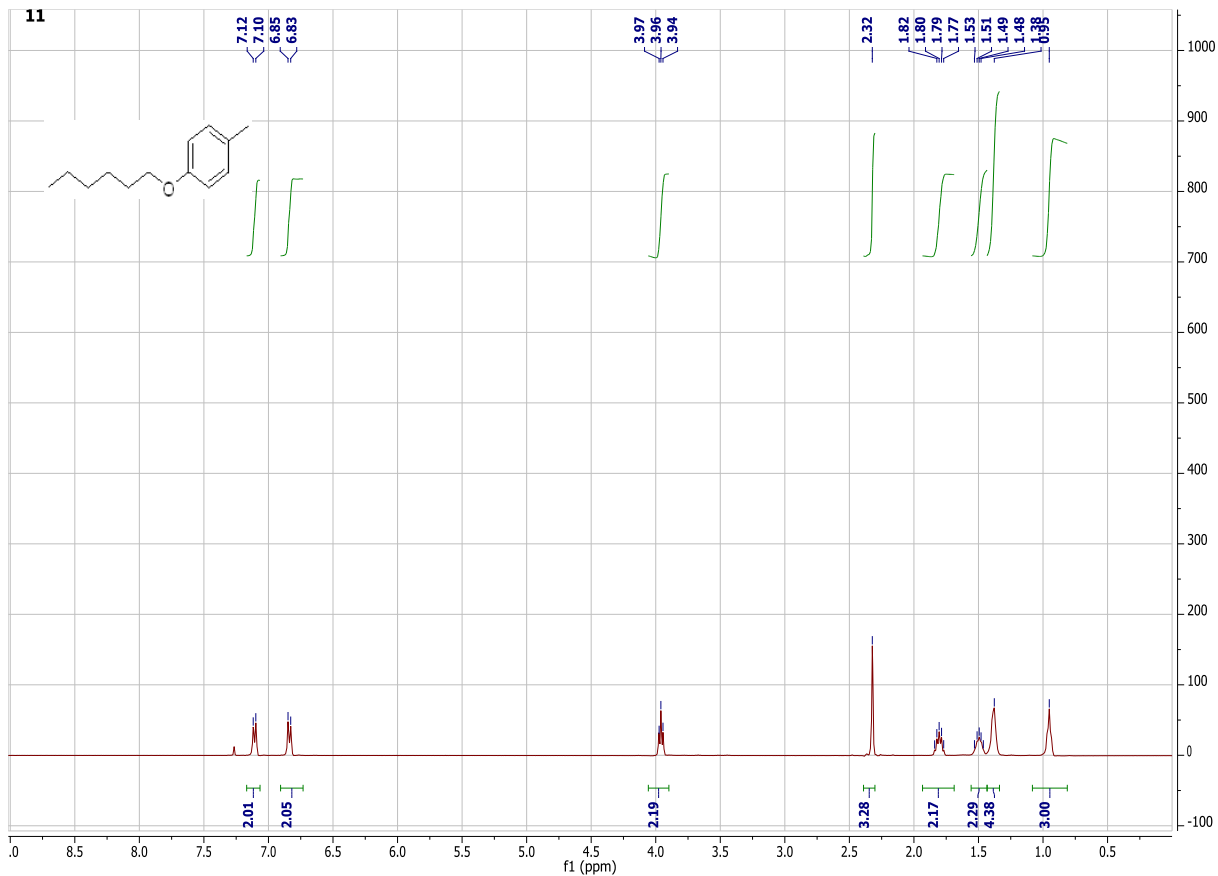


Appendix 8

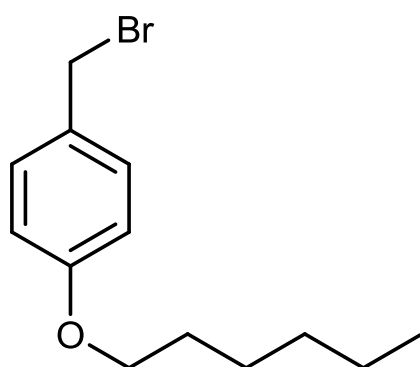


1-(hexyloxy)-4-methylbenzene

11

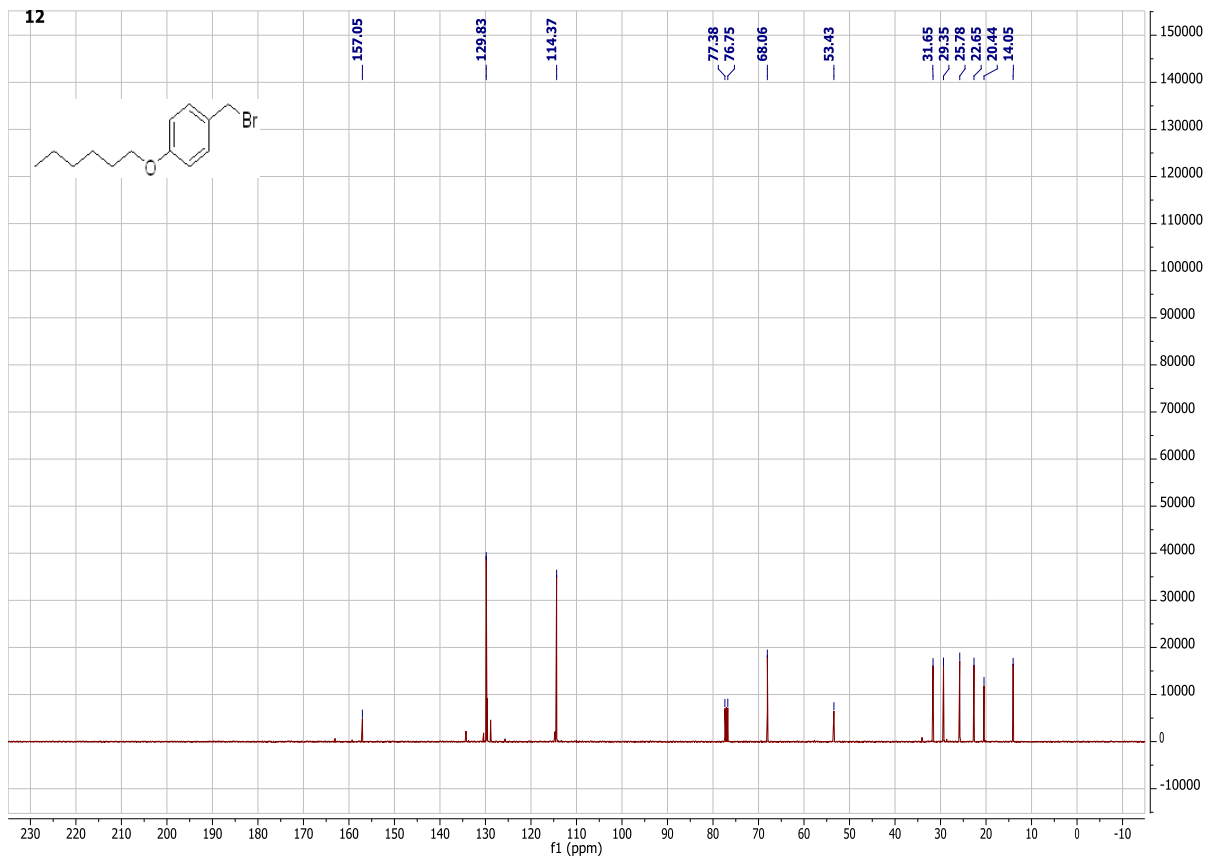
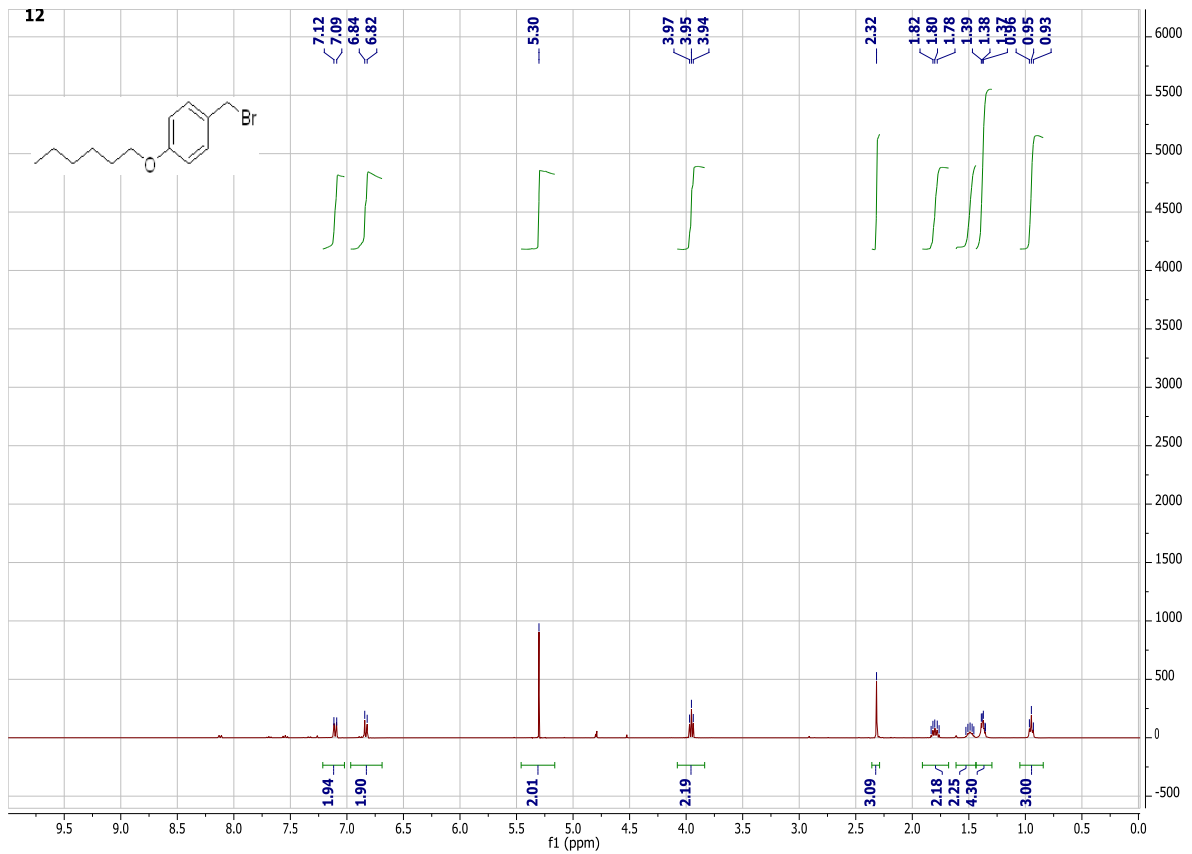


Appendix 9

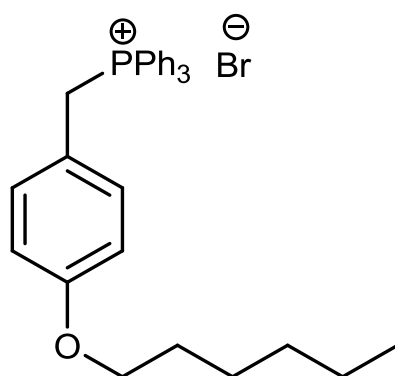


1-(bromomethyl)-4-(hexyloxy)benzene

12

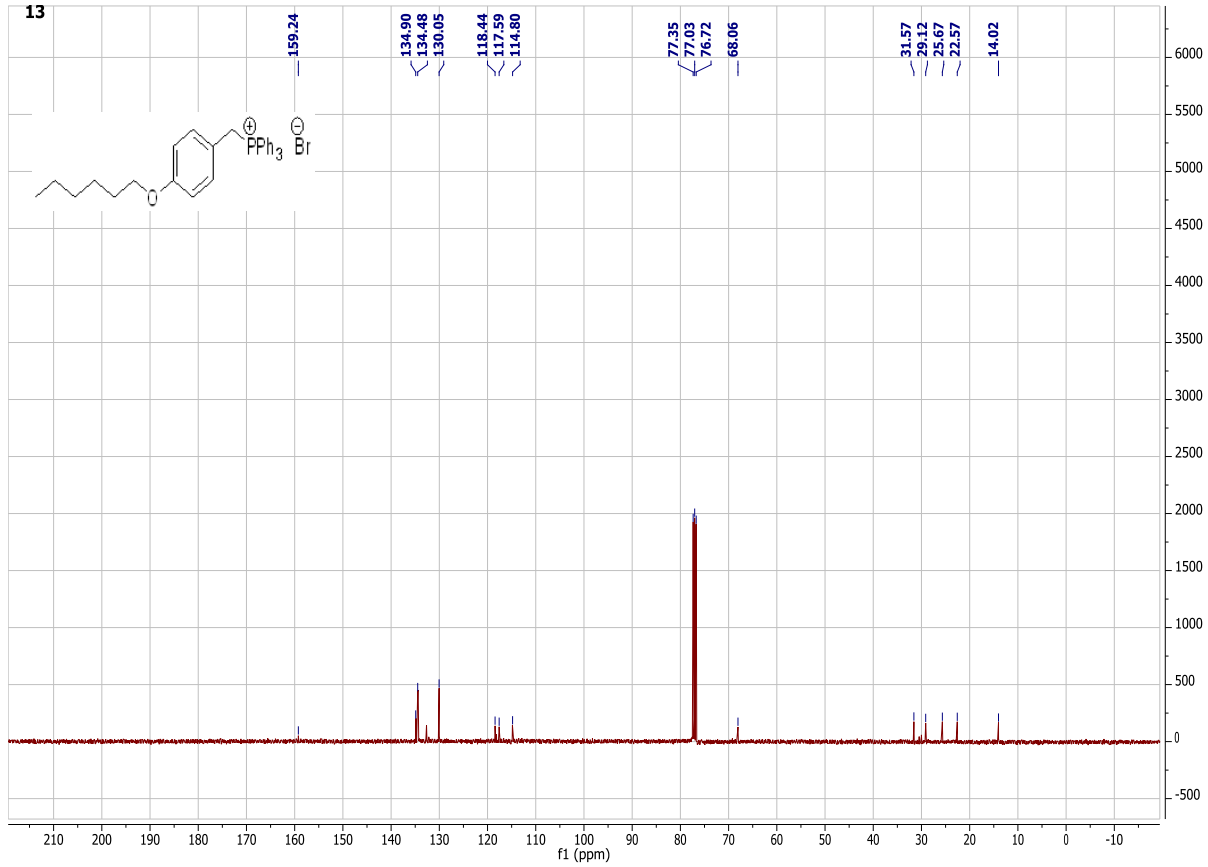
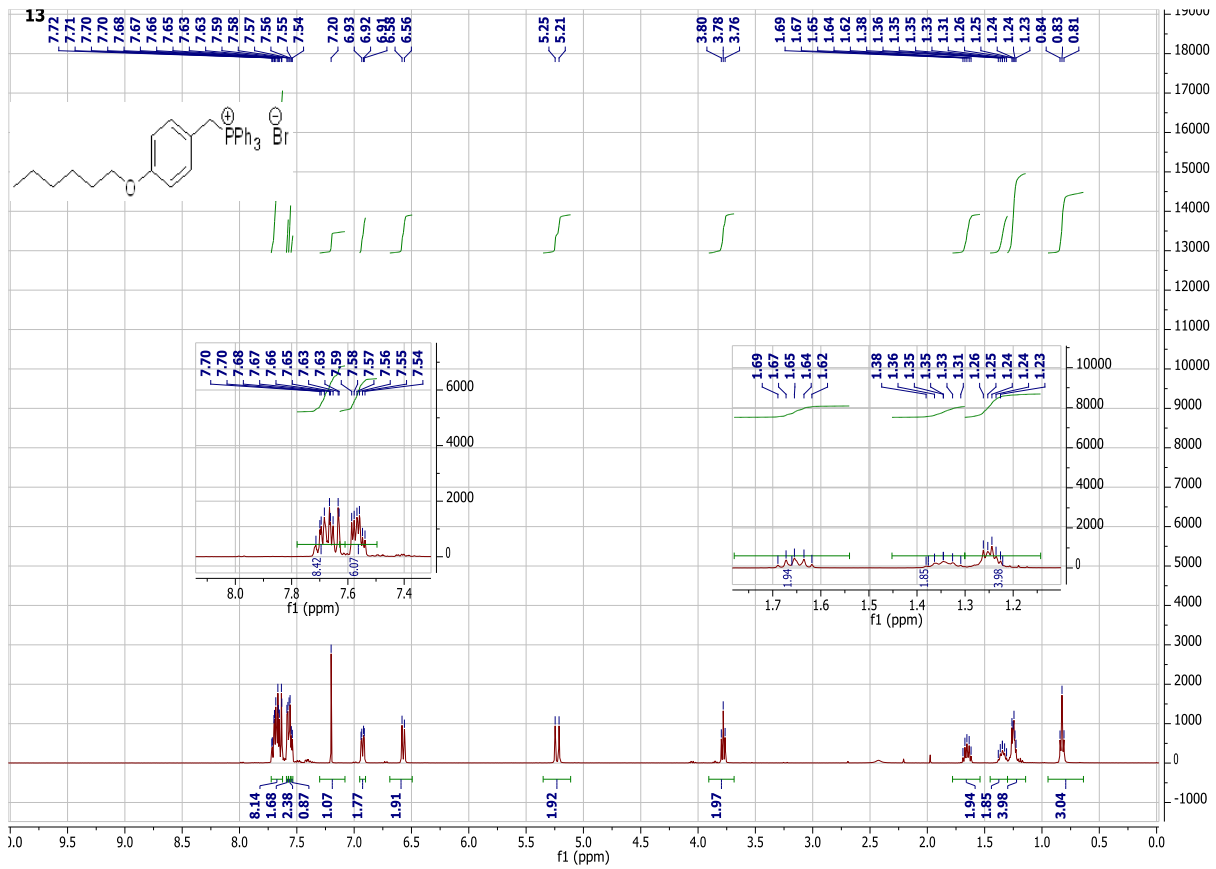


Appendix 10

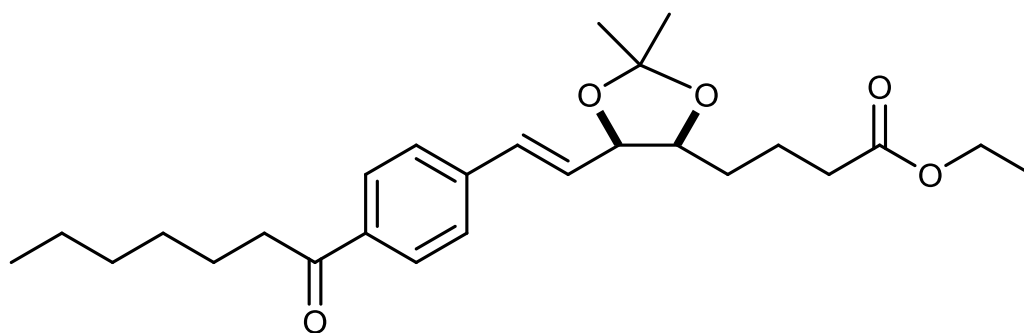


(4-(hexyloxy)benzyl)triphenylphosphonium bromide

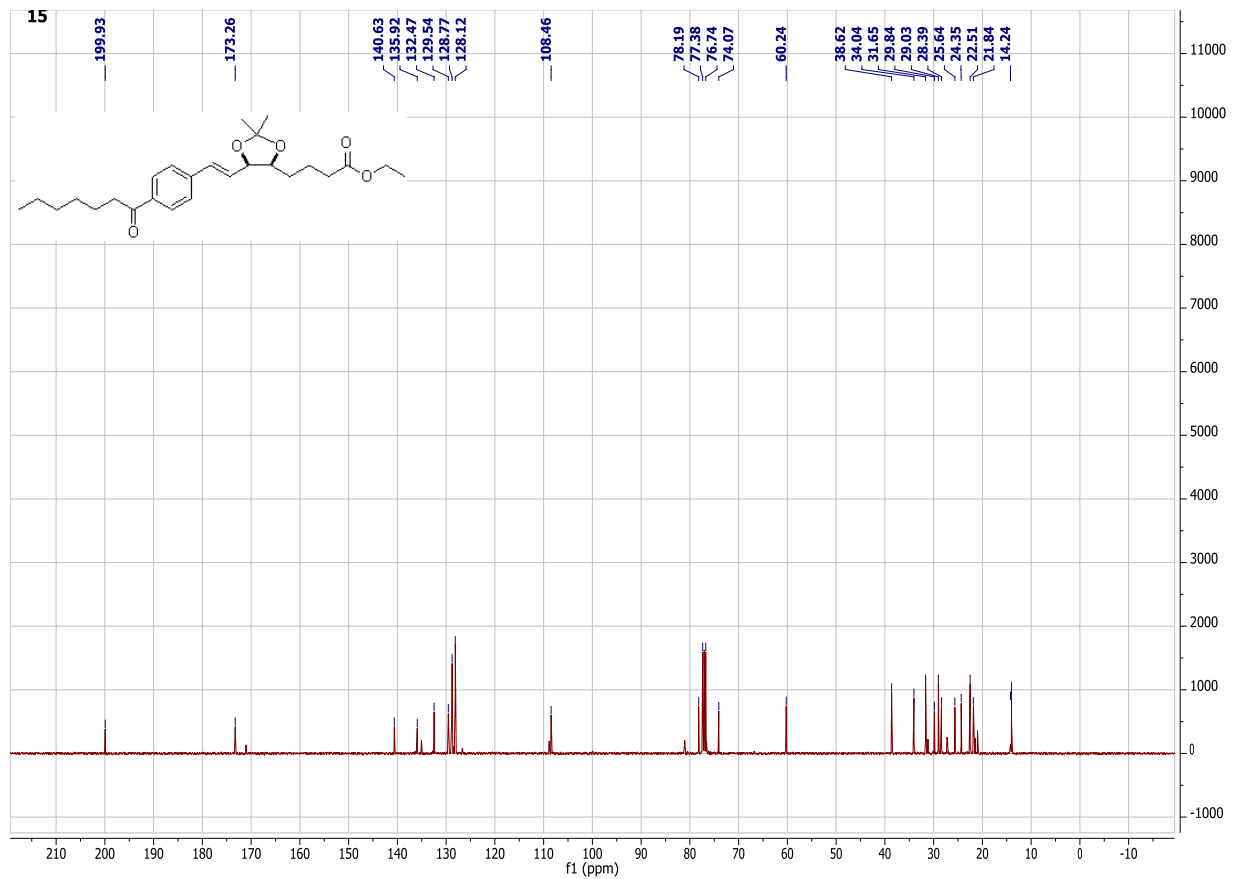
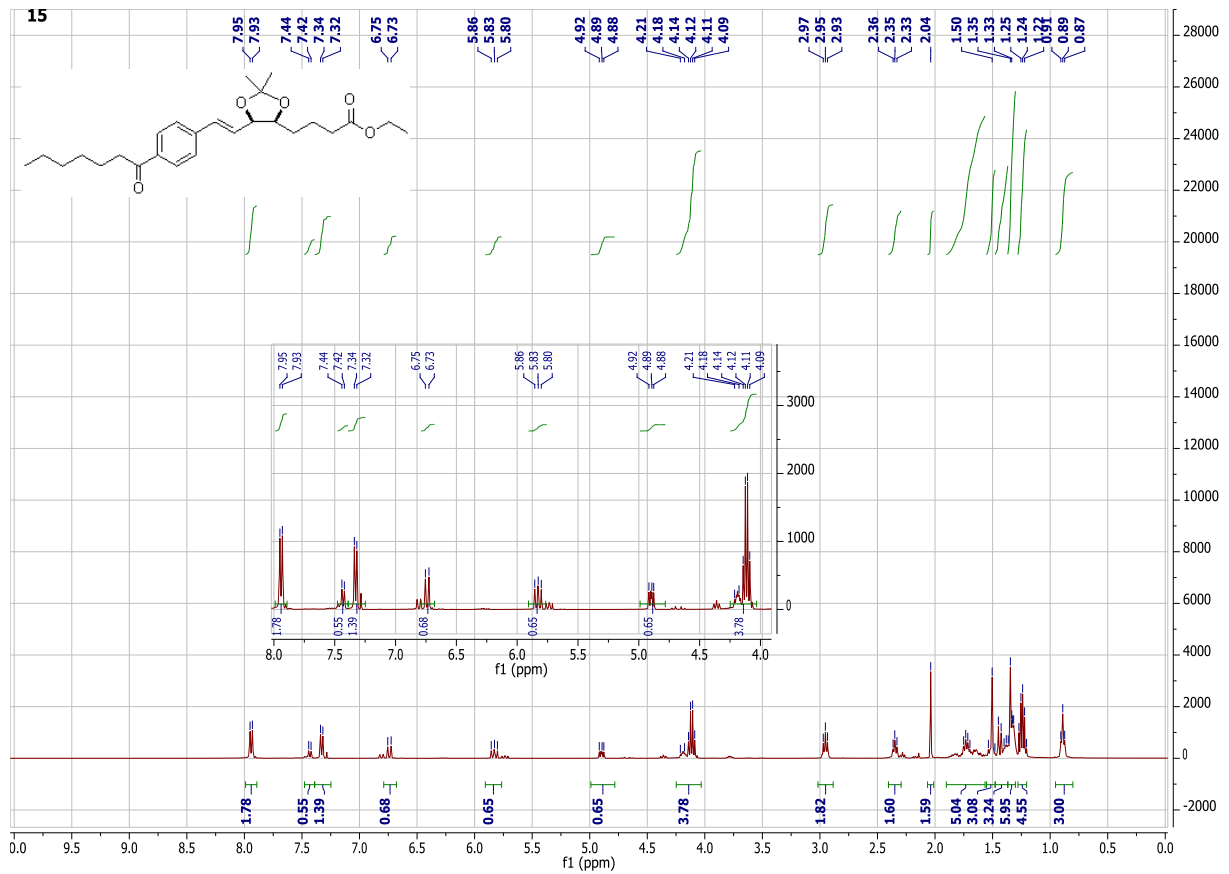
13



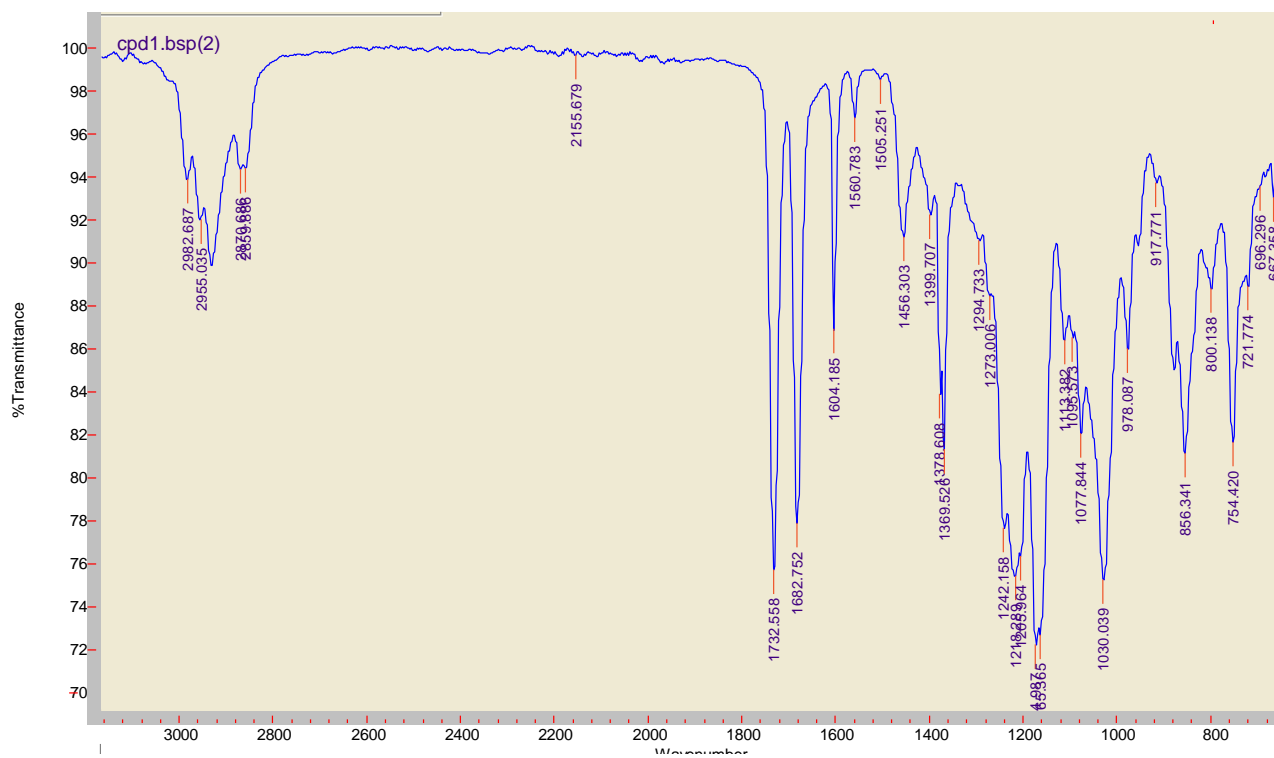
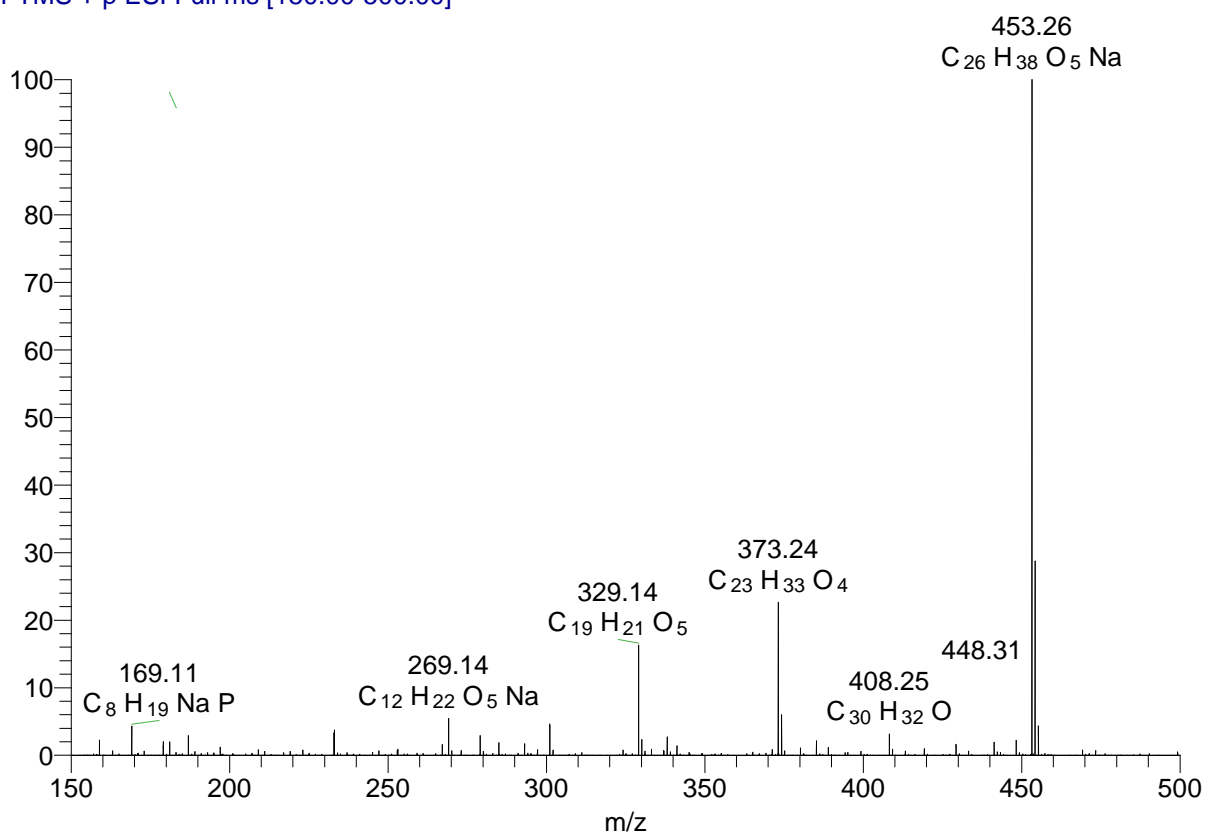
Appendix 11



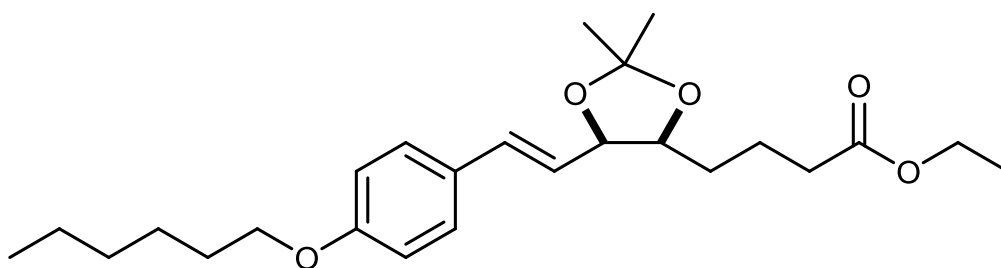
ethyl 4-((4S,5R)-5-(4-heptanoylstyryl)-2,2-dimethyl-1,3-dioxolan-4-yl)butanoate



bi_150930155903 #1 RT: 0.01 AV: 1 NL: 1.47E7
T: FTMS + p ESI Full ms [150.00-500.00]

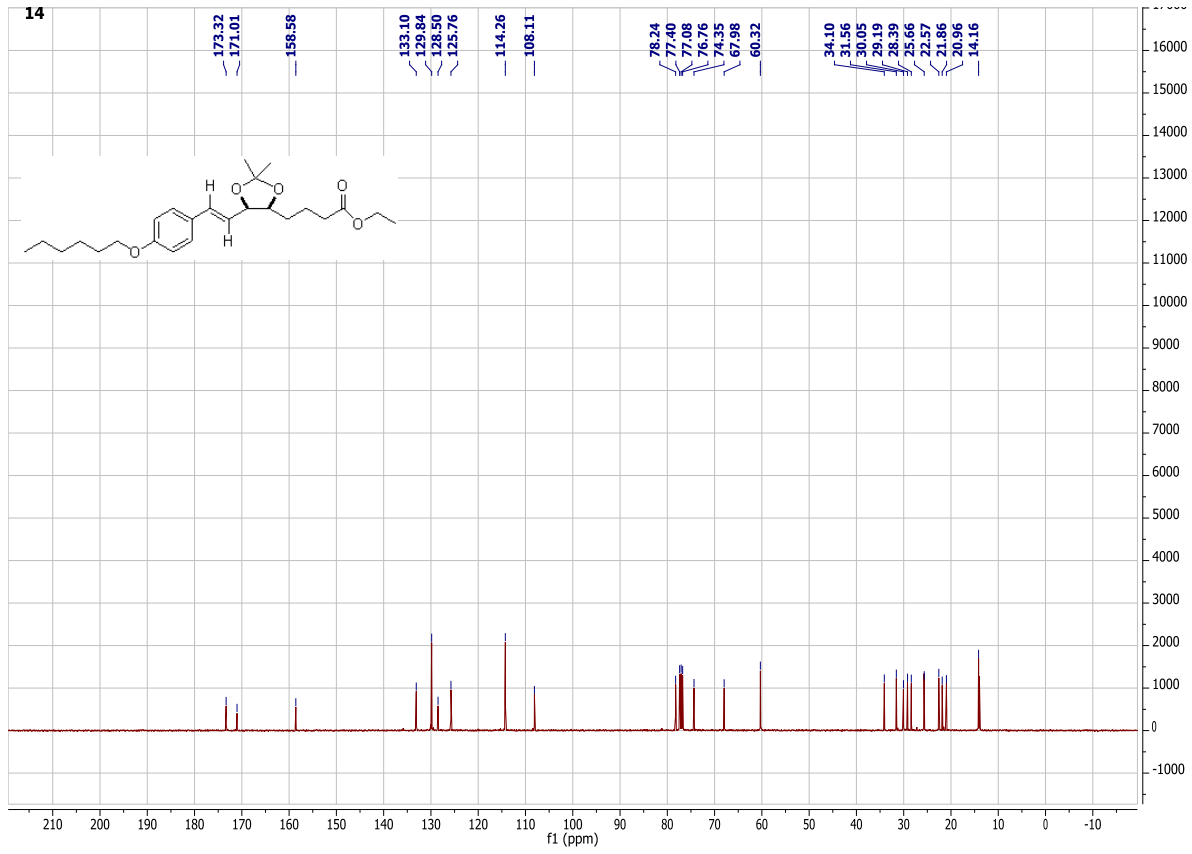
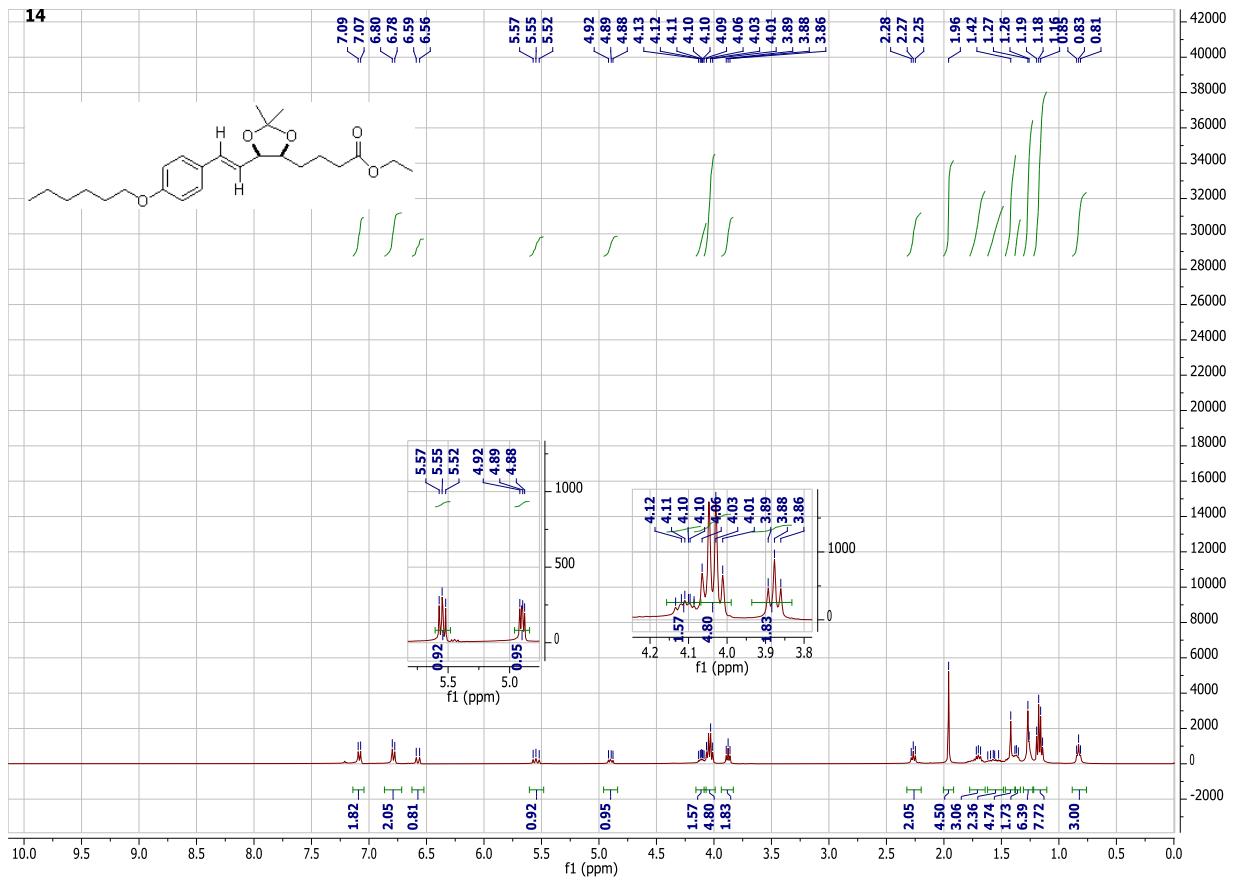


Appendix 12

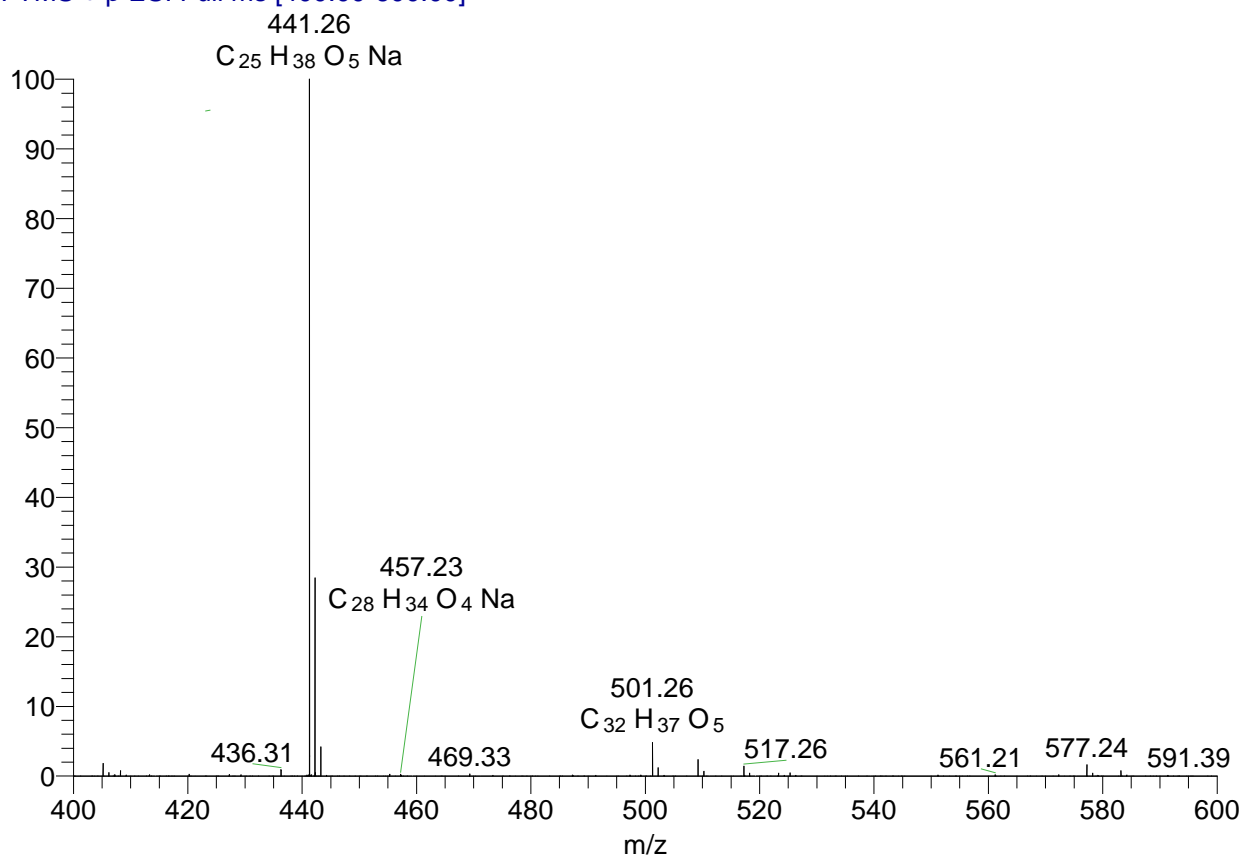


ethyl 4-((4S,5R)-5-(4-(hexyloxy)styryl)-2,2-dimethyl-1,3-dioxolan-4-yl)butanoate

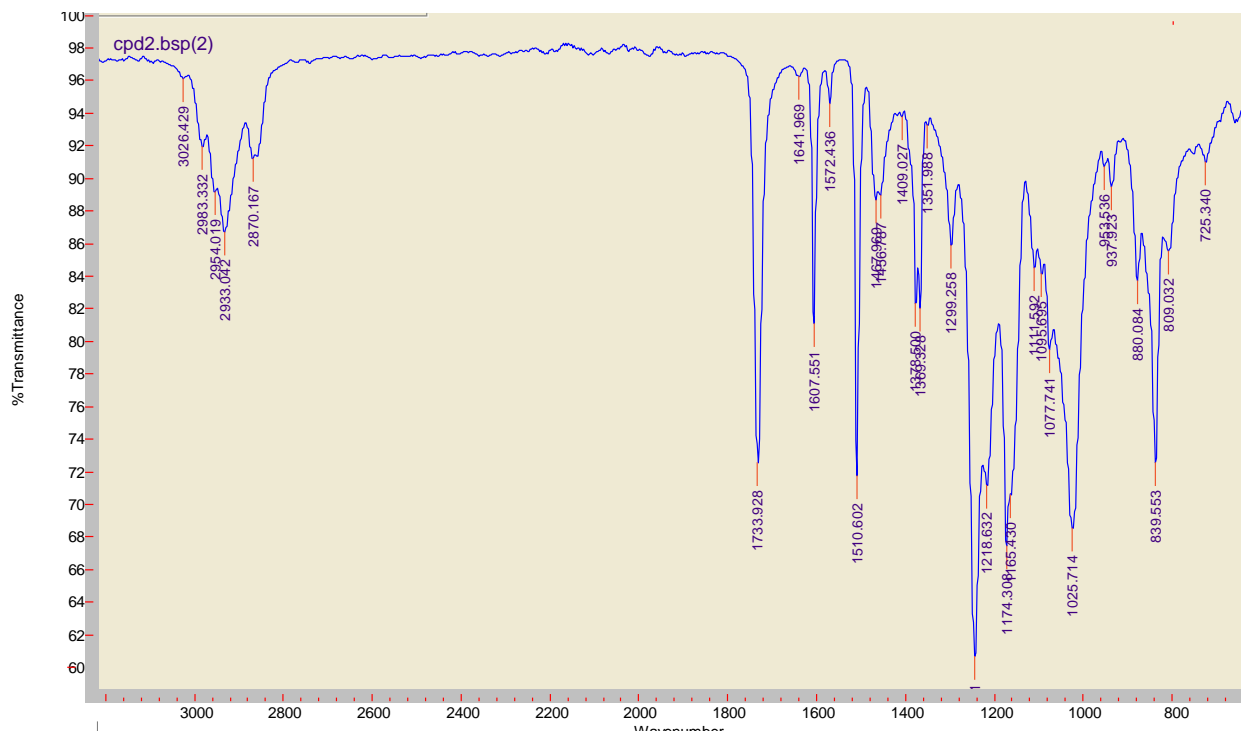
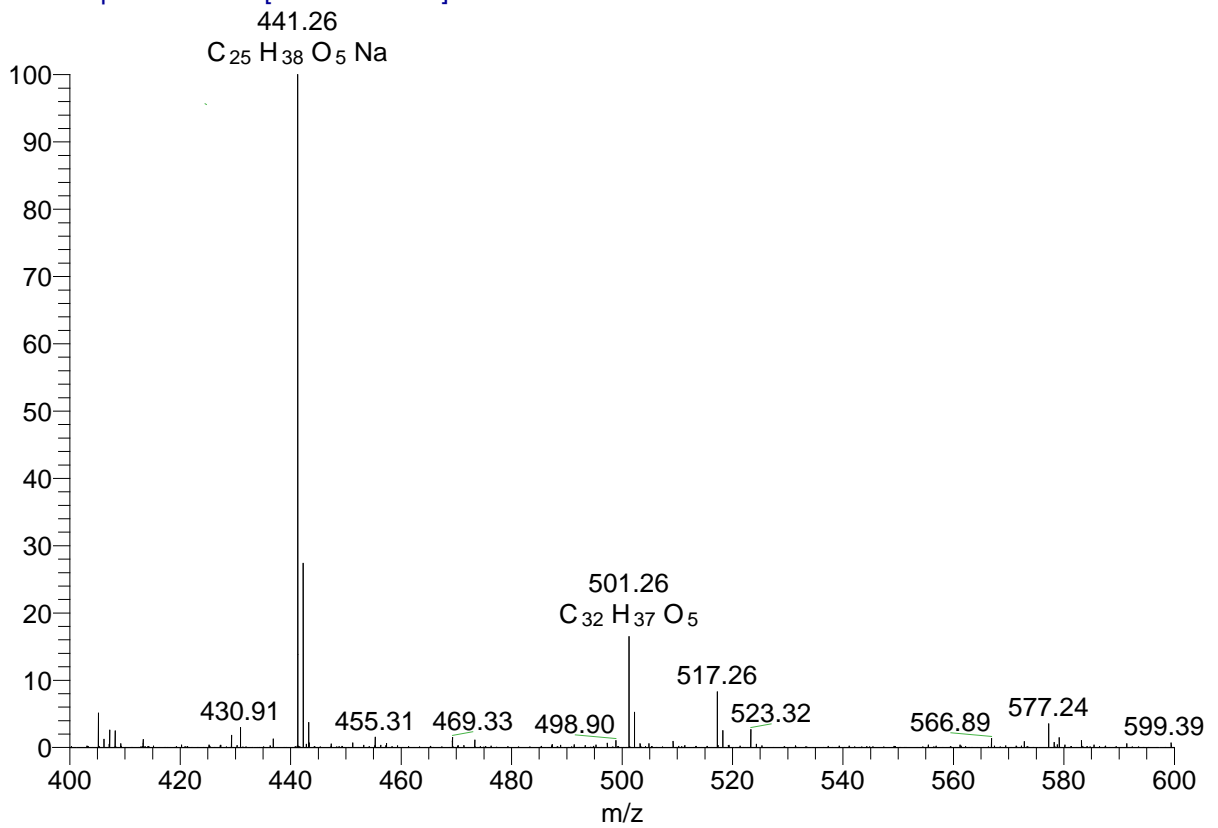
14



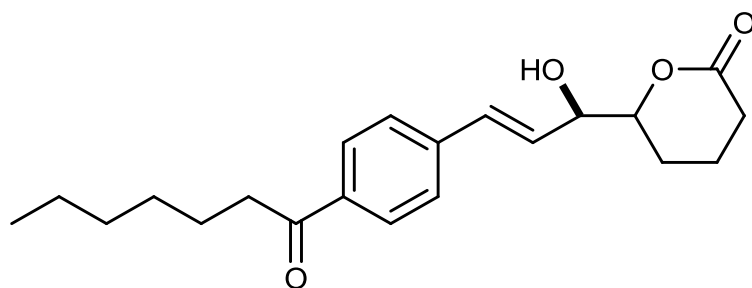
h_151007161342 #1 RT: 0.01 AV: 1 NL: 3.74E7
T: FTMS + p ESI Full ms [400.00-600.00]



h_a #1 RT: 0.02 AV: 1 NL: 4.55E6
T: FTMS + p ESI Full ms [400.00-600.00]

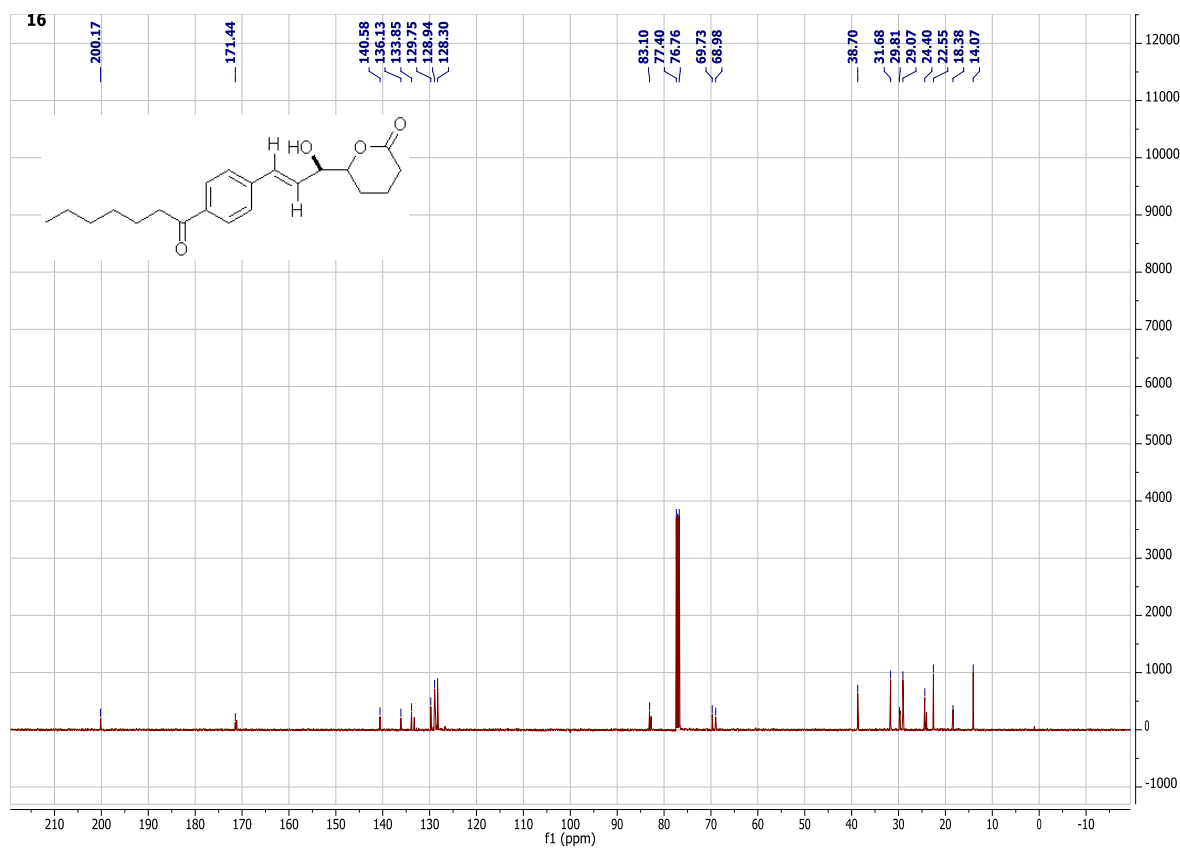
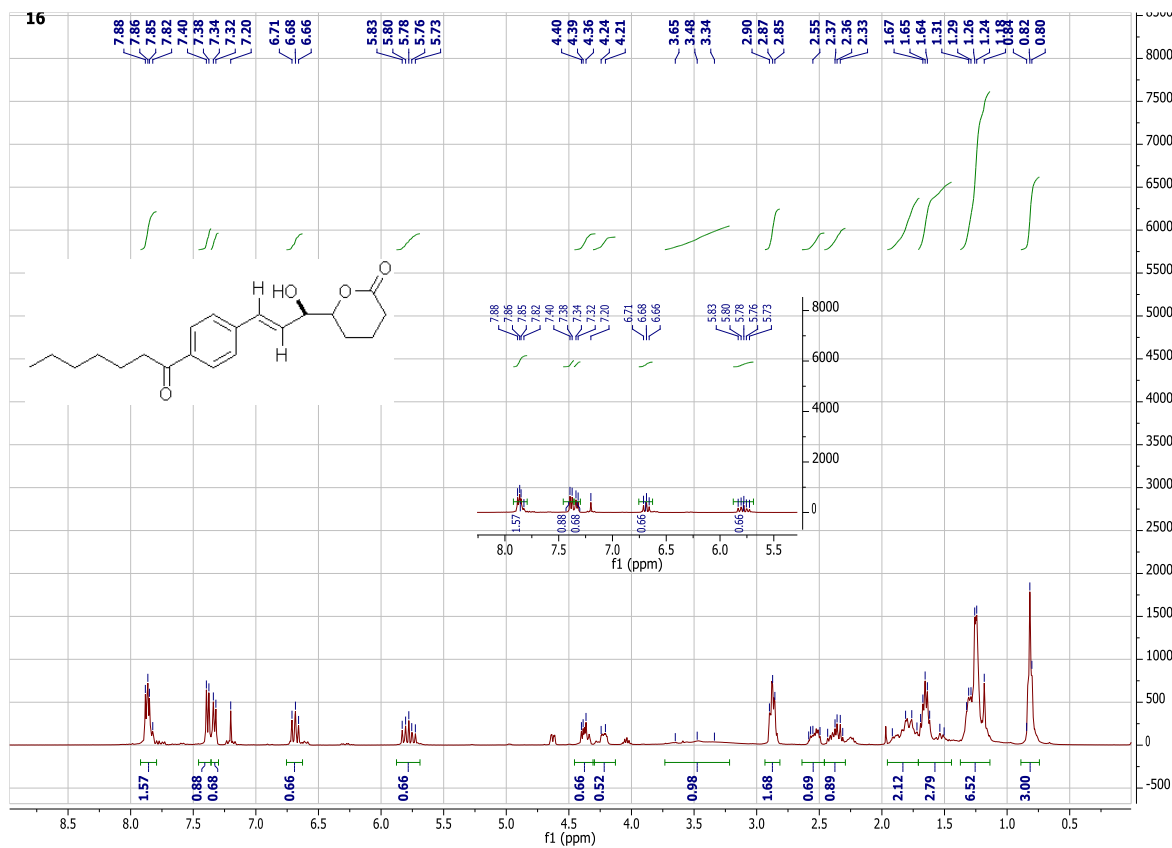


Appendix 13

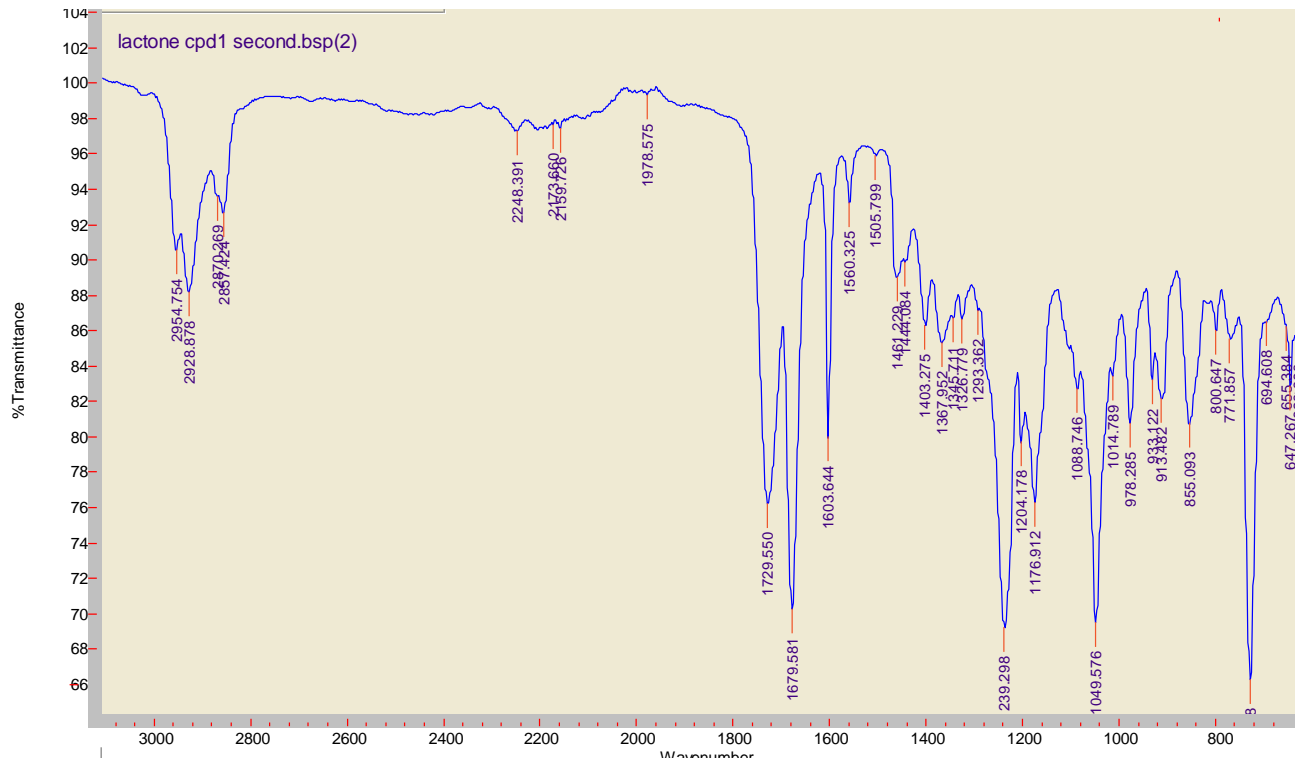
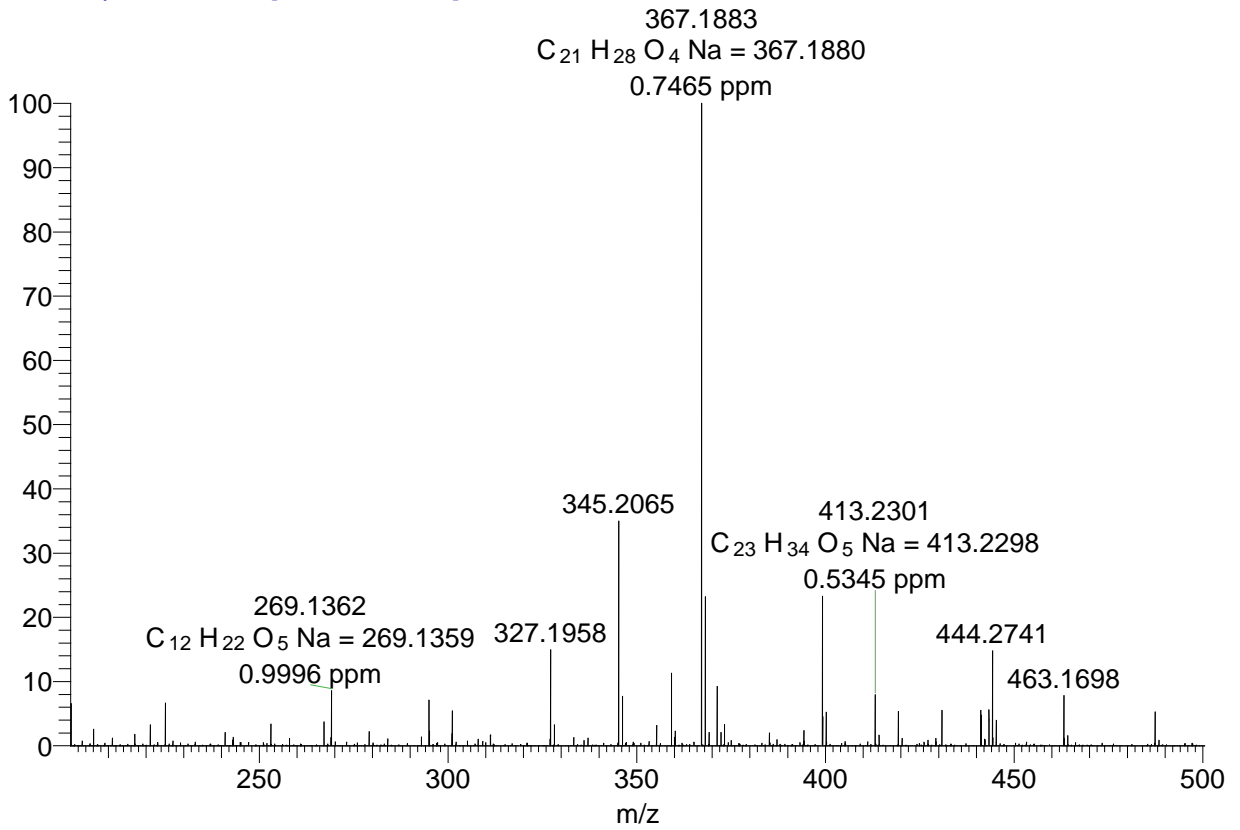


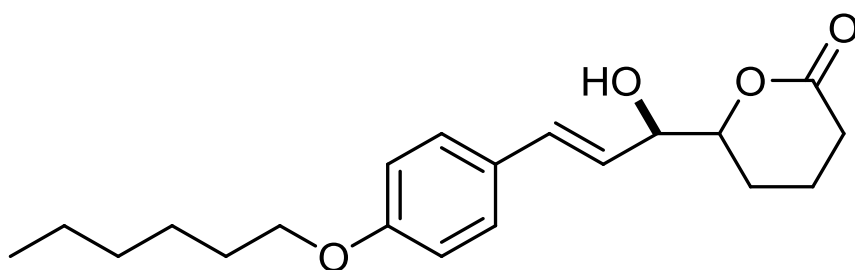
6-((*R,E*)-3-(4-heptanoylphenyl)-1-hydroxyallyl)tetrahydro-2*H*-pyran-2-one

16



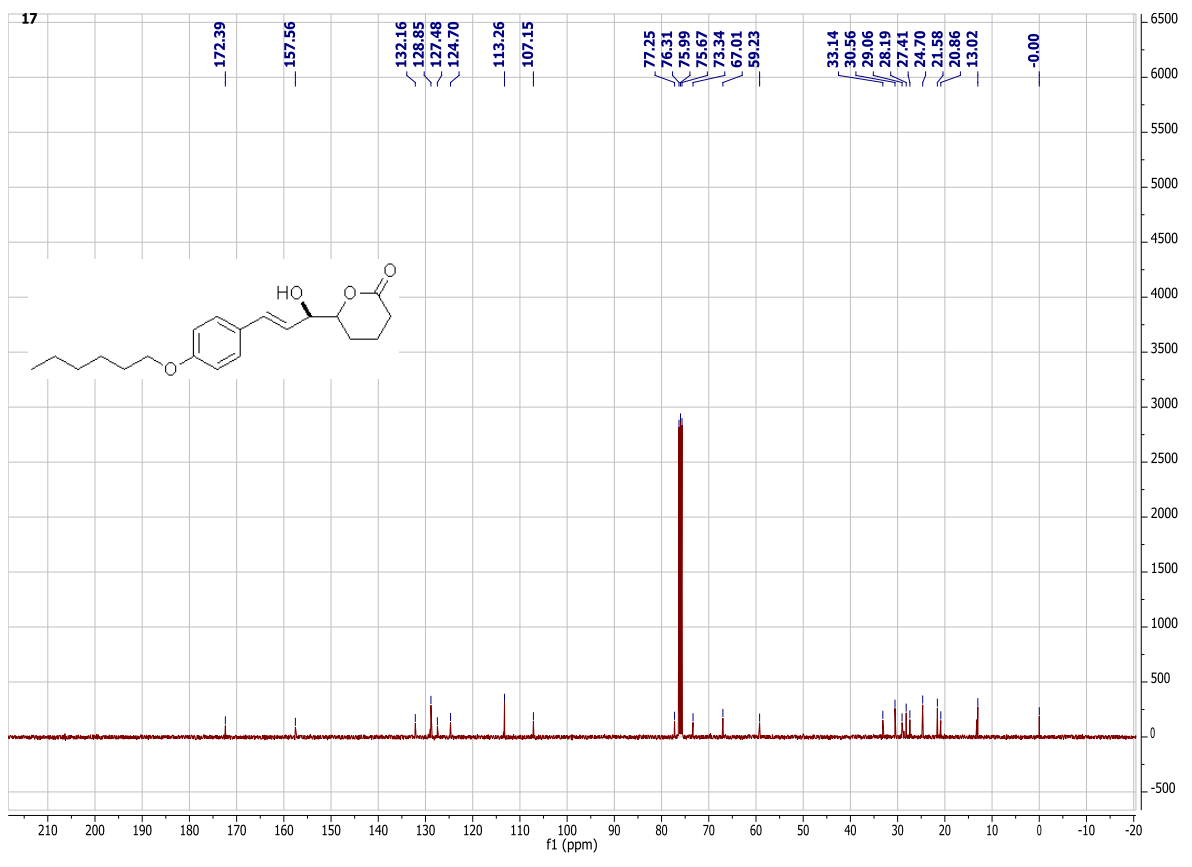
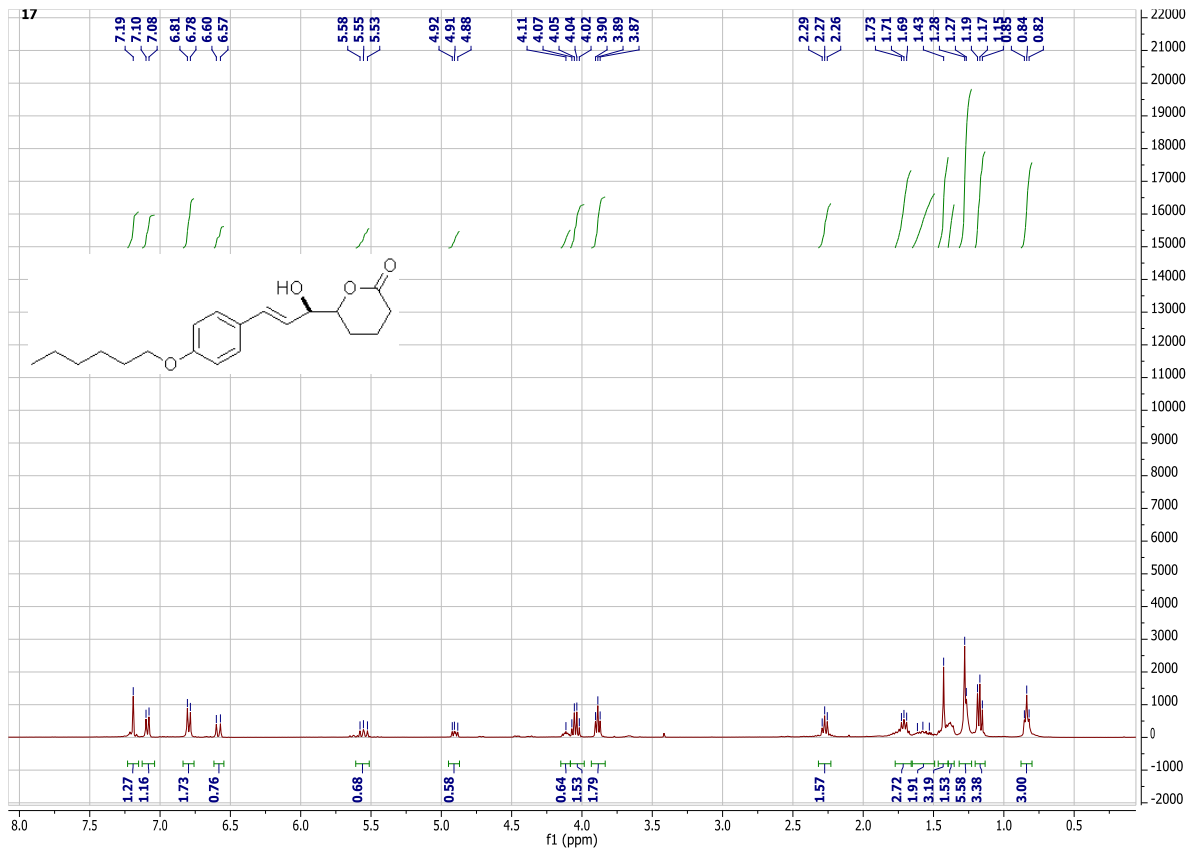
AB-180_151009115758 #1-4 RT: 0.02-0.11 AV: 4 NL: 1.81E6
T: FTMS + p ESI Full ms [200.00-500.00]



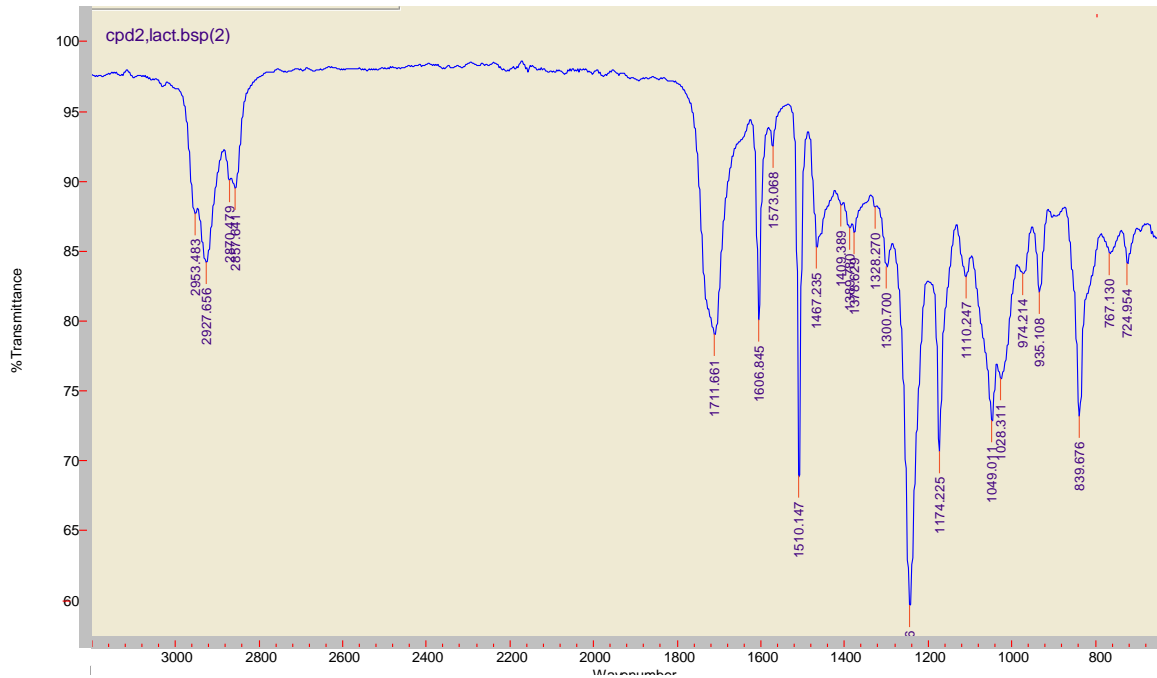
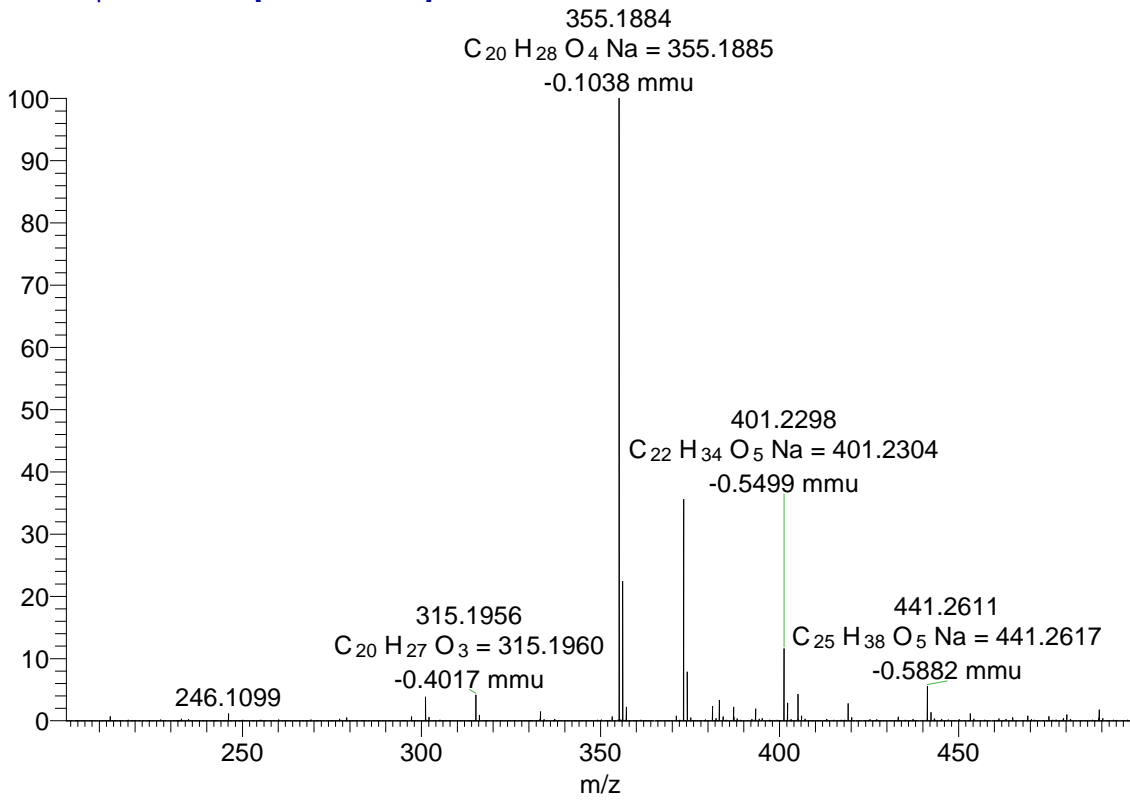


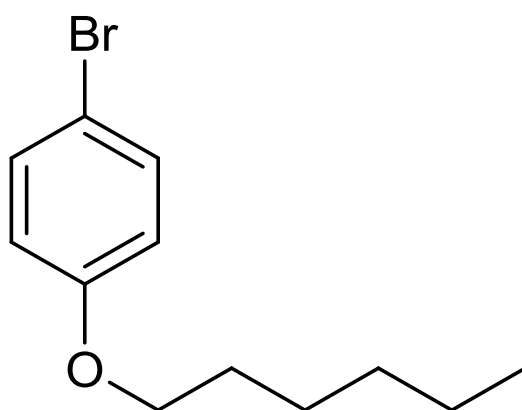
6-((*R,E*)-3-(4-(hexyloxy)phenyl)-1-hydroxyallyl)tetrahydro-2*H*-pyran-2-one

17



etherhydchl_151029153725 #1-5 RT: 0.00-0.11 AV: 5 NL: 7.66E7
T: FTMS + p ESI Full ms [200.00-600.00]





1-bromo-4-(hexyloxy)benzene

20

